METEOR-Berichte 01-2

Trans Atlantic 2000

Part 3

Cruise No. 47, Leg 3

1 June – 3 July 2000, Libreville – Walvis Bay

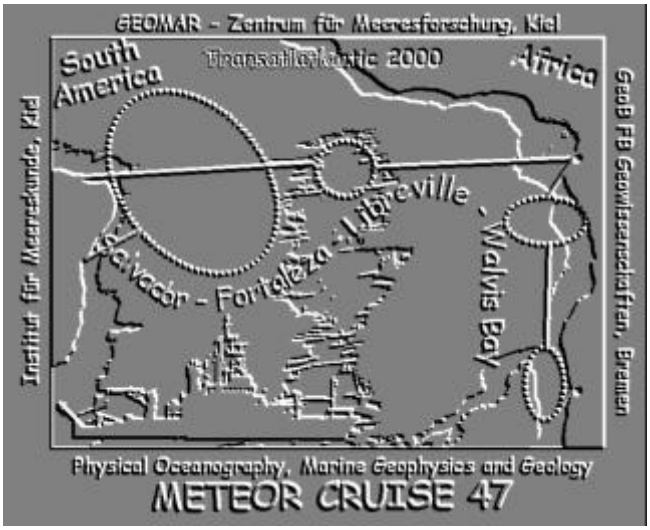

V. Spieß, W. Böke, M. Breitzke, K. Enneking, D. Grother, M. Gutowski, C. Hensen, C. Joppich, S. Kasten, F. Meier, B. Meyer-Schack, A. Reitz, A. Ringelhan, U. Rosiak, M. Salem, R. Schneider, S. Schulte, T. Schwenk, G. Verstegh, T. von Larcher, W.-T. Ochsenhirt, L. Zühlsdorff

Editorial Assistance:

Frank Schmieder
Fachbereich Geowissenschaften, Universität Bremen

Leitstelle METEOR
Institut für Meereskunde der Universität Hamburg

2002

Table of Contents

3.1 Participants M 47/3

Name	Discipline	Institution
Spieß, Volkhard, Prof. Dr., chief scientist	Geophysics	GeoB
Böke, Wolfgang, technician	Geophysics	GeoB
Breitzke, Monika, Dr., scientist	Geophysics	GeoB
Enneking, Karsten, technician	Geochemistry	GeoB
Grother, Dietmar, technician	Marine Geology	GeoB
Gutowski, Martin, student	Marine Geology	GeoB
Hensen, Christian, Dr., scientist	Geochemistry	GeoB
Joppich, Christoph, scientist	Meteorology	DWD
Kasten, Sabine, Dr., scientist	Geochemistry	GeoB
Meier, Florian, student	Geophysics	GeoB
Meyer-Schack, Birgit, technician	Marine Geology	GeoB
Ochsenhirt, Wolf-Thilo, technician	Meteorology	DWD
Reitz, Anja, student	Geochemistry	GeoB
Ringelhan, Alexander, student	Geophysics	GeoB
Rosiak, Uwe, technician	Marine Geology	GeoB
Salem, Mohamed, scientist	Geophysics	GeoB
Schneider, Ralf, Dr., scientist	Marine Geology	GeoB
Schulte, Sonja, Dr., scientist	Marine Geology	GeoB
Schwenk, Tilmann, scientist	Geophysics	GeoB
Spinelli, Glenn, scientist	Physical Properties	UCSC
Verstegh, Gerald, Dr., scientist	Marine Geology	GeoB
von Larcher, Thomas, student	Geophysics	GeoB
Zühlsdorff, Lars, Dr., scientist	Geophysics	GeoB

DWD	Deutscher Wetterdienst – Geschäftsfeld Seeschiffahrt – Bernhard-Nocht-Str. 76, 20359 Hamburg, Germany
GeoB	Department of Geosciences, Bremen University Klagenfurterstr., 28359 Bremen, Germany
UCSC	University of Santa Cruz, Hydrogeology, Earth Sciences Department, University of California, Sta. Cruz, CA 95064, U.S.A.

3.2 Research Program

For R/V METEOR Cruise M47/3 a variety scientific objectives were defined to be investigated through the combination of multichannel seismic surveying and geological and geochemical sampling of sediments and water column. Among the major topics were: fluid migration, channel-levee and canyon systems, sediment tectonics, Neogene sedimentation history and seismic imaging of dolomitic layers.

The regions of investigation were located at the African continental slopes in the southern equatorial Atlantic north and south of the Congo Canyon near 5°S as well as the region between Walvis Ridge at 18°40'S and the African continental slope at 25°40'S off Lüderitz in the Namibian upwelling system (Fig. 3.1).

The continental slope off the Congo River was subject to the first part of the ODP (Ocean Drilling Program) Drilling Campaign Leg 175, when 3 drill sites had been visited to study the Quaternary climatic and paleoceanographic history of the region. Due to the proximity of the continental slope north of the Congo Canyon to the mouth of the Congo River as a source of terrigenous sediment input, the sediments serve as a recorder of paleoclimatic signals from land as well as of marine signals. However, calibration of the riverine sediment flux versus the variability of marine productivity and current controlled sediment transport is required to decipher changes in sedimentation rates, provenance and composition as a function of land climate and regional oceanography. Selected seismic lines had been planned across the continental margin to both link the ODP Sites 1075 through 1077 with very high resolution seismic data, superior to the original pre-site survey data, and to reach an areal coverage, which should allow the reconstruction of spatial depositional patterns.

It has been speculated that regional tectonics has controlled the location of terrigenuous sediment sources as rivers and coastal mountain ranges, and the network of seismic lines in the study area was therefore designed to also image depositional patterns, stratigraphy and changes in sediment supply through Neogene times. Furthermore, the role of the Congo Canyon as an efficient trap for coarse sediment within the deep canyon flanks is not very well understood. Nowadays, most of the sand fraction is trapped and transported into the deep sea fan, and only fine-grained sediment in the suspension cloud is released from the Congo river into the region. Seismic lines across and near the canyon as well as selected coring should provide more information on the Holocene sedimentation and its climate control. Precise seismostratigraphic control should be provided by several crossings of ODP Sites 1075 through 1077 through the subsequent calculation of synthetic seismograms from sediment core data.

It is well known that the continental margin from Gabon to Angola (13°S) is shaped by massive diapirism of salt, creating the steep Angola escarpment, a marginal plateau and local uplift and subsidence on lateral scales of 10's of kilometers. However, a structure as the Angola escarpment seems to be absent in the vicinity of the Congo Canyon, but may have still controlled sediment distribution on the continental margin through episodic uplift of barriers. The seismic survey in the Congo Region was designed to image variations on local and regional scales to develop an understanding of the role of salt tectonism from sediment distribution and fan development.

A major topic of the research carried out during R/V METEOR Cruise M47/3 is related to fluid migration and active venting. Based on few seismic and sediment echosounder data from the R/V SONNE Cruise SO 86 in 1997, areas of apparent focused fluid flow, pockmarks, anomalous

amplitude distributions in surface sediments and intense small scale and large scale sediment tectonism was observed north of the Congo Canyon at the continental slope around 3000 m water depth.

A detailed survey and sampling program was designed to identify locations of assumed fluid flow and venting and to characterize both geochemical anomalies and sediments in the vicinity of such venting zones. The GeoB high resolution multichannel seismic systems should be used to gain detailed insights in near-surface structures and processes from digital echosounder and water gun seismic data as well as information from deeper levels through two different GI Guns, ranging in frequency between watergun and conventional seismic sources. Those data are acquired in an alternating trigger mode, which provides simultaneously 4 different seismic data sets on each seismic line, allowing studies on frequency dependent seismic properties and optimum structural imaging at different depth levels.

Another study area was chosen south of the Congo Canyon, where potential fluid migration was studied in an area of intense salt diapirism, which dominates sediment structures and deformation. A local survey was planned in conjunction with selected geologic and geochemical sampling.

As the last part of the research program, seismic surveying was planned along a latitudinal transect between Walvis Ridge at 19°S and the Namibia Upwelling Area off Lüderitz at 25°S. Target of the survey was the occurrence of dolomitic layers, which were drilled in ODP Leg 175 Sites 1081 through 1084. These layers had not been detected in the original seismic site survey data, since the layers were only a few decimeters thick, which was below the seismic resolution. New seismic data acquired with frequencies up to 1 kHz should be more suitable to detect these layers and in particular to map out their distribution as a function of burial depth, water depth and sediment supply as well as their relationship to an intermediate water bottom current, which is also responsible for erosion and the development of small scale mud waves.

3.3 Narrative of the Cruise

R/V METEOR Cruise M47/3 started in Libreville/Gabon on May, 31st, to carry out basic research in marine geophysics, marine geology and marine geochemistry at the southwest African continental margin. In preparation of the cruise, 5 countries, Gabon, Congo (cap. Kinshasa), Congo (cap. Brazzaville), Angola and Namibia, had been contacted for permission of this research operation, since most of the multichannel seismic surveying and coring was planned at the continental margin between 200 and 4000 m water depth within a zone of 200 nm from the coast. Before departure from Libreville, the missing permission from Congo (Brazzaville) was negotiated with the greatly appreciated help of the German embassy and the embassador of Congo in Libreville, which finally led to a positive response. Therefore, the scientific programme of the cruise could be carried out as originally planned. The last port activity was a mutual visit of crew members with the USNS HENSON, which was carrying out high precision bathymetric and side scan survey work in the Bay of Libreville

After departure on June, 1st, we started immediately with the setup of the seismic equipment and the labs to be ready for work on arrival in the first working area next day. In the evening of June, 2nd, the first station was visited and different sediment and water sampling devices were tested and used in 700 m water depth. A 3-day seismic survey was carried out running long

seismic lines across the continental margin to image the sedimentation as a function of distance from the Congo River, water depth, tectonic processes and the underlying morphology of salt diapirs. The lines were linked to a drill site of the Ocean Drilling Programm Leg 175, Site 1075, which provides high resolution stratigraphic information for age control of seismic reflectors.

The survey ended in one of the main working areas of the cruise, where we had planned an integrated study for the search of geologic structures related to the presence of gas hydrates and fluid or gas migration. Besides a detailed network of seismic, sediment acoustic and bathymetric lines in the vicinity of sampling sites, which was completed in several phases during the cruise, an extended geochemical and geological sampling program was carried out, which also included measurements and sampling in the water column for the search of methane. On May, 5th, the first sampling site was visited, which provided typical hemipelagic, water and organic-rich sediments.

Surveying of the continental margin was continued for two more days until May, 7th, on the margin north of the Congo Canyon, where most of the suspended matter from the river plume is deposited. Several crossings, a good areal coverage, and an extraordinary penetration of high frequency signals will allow a high resolution spatial reconstruction of sediment accumulation variability, which is expected to be a function of global and regional oceanographic and climatíc changes.

In contrast, in the vicinity of the fluid migration study area, which was chosen from few seismic lines of the R/V SONNE Cruise SO 86 in 1993, penetration of all seismic signals was limited by a high reflectivity zone in some hundred meters sub-bottom depth. This zone was assumed to be caused by high gas content, originating from migration from deeper layers. In addition, narrow columnar zones of acoustic blanking were found, which we interpreted as indicator for fluid or gas upflow towards the sea floor. Here, we visited in the first phase 6 sites, where we deployed 17 devices including the gravity corer with 6, 12 or 18 m length, box corer, multi corer with 12 samples, methane sensor and the CTD/rosette system for water analysis.

At several sites, indirect evidence for recent and past fluid migration was found, which includes methane in the bottom water, carbonate concretions at several sub-bottom depth levels, densely distributed worm tubes, shell fragments up to 8 cm long and steep geochemical gradients, but further shorebased studies are required to determine the source of the gas, the age of concretions and sediments and further geochemical parameters. Most pronounced features of the seismic and sediment acoustic measurements were socalled 'pockmarks', which are known from shallow water to indicate intense fluid or gas expulsion associated with subsequent collapse of the sea floor. Beneath the pockmarks, narrow zones can be traced to more than 100 m sub-bottom depth, where reflector amplitudes are reduced or reflections are completely absent. The detailed surveys carried out between the coring activities confirmed the circular shape of these zones, with morphologic expression at the sea floor between few meters and 30 m. Different seismic frequencies used simultaneously all show the same lateral amplitude change. Enhancement of some reflections in the vicinity of the pockmarks indicated on the other hand, that post-depositional processes have modified the laterally homogeneous pattern of hemipelagic sediment input, and may be attributed to the presence of gas or gas hydrates at depth.

On May, 10th, we left the fluid migration working area towards the deep Angola Basin, where we tried to trace the sediment transport from the Congo Canyon and the continental margin into the deep sea. Several long seismic lines during a 3.5 day survey provided interesting insights into the lateral sediment transport both in the suspension cloud of the river and at the bottom through

deep sea channels, and will be used to estimate spatial and temporal changes of the overall sediment input into the Congo Fan. The seismic data confirm the absence of fan sediments in the northern part of the Congo Fan and an untypical seismic signature with limited signal penetration independent of source frequency, which may be attributed to anomalously high attenuation due to high gas content. Two coring sites were visited on May, 15th, in the vicinity of an abandoned channel to recover coarser terrigenous material, which had been transported through the Congo Canyon directly from shelf basins into the fan and which may directly image changes in continental climate and erosion.

The following day, on May 16th, we started another seismoacoustic survey related to fluid migration, now south of the Congo Fan in an area, where intense salt diapirism has caused local uplift, subsidence and faulting and created pathways for migration of fluids, gas and hydrocarbons. Close to the salt front at the border to the abyssal plain, a 3-day seismic and acoustic survey was carried out to determine the major structural units in the surface sediments, to search for columnar or fault-related acoustic blanking zones as indicators for fluid migration and to completely cover the area with swath bathymetry, which provides the most distinct dataset for the reconstruction of tectonic movements. Due to the complex structural situation, data quality can only be evaluated after thorough processing on land, but online data clearly indicated local surface anomalies and assumed zones of fluid upflow, which also had been sampled by 4 gravity cores during May, 19th.

High accumulation sediment cores were expected from a core transect across the Congo Canyon close to the mouth of the Congo River, which documents the relationship of the river system and its suspension cloud as a function of global and regional climatic conditions. After a PARASOUND survey to identify undisturbed Holocene sequences we sampled at 4 sites on June, 20th with long gravity cores and surface samples.

On the transit to the fluid migration study area, which we had visited at the beginning of the cruise, we ran several seismic lines downslope the continental margin north of the Congo Canyon to link the Leg 175 ODP drill sites with high resolution seismics for a detailed seismostratigraphic study. On June, 22nd, we finished the seismic work in this region and continued sampling at two other sites, which were identified from the previous bathymetric survey as pockmark surface expressions of 20 to 30 m depth and the final seismic line.

A few hours before the end of the sampling program we collected a big surprise - massive gas hydrates below 4 meters depth in a nearly 10 m long gravity core! Although we had hypothesized that features in the sediment column at depth originated from the presence of gas hydrates, we never had expected to find them at the sea floor or a few meters beneath. A second core provided a piece of gas hydrate directly from the sea floor. Distinct acoustic reflectivity anomalies in the sediment echosounder data as well as seismic data, which indicate a connection to gas accumulations at greater depth, were the basic data sets, which are linked to sea floor observations of coexisting gas hydrates, carbonate concretions, shell horizons, living species and pronounced geochemical anomalies in sediment and water, all leading to the conclusion of active venting and continuous supply of methane and growth of hydrates. Although the hydrate was disintegrating on the way up to the ship due to pressure release and temperature increase, most material was preserved and frozen for further shorebased analyses. Unusual was also the location of the hydrate site at a passive margin in greater water depth compared to many other findings worldwide. Based on these findings, we had extended our sampling program and also added a

detailed sediment echosounder survey in the vicinity of the hydrate site to understand the local structures, which result from the interaction of pelagic sedimentation, fluid upflow and venting and hydrate growth. In the evening of June, 23rd, we finished geologic sampling work of the cruise and left for the last part of the cruise, a seismic survey in the Namibia upwelling system south of the Walvis Ridge.

On June, 27th, we deployed the seismic equipment a last time north of the Walvis Ridge at 19°40'S. Along a zickzack course we headed southward through one of the main study areas of ODP Leg 175, crossing the four sites 1081 through 1084 in water depths between 500 and 2500 m to 25°40'S off Lüderitz. Beside the seismostratigraphic correlation between sites and to the coring and downhole logging data, we targeted our high resolution survey to the identification of dolomitic horizons, which had been found frequently in three of the four drill sites, but had not been identified in older seismic data due to their limited resolution. Higher source frequencies up to a factor of 5 were used to overcome this problem, and we hope to be able in shorebased analyses to map and analyze the spatial distribution of these dolomites and understand their relation to upwelling, deposition and bottom currents in the area. On July, 2nd, we finished the very successful scientific program of R/V METEOR Cruise M47/3 after 5 days of seismic surveying, heading for Walvis Bay as the final port. In the morning of July, 3rd, we left the ship and the ship's crew, which is and specifically was during this cruise by their professional support one of the important factors for a success of a scientific cruise.

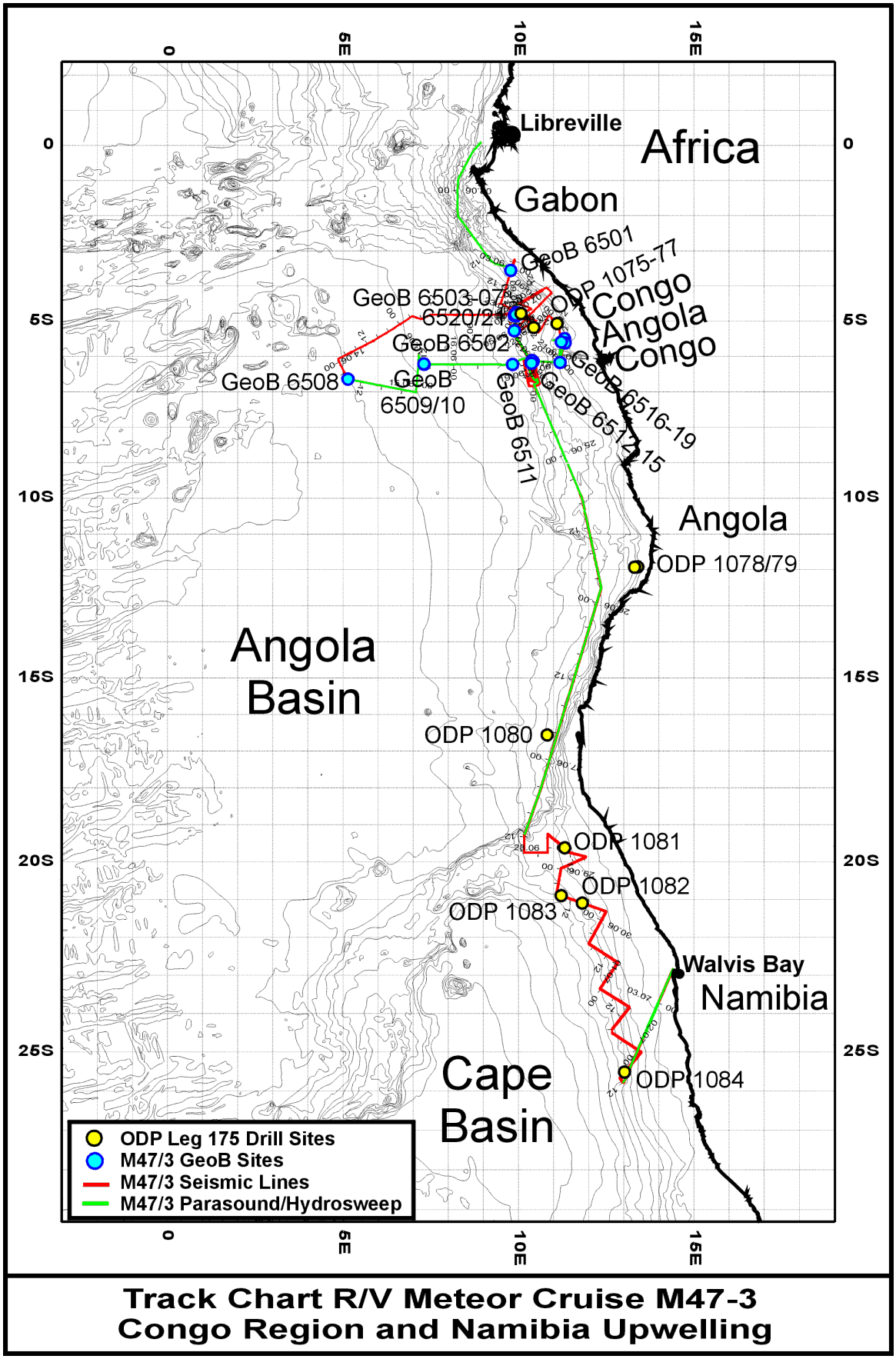

Fig. 3.1: Cruise track of R/V METEOR Cruise M 47/3 and locations of GeoB stations and ODP Drill Sites. Red: Seismic lines, green: PARASOUND/HYDROSEEP tracks.

3.4 Preliminary Results

3.4.1 Geophysical Profiling Methods

(V. Spieß, M. Breitzke, W. Böke, M. Gutowski, F. Meier, A. Ringelhan, T. Schwenk, T. von Larcher, L. Zühlsdorff)

Multichannel seismic surveying was carried out in all study areas of Cruise M47/3, including the Southwest African continental margin north and south of the Congo Canyon, the deep Congo Fan and the Namibia Upwelling System between Walvis Ridge and Lüderitz. With the GeoB high-resolution multichannel seismic equipment, small scale sedimentary structures and closely spaced layers can be imaged on a meter to sub-meter scale, which can usually not be resolved with conventional seismic systems. The alternating operation of a small chamber watergun (0.16 L; 200 – 1600 Hz), a GI airgun with reduced chamber volume (0.4 L; 100 – 500 Hz), and a GI airgun with normal chamber volume (1.7 L; 30 –200 Hz) yields three seismic data sets simultaneously. Guns with larger chamber volume are of greater penetration into the sea floor, revealing the larger scale structural framework, whereas guns with smaller chamber volume are of higher resolution, revealing finer details of the upper 200-400 m of the sediment cover beyond the penetration of the PARASOUND sedimet echosounder (50-100 m).

All seismic profiling activities during R/V METEOR Cruise M47/3 included continuous operation of two hydro-acoustic systems (PARASOUND sediment echosounder and HYDROSWEEP swath sounder) to determine the sea floor morphology, to characterize and analyze sediment deposition processes and sediment structures, and to provide information for site selection of coring and in situ measurements. Both hydro-acoustic data sets were acquired digitally.

3.4.1.1 PARASOUND Sediment Echosounding

(V. Spieß, M. Breitzke, W. Böke, M. Gutowski, F. Meier, A. Ringelhan, T. Schwenk, T. von Larcher, L. Zühlsdorff)

The PARASOUND system works both as a low-frequency sediment echosounder and as high-frequency narrow beam sounder to determine the water depth. It makes use of the parametric effect, which produces additional frequencies through nonlinear acoustic interaction of finite amplitude waves. If two sound waves of similar frequencies (here 18 kHz and e.g. 22 kHz) are emitted simultaneously, a signal of the difference frequency (e.g. 4 kHz) is generated for sufficiently high primary amplitudes. The new component is traveling within the emission cone of the original high frequency waves, which are limited to an angle of only 4° for the equipment used. Therefore, the footprint size of 7% of the water depth is much smaller than for conventional systems and both vertical and lateral resolution are significantly improved.

The PARASOUND system is permanently installed on the ship. The hull-mounted transducer array has 128 elements on an area of ~1 m^2. It requires up to 70 kW of electric power due to the low degree of efficiency of the parametric effect. In 2 electronic cabinets, beam forming, signal generation and the separation of primary (18, 22 kHz) and secondary frequencies (4 kHz) is carried out. With the third electronic cabinet in the echosounder control room, the system is operated on a 24 hour watch schedule.

Since the two-way travel time in the deep sea is long compared to the length of the reception window of up to 266 ms, the PARASOUND System sends out a burst of pulses at 400 ms intervals, until the first echo returns. The coverage of this discontinuous mode depends on the water depth and produces non-equidistant shot distances between bursts. On average, one seismogram is recorded about every second providing a spatial resolution on the order of a few meters on seismic profiles at 4.9 knots.

The main tasks of the operators are system and quality control and the adjustment of the start of the reception window. Because of the limited penetration of the echosounder signal into the sediment, only a short window close to the sea floor is recorded.

Beyond the analog recording features with the b/w DESO 25 device, the PARASOUND System was equipped with the digital data acquisition system PARADIGMA, which was developed at the University of Bremen (Spieß, 1993). The data were stored on two exchangable disc drives of 4 GigaByte capacity, allowing continuous recording between 5 and 10 days dependant on water depth and shot rate. The Pentium-processor based PC allows the buffering, transfer and storage of the digital seismograms at very high repetition rates. From the emitted series of pulses usually every second pulse is digitized and stored, resulting in recording intervals of 800 ms within a pulse sequence. The seismograms were sampled at a frequency of 40 kHz, with a typical registration length of 266 ms for a depth window of ~200 m. The source signal was a band limited, 2-6 kHz sinusoidal wavelet of 4 kHz dominant frequency with a duration of 2 periods (~500 µs total length).

Already during the acquisition of the data an online processing was carried out. For all profiles, PARASOUND sections were plotted with a vertical scale of several hundred meters. Most of the changes in window depth could thereby be eliminated. From these plots, a first impression of variations in sea floor morphology, sediment coverage and sedimentation patterns along the ships track could be gained. To improve the signal-to-noise ratio, the echogram sections were filtered with a wide band pass filter. In addition, the data were normalized to a constant value much smaller than the average maximum amplitude, to amplify in particular deeper and weaker reflections.

During the entire cruise, the combined PARASOUND/PARADIGMA system worked without significant problems. The storage procedure with exchangable hard discs worked successfully and reliable and avoided previously more frequent alert situations due to errors of magnetic tape recording.

3.4.1.2 HYDROSWEEP Bathymetry

(V. Spieß, M. Breitzke, W. Böke, M. Gutowski, F. Meier, A. Ringelhan, T. Schwenk, T. von Larcher, L. Zühlsdorff)

The multibeam echosounder HYDROSWEEP on R/V METEOR was routinely used during the cruise and serviced by the PARASOUND operator during a 24-hour watch. Sounding 59 pre-formed beams over an opening angle of 90 degrees, the hull-mounted system provides an image of the sea floor topography with a path width of twice the water depth. The system operates at a frequency of 15.5 kHz. To compress refraction effects on the outer beams, the system uses a calibration mode to compare depth values of the central and outer beams in order to calculate a

mean sound velocity by producing the best fit between both values. This configuration minimizes residual errors to values smaller than 0.5% of water depth (Grant and Schreiber, 1990).

Processing of the bathymetric data was carried out with the public domain software MULTIBEAM (Caress and Chayes, 1996). In particular, outer beams were zapped, artifacts were identified and flagged using automatic tools as well as an interactive editor, and the depth values were recalculated by full raytracing through a water velocity profile from the Levitus database. After gridding, the data were imaged as contour plots with the GMT software package (Wessel and Smith, 1998).

A comparison of the data of Cruise M47/3 with Cruises M16/1, M20/1, M41/1 and SO 86 revealed that the recently acquired data are much noisier (independent of weather conditions) than older data, indicating some significant change in the hardware and/or software of the acquisition system.

3.4.1.3 Multichannel Seismics

(V. Spieß, M. Breitzke, W. Böke, M. Gutowski, F. Meier, A. Ringelhan, T. Schwenk, T. von Larcher, L. Zühlsdorff)

The GeoB multichannel seismic system is specifically designed to acquire high resolution seismic data through optimizing all system components and procedural parameters. Figure 3.2 gives an outline of the system setup as it was used during R/V METEOR Cruise M47/3.

Seismic Sources and Compressor

During seismic surveying, four different seismic sources, two GI-Guns and two waterguns, were triggered in a quasi-simultaneous mode at a time interval between 10 and 13 s (see also trigger unit). Owing to an average ship speed of 5.0 kn, a shot distance of appx. 25 m to 34 m was thus obtained for the alternating mode operation of each gun type.

Each source type was shot more than 130000 times at an air pressure of about 165-190 bar. Due to rough weather, the systems were temporarily operating under heavy conditions and pressure lines were broken several times. Complete data gaps, however, could be avoided, since only one of the sources had to be turned off at a time.

The geometry of source and receiver systems during the measurements is shown in Figure 3.3. Ship velocity during deployment and retrieval was between 2.5 and 3.5 kn, respectively, depending on weather conditions and surface currents.

One standard GI-Gun (Generator-Injector gun; SODERA) with normal chamber volume (2 x 1.7 L) as well as a second GI-Gun with reduced chamber volume (2 x 0.41 L) were towed together with a towing frame on starboard side, appx. 10-15 m behind the stern with a lateral offset of appx. 4 meters. The towing wire was connected to a bow with both GI-Guns hanging on two chains 40 cm beneath (Fig. 3.4). An elongated buoy, which stabilized the gun in a horizontal position at a water depth of ~1.4 m, was connected to the bow by two rope loops. The Injector was triggered with a delay of 30 ms with respect to the Generator signal, which basically eliminated the bubble signal.

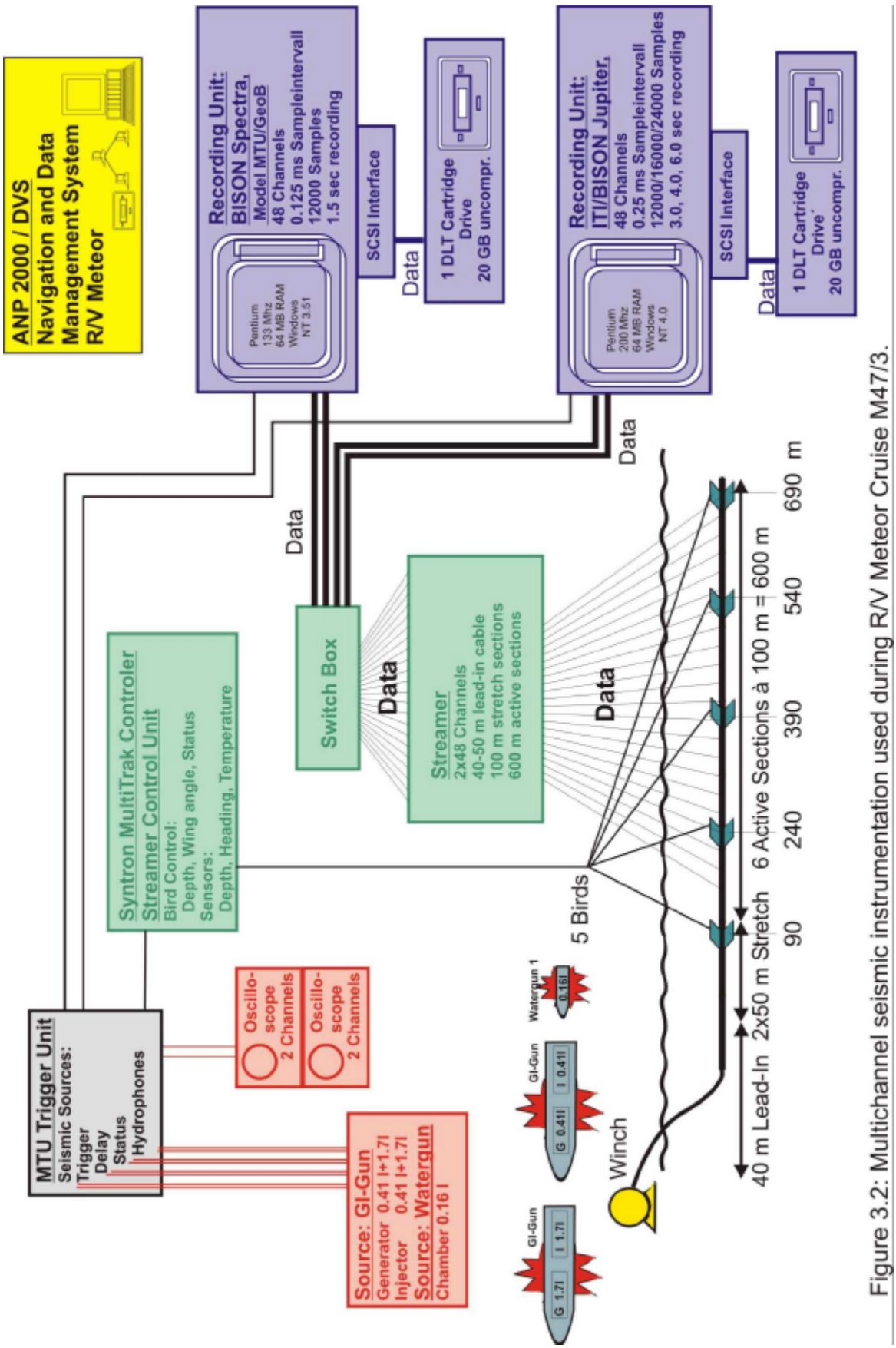

Figure 3.2: Multichannel seismic instrumentation used during R/V Meteor Cruise M47/3.

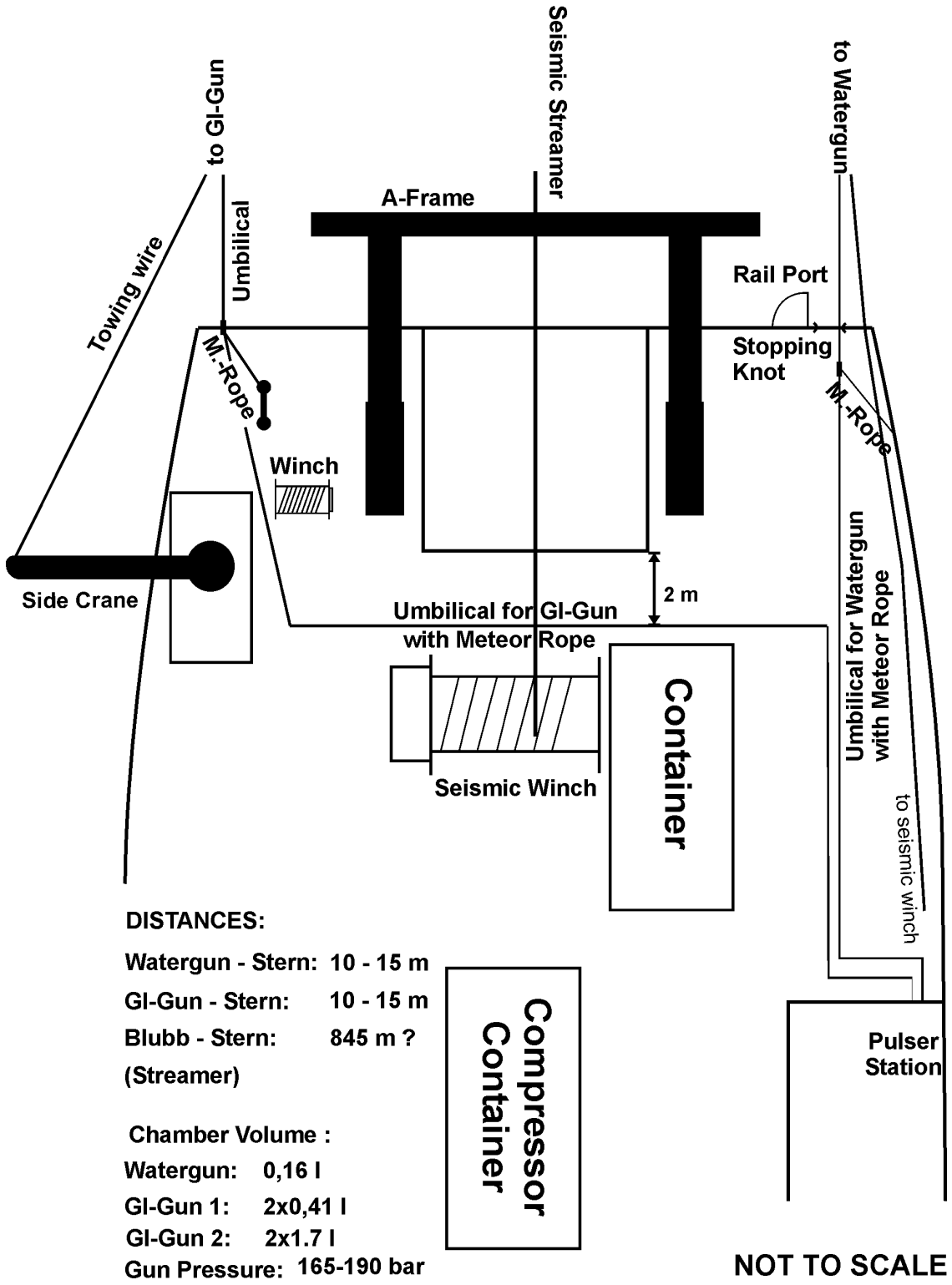

Fig. 3.3: Working deck setting during R/V METEOR Cruise M47/3

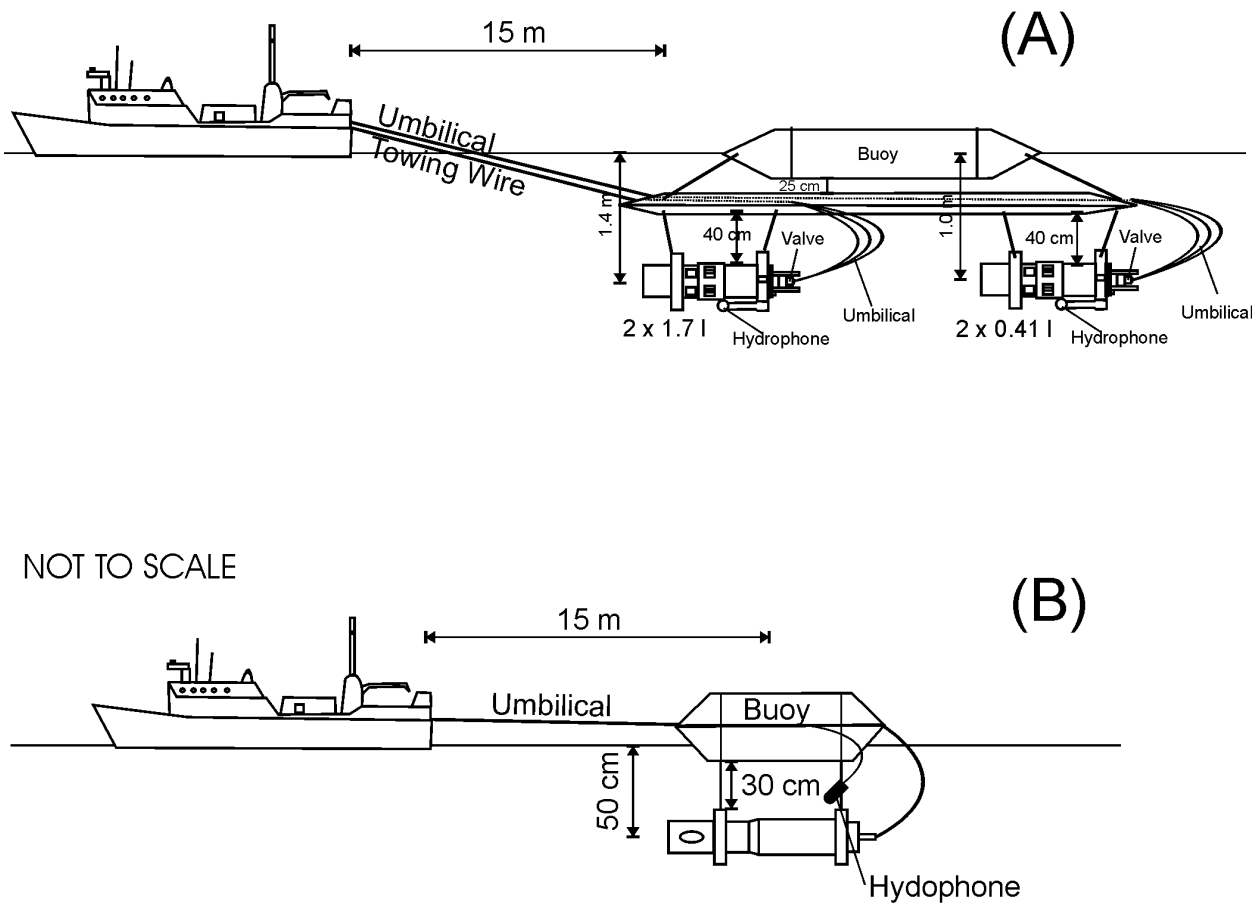

Fig. 3.4: Towing gear and arrangement for (A) GI Gun 0.41 L + 1.7 L and (B) Watergun 0.16 L.

The other source type was a S15 watergun (SODERA) with a volume of 0.16 L. One was towed by an outrigger at port side, providing an offset of appx. 16 m from the ship's axis. The other one was towed by a starboard side crane providing about 9 m offset from the ship's axis. Owing to the lateral offset between sources and receivers, two parallel watergun profiles with a distance of appx. 12.5 m were measured simultaneously. Since the line spacing at the most important survey areas was chosen to be 25 m, the effective line spacing for watergun data was therefore further reduced to 12.5 m. For both waterguns, the distance to the ship's stern was about 25 m. The umbilicals were secured by strong ropes to avoid damage of pressure lines and electric cables due to rubbing or bending. Steel frames held the waterguns in a tight position parallel to the elongated buoy in a depth of approximately 0.5 m (Fig. 3.4). During operations, the near field source signature of all four guns was checked on a digital scope in the seismic lab.

High-pressure air for gun operation was provided by the new LMF compressor. It was set up in a oversize container on the working deck of R/V METEOR and maintained by the ship's crew. Only minor technical problems occured during the cruise, providing continuous supply of high pressures up to 190 bar. However, for high resolution seismics with relatively small airguns, 90% of the air production (28 m^3 per minute) had to be blown into the air, causing a very noisy environment, which was adding to the high noise level of the diesel aggregate. The air consumption of the airguns used sums up to:

- Watergun + GI Gun 2x0.41 L in alternating mode at 10 s: **0.56 m^3 / min**
- Watergun + GI Gun 2x0.41 L in quasi-continuous mode at 12 s: **0.93 m^3 / min**
- Watergun + GI Gun 2x1.7 L in quasi-continuous mode at 12 s: **3.38 m^3 / min**

Streamer

The multichannel seismic streamer (SYNTRON) includes a tow-lead, two stretch sections of 50 m and six active sections of 100 m length each. A 100 m long METEOR rope with a buoy at the end was connected to the tail swivel. A 30 m long deck cable connected the streamer to the recording system. The winch location on the working deck is shown in Fig. 3.3. During operations, the streamer (tow lead) was fixed with two METEOR ropes. The tow lead was laid out ~35 m, the distance from ship to stretch section was 30 m.

Active sections are subdivided in 16 hydrophone groups (Fig. 3.5). Each of the 6.25 m long hydrophone groups is again subdivided into 5 subgroups of different length. One of the subgroups is a high-resolution hydrophone with pre-amplifier. A programming module distributes the subgroups of 4 hydrophone groups, i.e. a total of 20 groups, to 5 channels. As illustrated in Figure 3.5, every second 6.25 m hydrophone subgroup was completely used with all 13 hydrophones, whereas the two additional channels were reduced in length to 2.2 m and 3.3 m, respectively. Locations of individual hydrophone groups are given in Table 3.1.

A switch box connects the streamer via deck cable with the seismograph and allows the assignment and optional stacking of streamer hydrophone subgroups to individual recording channels. The incoming 120 channels (96 hydrophone groups and 24 single hydrophones) were distributed to the output channels of the recording system(s) as shown in Table 3.2 with two different patterns.

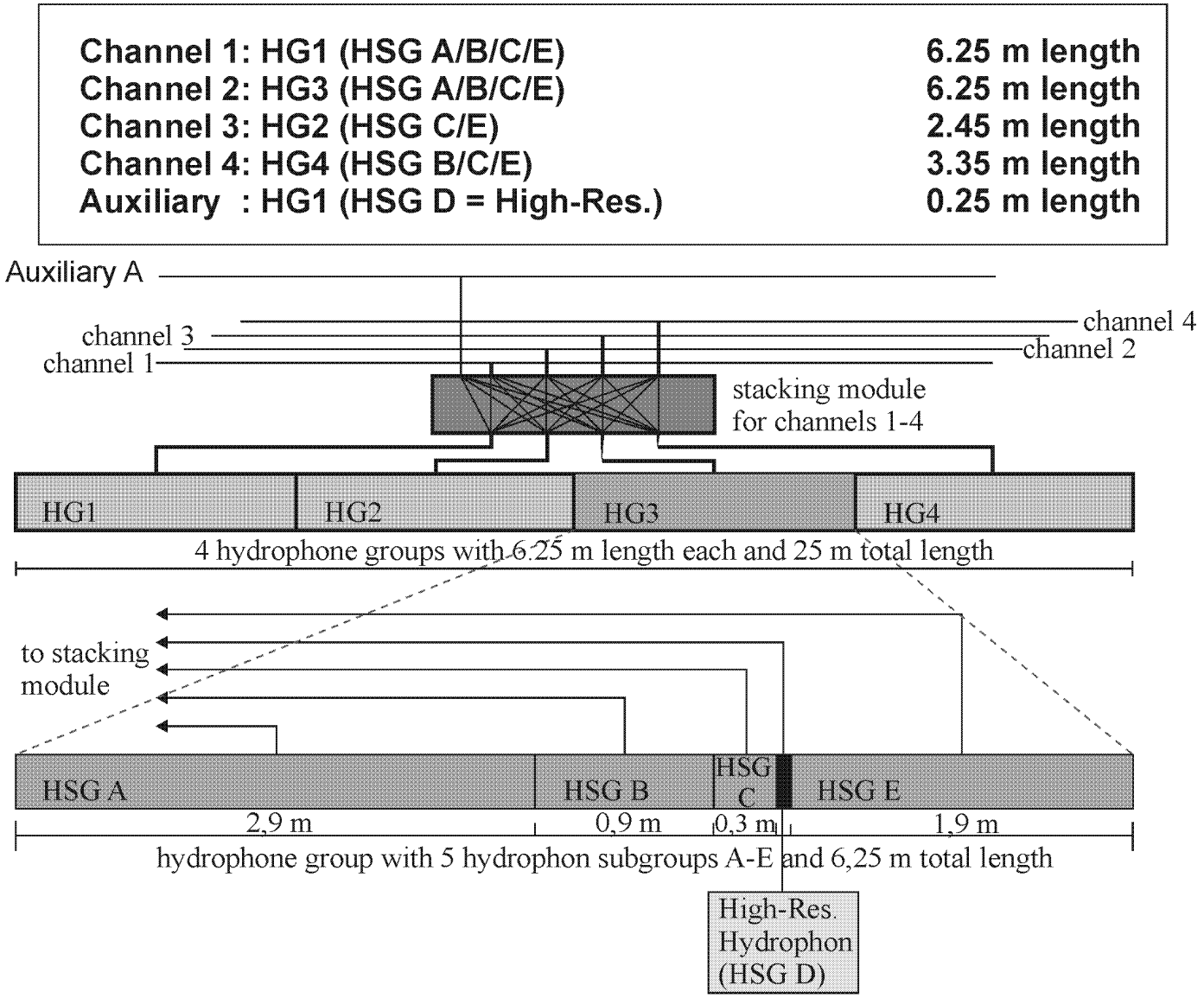

Figure 3.5: Multichannel streamer design used during R/V Meteor Cruise M47/3. The hydrophone group combination repeats after every 5 channels.

Output channels 1 to 48 were connected to the Jupiter recording system (alternating mode of small-chamber and large-chamber GI Gun), channels 49 to 96 to the Spectra recording system (alternating mode of waterguns) (Table 3.2). Single hydrophones (streamer channels 97 to 120) were not recorded.

Deployment and retrieval lasted appx. 45 minutes including installation of the five Remote Bird Units (RUs; see below).

Segment of 25 m length	Hydrophone Group No.	Channel No. In Section	Midpoint Distance
A (0-25 m)	1	1	3.1 m
A	2	3	11.3 m
A	3	2	15.6 m
A	4	4	23.3 m
B (25-50 m)	1	5	28.1 m
B	2	7	36.3 m
B	3	6	40.6 m
B	4	8	48.3 m
C (50-75 m)	1	9	53.1 m
C	2	11	61.3 m
C	3	10	65.6 m
C	4	12	73.3 m
d (75-100 m)	1	13	78.1 m
D	2	15	86.3 m
D	3	14	90.6 m
D	4	16	98.3 m

Table 3.1: Channel assignment and midpoint distances of hydrophone groups from begin of each active section.

MULTITRAK Bird Controller

In operation, 5 MULTITRAK Remote Units (RU) were attached to the streamer. The positions of the RUs are listed in Table 3.3. Each RU includes a depth and a heading sensor as well as adjustable wings. The RUs are controlled by the MULTITRAK Bird controller in the seismic lab. Controller and RUs communicate via communication coils nested within the streamer. A twisted pair wire within the deck cable connects controller and coils.

Each shot trigger started the bird scan of water depth, wing angle and heading data (delay 0.0 s, duration 1.0 s). The current location of the streamer can be displayed as a depth or heading profile on a monitor. All parameters are digitally stored on the controller PC, together with shot number, date and time.

There are two ways of controlling the streamer depth. The most common way is to send an operating depth range to the RUs (typically 3 meters during Cruise M47/3). The RUs try to force the streamer to the chosen depth by adjusting the wing angles accordingly. Another option is to set a constant wing angle, which did not have to be applied during this cruise. Depth and wing angle statistics help to set appropriate parameters.

Table 3.2a: Streamer channel 1 to 48 assignment to output channel for Jupiter recording system (GI Gun) for seismic lines GeoB 00-052 to the end of the cruise.

Input Channel	Output Channel	Hydrophone Group	Number of Hydrophones per Group	Hydrophone Group Length [m]	Hydrophone Group distance [m]
1	1	HG1	13	6.25	12.5
2	2	HG3	13	6.25	12.5
5	3	HG1	13	6.25	12.5
6	4	HG3	13	6.25	12.5
9	5	HG1	13	6.25	12.5
10	6	HG3	13	6.25	12.5
13	7	HG1	13	6.25	12.5
14	8	HG3	13	6.25	12.5
17	9	HG1	13	6.25	12.5
18	10	HG3	13	6.25	12.5
21	11	HG1	13	6.25	12.5
22	12	HG3	13	6.25	12.5
25	13	HG1	13	6.25	12.5
26	14	HG3	13	6.25	12.5
29	15	HG1	13	6.25	12.5
30	16	HG3	13	6.25	12.5
33	17	HG1	13	6.25	12.5
34	18	HG3	13	6.25	12.5
37	19	HG1	13	6.25	12.5
38	20	HG3	13	6.25	12.5
41	21	HG1	13	6.25	12.5
42	22	HG3	13	6.25	12.5
45	23	HG1	13	6.25	12.5
46	24	HG3	13	6.25	12.5
49	25	HG1	13	6.25	12.5
50	26	HG3	13	6.25	12.5
53	27	HG1	13	6.25	12.5
54	28	HG3	13	6.25	12.5
57	29	HG1	13	6.25	12.5
58	30	HG3	13	6.25	12.5
61	31	HG1	13	6.25	12.5
62	32	HG3	13	6.25	12.5
65	33	HG1	13	6.25	12.5
66	34	HG3	13	6.25	12.5
69	35	HG1	13	6.25	12.5
70	36	HG3	13	6.25	12.5
73	37	HG1	13	6.25	12.5
74	38	HG3	13	6.25	12.5
77	39	HG1	13	6.25	12.5
78	40	HG3	13	6.25	12.5
81	41	HG1	13	6.25	12.5
82	42	HG3	13	6.25	12.5
85	43	HG1	13	6.25	12.5
86	44	HG3	13	6.25	12.5
89	45	HG1	13	6.25	12.5
90	46	HG3	13	6.25	12.5
93	47	HG1	13	6.25	12.5
94	48	HG3	13	6.25	12.5

Table 3.2b: Streamer channel 1 to 48 assignment to output channel for Jupiter recording system (GI Gun) for seismic lines GeoB 00-040 through GeoB 00-051.

Input Channel	Output Channel	Hydrophone Group	Number of Hydrophones per Group	Hydrophone Group Length [m]	Hydrophone Group distance [m]
1	1	HG1	13	6.25	8.15
3	2	HG2	6	2.45	16.85
5	3	HG1	13	6.25	8.15
7	4	HG2	6	2.45	16.85
9	5	HG1	13	6.25	8.15
11	6	HG2	6	2.45	16.85
13	7	HG1	13	6.25	8.15
15	8	HG2	6	2.45	16.85
17	9	HG1	13	6.25	8.15
19	10	HG2	6	2.45	16.85
21	11	HG1	13	6.25	8.15
23	12	HG2	6	2.45	16.85
25	13	HG1	13	6.25	8.15
27	14	HG2	6	2.45	16.85
29	15	HG1	13	6.25	8.15
31	16	HG2	6	2.45	16.85
33	17	HG1	13	6.25	8.15
35	18	HG2	6	2.45	16.85
37	19	HG1	13	6.25	8.15
39	20	HG2	6	2.45	16.85
41	21	HG1	13	6.25	8.15
43	22	HG2	6	2.45	16.85
45	23	HG1	13	6.25	8.15
47	24	HG2	6	2.45	16.85
49	25	HG1	13	6.25	8.15
51	26	HG2	6	2.45	16.85
53	27	HG1	13	6.25	8.15
55	28	HG2	6	2.45	16.85
57	29	HG1	13	6.25	8.15
59	30	HG2	6	2.45	16.85
61	31	HG1	13	6.25	8.15
63	32	HG2	6	2.45	16.85
65	33	HG1	13	6.25	8.15
67	34	HG2	6	2.45	16.85
69	35	HG1	13	6.25	8.15
71	36	HG2	6	2.45	16.85
73	37	HG1	13	6.25	8.15
75	38	HG2	6	2.45	16.85
77	39	HG1	13	6.25	8.15
79	40	HG2	6	2.45	16.85
81	41	HG1	13	6.25	8.15
83	42	HG2	6	2.45	16.85
85	43	HG1	13	6.25	8.15
87	44	HG2	6	2.45	16.85
89	45	HG1	13	6.25	8.15
91	46	HG2	6	2.45	16.85
93	47	HG1	13	6.25	8.15
95	48	HG2	6	2.45	16.85

Table 3.2c: Streamer channel 49 to 96 assignment to output channel for Spectra recording system (Watergun) for seismic lines GeoB 00-052 to the end of the cruise.

Input Channel	Output Channel	Hydrophone Group	Number of Hydrophones per Group	Hydrophone Group Length [m]	Hydrophone Group distance [m]
3	49	HG2	6	2.2	13
4	50	HG4	9	3.3	12
7	51	HG2	6	2.2	13
8	52	HG4	9	3.3	12
11	53	HG2	6	2.2	13
12	54	HG4	9	3.3	12
15	55	HG2	6	2.2	13
16	56	HG4	9	3.3	12
19	57	HG2	6	2.2	13
20	58	HG4	9	3.3	12
23	59	HG2	6	2.2	13
24	60	HG4	9	3.3	12
27	61	HG2	6	2.2	13
28	62	HG4	9	3.3	12
31	63	HG2	6	2.2	13
32	64	HG4	9	3.3	12
35	65	HG2	6	2.2	13
36	66	HG4	9	3.3	12
39	67	HG2	6	2.2	13
40	68	HG4	9	3.3	12
43	69	HG2	6	2.2	13
44	70	HG4	9	3.3	12
47	71	HG2	6	2.2	13
48	72	HG4	9	3.3	12
51	73	HG2	6	2.2	13
52	74	HG4	9	3.3	12
55	75	HG2	6	2.2	13
56	76	HG4	9	3.3	12
59	77	HG2	6	2.2	13
60	78	HG4	9	3.3	12
63	79	HG2	6	2.2	13
64	80	HG4	9	3.3	12
67	81	HG2	6	2.2	13
68	82	HG4	9	3.3	12
71	83	HG2	6	2.2	13
72	84	HG4	9	3.3	12
75	85	HG2	6	2.2	13
76	86	HG4	9	3.3	12
79	87	HG2	6	2.2	13
80	88	HG4	9	3.3	12
83	89	HG2	6	2.2	13
84	90	HG4	9	3.3	12
87	91	HG2	6	2.2	13
88	92	HG4	9	3.3	12
91	93	HG2	6	2.2	13
92	94	HG4	9	3.3	12
95	95	HG2	6	2.2	13
96	96	HG4	9	3.3	12

Table 3.2d: Streamer channel 49 to 96 assignment to output channel for Spectra recording system (Watergun) for seismic lines GeoB 00-040 through GeoB 00-051.

Input Channel	Output Channel	Hydrophone Group	Number of Hydrophones per Group	Hydrophone Group Length [m]	Hydrophone Group distance [m]
2	49	HG3	13	6.25	7.7
4	50	HG4	9	3.35	17.3
6	51	HG3	13	6.25	7.7
8	52	HG4	9	3.35	17.3
10	53	HG3	13	6.25	7.7
12	54	HG4	9	3.35	17.3
14	55	HG3	13	6.25	7.7
16	56	HG4	9	3.35	17.3
18	57	HG3	13	6.25	7.7
20	58	HG4	9	3.35	17.3
22	59	HG3	13	6.25	7.7
24	60	HG4	9	3.35	17.3
26	61	HG3	13	6.25	7.7
28	62	HG4	9	3.35	17.3
30	63	HG3	13	6.25	7.7
32	64	HG4	9	3.35	17.3
34	65	HG3	13	6.25	7.7
36	66	HG4	9	3.35	17.3
38	67	HG3	13	6.25	7.7
40	68	HG4	9	3.35	17.3
42	69	HG3	13	6.25	7.7
44	70	HG4	9	3.35	17.3
46	71	HG3	13	6.25	7.7
48	72	HG4	9	3.35	17.3
50	73	HG3	13	6.25	7.7
52	74	HG4	9	3.35	17.3
54	75	HG3	13	6.25	7.7
56	76	HG4	9	3.35	17.3
58	77	HG3	13	6.25	7.7
60	78	HG4	9	3.35	17.3
62	79	HG3	13	6.25	7.7
64	80	HG4	9	3.35	17.3
66	81	HG3	13	6.25	7.7
68	82	HG4	9	3.35	17.3
70	83	HG3	13	6.25	7.7
72	84	HG4	9	3.35	17.3
74	85	HG3	13	6.25	7.7
76	86	HG4	9	3.35	17.3
78	87	HG3	13	6.25	7.7
80	88	HG4	9	3.35	17.3
82	89	HG3	13	6.25	7.7
84	90	HG4	9	3.35	17.3
86	91	HG3	13	6.25	7.7
88	92	HG4	9	3.35	17.3
90	93	HG3	13	6.25	7.7
92	94	HG4	9	3.35	17.3
94	95	HG3	13	6.25	7.7
96	96	HG4	9	3.35	17.3

Table 3.3: RU positions along seismic streamer.

RU (No.)	Position	Distance to Tow-Lead
3	End of Stretch Section No. 2	90 m
4	Mid of Active Section No. 2	240 m
6	End of Active Section No. 3	390 m
5	Mid of Active Section No. 5	540 m
2	End of Active Section No. 6	690 m

Data Acquisition System

A 48 channel Jupiter/ITI/Bison seismograph, which allows a maximum sampling frequency of 4 kHz at 24 bit resolution, is based on a PENTIUM PC (200 MHz; 64 MB RAM) with a WINDOWS NT 4.0 operating system. The seismograph allows online data display (shot gather), online demultiplexing and storing in SEG-Y format on DLT4000 cartridge tape with 20 GByte uncompressed capacity. Data were recorded at a sampling frequency of 4 kHz over an interval of 1.5 or 3 or 6 seconds, resulting in 48 x 6000 or 48 x 12000 or 48 x 24000 samples of 4 Byte each per shot, respectively. Pre-amplifiers were set to 48 dB, low cut filter to 4 Hz. Despite some minor software problems, the instrument worked very reliable and data were routinely collected from the beginning of the seismic survey.

The second system, a 48 channel seismograph (BISON SPECTRA) was specially designed for the University of Bremen, which allows a continuous operation mode to acquire very high resolution seismic data (sampling with up to 20 kHz). The seismograph (PENTIUM PC; 133 MHz; 64 MB RAM) is a predator of the above mentioned Jupiter system, runs under WINDOWS NT 3.51 and reveals basically the same features. It allows online data display (shot gather), online demultiplexing and storing in SEG-Y format. Pre-amplifiers were set to 60 dB, analog filters to 16 Hz (low-cut) and 2000 Hz (high-cut). The sampling frequency was 8 kHz for watergun recording over a length of 1500 ms. All channels were pre-amplified by a factor of 1000 (60 dB) to keep the incoming signal within the optimum voltage range for digitzing. The data were stored on a DLT4000 cartridge tape.

On both systems, the recording delay had to be adjusted according to the current water depth and was controlled through the trigger unit.

Trigger Unit

The custom trigger unit controls seismic sources, seismographs, bird controller, online-plotter with separate filter and digital scope (near-field hydrophones). The unit is set up on an IBM compatible PC with a Windows NT 4.0 operating system and includes a real-time controller interface card (SORCUS) with 16 I/O channels, synchronized by an internal clock. The unit is connected to an amplifier unit and a gun amplifier unit. The PC runs a custom software, which allows to define arbitrary combinations of trigger signals, which we used to optimize the available recording time for two/three seismic sources and to minimize shot distance.

Trigger times can be changed at any time during the survey. Through this feature, the recording delay can be adjusted to water depth without interruption of data acquisition. The amplifier unit converts the controller output to positive or negative TTL levels. The gun

amplifier unit, which generates a 60V/8 Amp. trigger level, controls the magnetic valves of the individual seismic sources. It was placed in the pulser station close to the gun pressure controls for immediate shutdown of gun operation.

Figure 3.6 shows one of the quasi-simultaneous trigger schemes, which were used during the survey for two recording systems and three different source types. It consists of two trigger intervals, one controlling the first watergun and the GI-Gun with smaller chamber volume, the second controlling a second shot of the watergun and the larger volume GI-Gun (to increase signal energy and depth penetration). For the example in Figure 3.6, each trigger interval has a length of 9 seconds, which may be extended up to 11.5 seconds for greater water depth (see Table 3.4). The arrival times of multiple reflections (second and third) were considered for the construction of the trigger scheme. Furthermore, the GI-Guns were later shot separately to improve the source signature, i.e. the GI-Gun with smaller chamber volume was shot during the first trigger interval whereas the GI-Gun with larger chamber volume was shot during the second. If necessary, the scheme was also changed with respect to expected penetration depth, sediment thickness, and changes in water depth (e.g., to set the proper recording delay). Each source type was recorded on a separate tape, one at the Bison Spectra for the watergun sorces and one on the Bison Jupiter for the GI-Gun sources. Recording and data storage occured parallel on both systems. In this mode, an additional processing step of splitting records from different sources is required prior to standard seismic data processing. Each gun was fired every 18-26 seconds (depending on interval length of the trigger scheme, which was 9-13 seconds).

As a consequence of the parallel recording, acquisition parameters could be adjusted on each system to the properties of the source as signal penetration and frequency content. Watergun recording was reduced to 1.5 seconds at a sampling frequency of 8 KHz and GI Gun data were recorded for 3 or 6 seconds, respectively, at 4 kHz.

Table 3.4: Trigger times for sources and recording systems as a function of water depth (two-way traveltime), given in milliseconds. The total length of the trigger period is given in the last column. Depending on the strength of multiple returns, these times may have to be adjusted to avoid interference.

Depth [m]	TWT [ms]	Delay [ms]	Shot Time Watergun [ms]	Shot Time GI Gun [ms]	Recording Time Watergun [ms]	Recording Time GI Gun (BISON-2) [ms]	MTC-Controller [ms]	EPC Online Recording [ms]	Total Trigger Period [ms]
0	0	0	0	1500	0 - 1500	1500 - 4500	5000	0	9000
375	500	500	0	2000	500 - 2000	2500 - 5500	6000	500	9000
750	1000	1000	0	2500	1000 - 2500	3500 - 6500	7000	1000	9000
1125	1500	1500	0	3000	1500 - 3000	4500 - 7500	0	1500	9000
1500	2000	2000	0	1500	2000 - 3500	3500 - 6500	0	2000	9000
1875	2500	2500	0	1500	2500 - 4000	4000 - 7000	0	2500	9000
2250	3000	3000	0	1500	3000 - 4500	4500 - 7500	0	3000	9000
2625	3500	3500	0	1500	3500 - 5000	5000 - 8000	0	3500	9000
3000	4000	4000	0	1500	4000 - 5500	5500 - 8500	0	4000	9000
3375	4500	4500	0	1500	4500 - 6000	6000 - 9000	0	4500	9000
3750	5000	5000	0	1500	5000 - 6500	6500 - 9500	0	5000	9500
4125	5500	5500	0	1500	5500 - 7000	7000 - 10000	0	5500	10000
4500	6000	6000	0	1500	6000 - 7500	7500 - 10500	0	6000	10500
4875	6500	6500	0	1500	6500 - 8000	8000 - 11000	0	6500	11000
5250	7000	7000	0	1500	7000 - 8500	8500 - 11500	0	7000	11500

3.4.1.4 Preliminary Results from Geophysical Profiling

(V. Spieß, M. Breitzke, W. Böke, M. Gutowski, F. Meier, A. Ringelhan, T. Schwenk, T. von Larcher, L. Zühlsdorff)

The survey and sampling activity in the Congo region was carried out from June, 1st through June, 22nd, when investigations with different objectives, as fluid migration, regional stratigraphy, fan sedimentation were combined. Figure 3.7 and Table 3.5 summarize the seismic and echosounder tracks as well as all sampling sites in this region.

Northern Congo Continental Margin

The Congo continental margin is characterized by sedimentation originating from higher productivity in surface waters and terrigenuous input through the suspension cloud of the Congo River. Coarser particles are trapped in the Congo Canyon, which incises the shelf across the coast as an efficient trap for bedload. Due to the northward directed Benguela coastal current, most of the suspended material is deposited on the slope north of the Congo Canyon.

The strong coastal currents have inhibited sedimentation on the shelf as illustrated in Figure 3.8. Older, inclined strata are exposed at the sea floor, which represents an erosional surface created during sea level low stand at appx. 115 m water depth. The digital PARASOUND example is typical for wide shelf areas off the SW African coast.

Sediments are composed of fine grained terrigenuous material, biogenic opal and organic matter. As known from other regions, these sediments preserve a high water content, which supports failure of the material during early diagenesis and compaction. Mass wasting is therefore a frequent process shaping the continental margin north of the Congo Canyon. The digital PARASOUND example along seismic line GeoB 00-045 (Fig. 3.9) reveals a continuous layering, but reflectors are interrupted by densely distributed small scale faults. The slightly undulating sea floor is another indicator for sediment tectonics and perhaps compression.

A part of seismic line GeoB 00-047 (Fig. 3.10), shot with GI Guns, shows several transparent units, which typically represent debris flows. Undulating reflectors at depth reveal that salt diapirism may be responsible for local uplift and associated fracturing above, but penetration of seismic data is not sufficient to confirm this.

Intermediate in resolution and penetration between GI Gun and digital echosounder data are watergun records as the example from line GeoB 00-047 (Fig. 3.11), which reveals significant variations in reflection amplitudes. Although an unequivocal interpretation is not possible at this stage, the pronounced amplitude changes cannot be associated with lithologic changes, but are more likely caused by postsedimentary changes related to gas charge, gas or fluid migration, or sediment deformation. However, it must be taken into account that in particular for high frequency seismic signal, structure and geometry may significantly affect reflection amplitude, which can be partially corrected by careful onshore processing including seismic migration.

All examples shown are typical for the continental slope north of the Congo Canyon between shelf break and 3500 m water depth, where hemipelagic sedimentation is dominating. At greater water depth, fan deposition is present, which is associated with coarser grain sizes, channel-levee systems, and intercalation of depositional lobes (see example below).

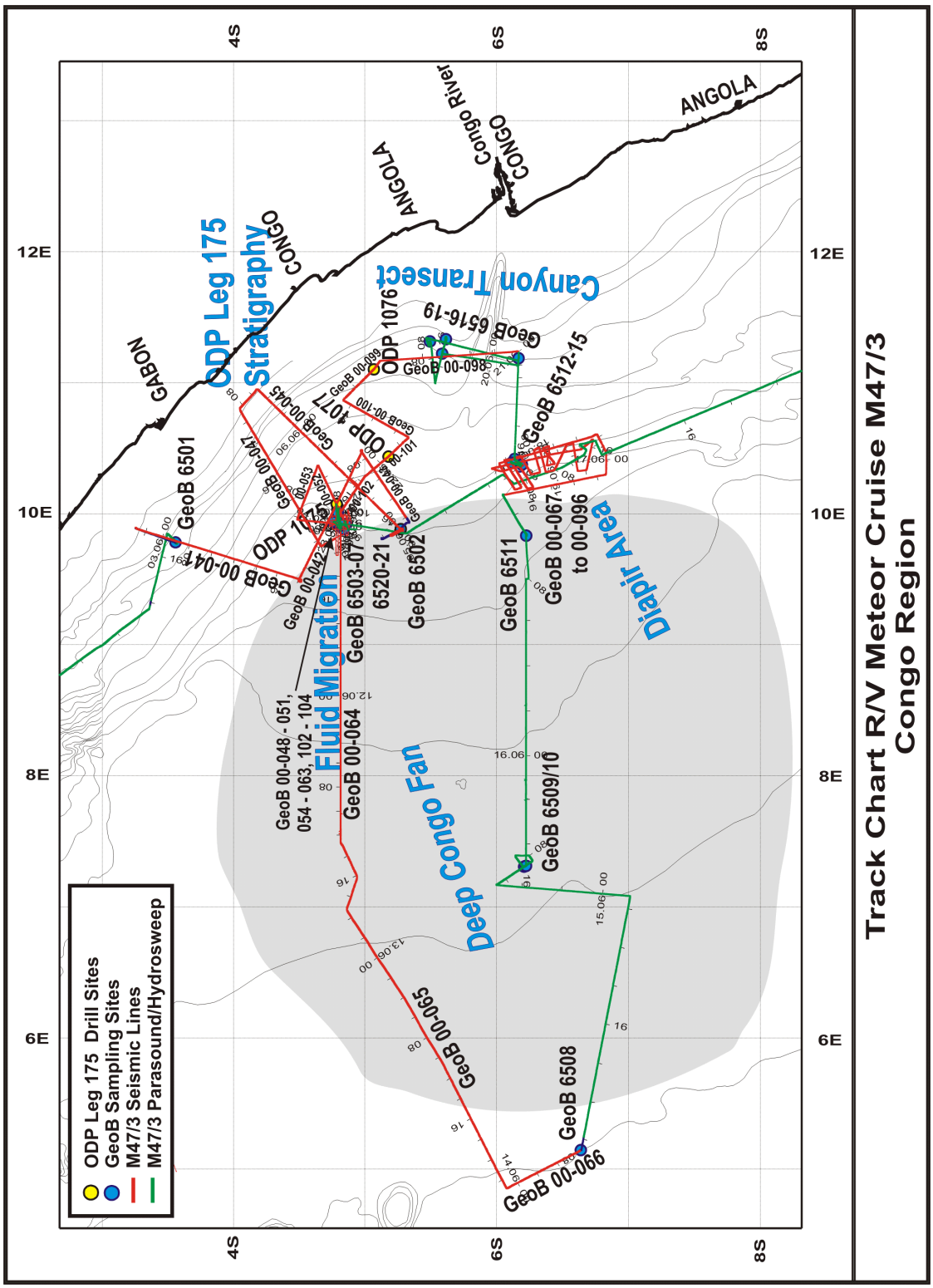

Fig. 3.7: Track Chart of R/V METEOR Cruise M47/3 in the Congo region with seismic lines (red), echosounder lines (green), GeoB coring sites (blue) and ODP drill sites (yellow).

Table 3.5: Multichannel Seismic Profiles of R/V METEOR Cruise M47/3

Profile	Start						End						Length	Shots
	Date	Time	Lat [° ' S]		Lon [° ' W]		Date	Time	Lat [° ' S]		Lon [° ' W]		km	
Northern Congo Margin and *Pockmark Area*														
GeoB00-041	03.06.2000	05:00	03	25.2	09	50.1	03.06.2000	18:27	04	30.6	09	28.8	127	6916
GeoB00-042	03.06.2000	18:54	04	30.1	09	30.1	04.06.2000	06:45	04	58.5	10	27.9	119	9231
GeoB00-043	04.06.2000	07:11	04	58.1	10	29.0	04.06.2000	14:51	05	19.7	09	55.9	73	5946
GeoB00-044	05.06.2000	02:41	05	08.9	09	48.8	05.06.2000	07:52	05	16.5	09	52.9	16	684
GeoB00-045	05.06.2000	08:27	05	16.4	09	52.8	06.06.2000	05:09	04	11.1	10	56.9	169	15162
GeoB00-046	06.06.2000	07:20	04	05.6	10	51.2	06.06.2000	08:35	04	02.8	10	48.1	8	496
GeoB00-047	06.06.2000	08:54	04	03.3	10	47.0	06.06.2000	22:31	04	39.9	09	45.2	133	10604
GeoB00-048	*06.06.2000*	*22:38*	*04*	*40.3*	*09*	*45.3*	*07.06.2000*	*00:30*	*04*	*49.0*	*09*	*50.2*	*18*	*1505*
GeoB00-049	*07.06.2000*	*00:50*	*04*	*50.3*	*09*	*51.0*	*07.06.2000*	*02:21*	*04*	*50.3*	*09*	*54.4*	*16*	*1208*
GeoB00-050	*07.06.2000*	*02:40*	*04*	*51.5*	*09*	*58.9*	*07.06.2000*	*04:07*	*04*	*51.3*	*09*	*50.0*	*16*	*1164*
GeoB00-051	*07.06.2000*	*04:38*	*04*	*52.3*	*09*	*51.0*	*07.06.2000*	*06:12*	*04*	*52.3*	*09*	*59.1*	*15*	*1267*
GeoB00-052	07.06.2000	23:36	04	51.2	09	55.4	08.06.2000	05:49	04	37.5	10	19.4	51	4776
GeoB00-053	08.06.2000	05:49	04	37.5	10	19.4	08.06.2000	09:43	04	29.7	09	59.2	40	3142
GeoB00-054	*09.06.2000*	*00:29*	*04*	*48.8*	*09*	*54.8*	*09.06.2000*	*01:50*	*04*	*48.8*	*10*	*02.4*	*14*	*963*
GeoB00-055	*09.06.2000*	*02:12*	*04*	*47.7*	*10*	*02.3*	*09.06.2000*	*05:55*	*04*	*47.8*	*09*	*41.8*	*38*	*3014*
GeoB00-056	*09.06.2000*	*06:30*	*04*	*46.8*	*09*	*42.0*	*09.06.2000*	*10:36*	*04*	*46.8*	*10*	*03.2*	*39*	*3244*
GeoB00-057	*10.06.2000*	*00:01*	*04*	*52.6*	*09*	*52.9*	*10.06.2000*	*01:25*	*04*	*52.9*	*09*	*52.9*	*13*	*1113*
GeoB00-058	*10.06.2000*	*02:00*	*04*	*46.1*	*09*	*54.9*	*10.06.2000*	*03:18*	*04*	*53.2*	*09*	*55.0*	*13*	*1060*
GeoB00-059	*10.06.2000*	*03:54*	*04*	*53.1*	*09*	*57.0*	*10.06.2000*	*05:11*	*04*	*45.9*	*09*	*57.0*	*13*	*1025*
GeoB00-060	*10.06.2000*	*05:53*	*04*	*46.0*	*09*	*59.0*	*10.06.2000*	*06:56*	*04*	*51.7*	*09*	*58.9*	*11*	*838*
GeoB00-061	*10.06.2000*	*07:01*	*04*	*51.8*	*09*	*58.4*	*10.06.2000*	*07:54*	*04*	*51.7*	*09*	*53.7*	*9*	*692*
GeoB00-062	*10.06.2000*	*08:29*	*04*	*42.3*	*09*	*55.3*	*10.06.2000*	*09:15*	*04*	*48.3*	*09*	*55.4*	*11*	*596*
GeoB00-063	*10.06.2000*	*09:38*	*04*	*48.8*	*09*	*55.4*	*10.06.2000*	*12:48*	*04*	*48.9*	*09*	*37.7*	*33*	*2672*
Congo Fan														
GeoB00-064	10.06.2000	13:15	04	48.9	09	35.4	12.06.2000	12:31	04	48.9	07	29.9	232	17857
GeoB00-065	12.06.2000	12:52	04	49.5	07	28.3	13.06.2000	22:49	06	04.6	04	51.3	321	13871
GeoB00-066	13.06.2000	22:49	06	04.6	04	51.3	14.06.2000	05:53	06	36.3	05	07.4	66	2656
Diapir Area														
GeoB00-067	16.06.2000	13:50	06	03.0	10	08.8	16.06.2000	22:45	06	49.8	10	18.0	88	7082
GeoB00-068	16.06.2000	22:45	06	49.8	10	18.0	17.06.2000	00:35	06	50.0	10	28.0	18	1442
GeoB00-069	17.06.2000	00:35	06	50.0	10	28.0	17.06.2000	02:12	06	46.0	10	36.1	17	1312
GeoB00-070	17.06.2000	02:12	06	46.0	10	36.1	17.06.2000	10:34	06	01.5	10	23.1	86	6682
GeoB00-071	17.06.2000	11:00	06	03.0	10	19.7	17.06.2000	13:15	06	08.8	10	11.1	19	1783
GeoB00-072	17.06.2000	13:15	06	08.8	10	11.1	17.06.2000	13:46	06	11.3	10	12.2	5	409
GeoB00-073	17.06.2000	13:46	06	11.3	10	12.2	17.06.2000	16:32	06	03.9	10	24.5	26	2205
GeoB00-074	17.06.2000	16:32	06	03.9	10	24.5	17.06.2000	16:53	06	05.7	10	24.9	3	264
GeoB00-075	17.06.2000	17:09	06	06.6	10	23.8	17.06.2000	19:45	06	13.8	10	11.9	26	2067
GeoB00-076	17.06.2000	19:45	06	13.8	10	11.9	17.06.2000	20:18	06	16.7	10	12.0	5	467
GeoB00-077	17.06.2000	20:18	06	16.7	10	12.0	17.06.2000	23:15	06	08.1	10	25.3	29	2310
GeoB00-078	17.06.2000	23:30	06	09.3	10	25.9	17.06.2000	23:48	06	10.7	10	26.4	3	223
GeoB00-079	18.06.2000	00:08	06	11.8	10	25.0	18.06.2000	01:55	06	15.9	10	18.2	15	1179
GeoB00-080	18.06.2000	01:55	06	15.9	10	18.2	18.06.2000	02:49	06	19.7	10	18.9	7	582
GeoB00-081	18.06.2000	02:49	06	19.7	10	18.9	18.06.2000	04:35	06	17.9	10	25.8	13	1029
GeoB00-082	18.06.2000	04:38	06	17.3	10	29.1	18.06.2000	05:04	06	18.9	10	30.1	3	336
GeoB00-083	18.06.2000	05:04	06	18.9	10	30.1	18.06.2000	07:13	06	26.3	10	20.0	23	1652
GeoB00-084	18.06.2000	07:13	06	22.5	10	19.2	18.06.2000	07:56	06	26.3	10	20.0	7	596

Table 3.5: (continued)

Profile	Start						End						Length	Shots
	Date	Time	Lat	[° ' S]	Lon	[° ' W]	Date	Time	Lat	[° ' S]	Lon	[° ' W]	km	
GeoB00-085	18.06.2000	07:56	06	26.3	10	20.0	18.06.2000	10:32	06	32.6	10	31.5	24	1938
GeoB00-086	18.06.2000	10:32	06	2.6S	10	31.5	18.06.2000	11:00	06	34.9	10	31.9	4	381
GeoB00-087	18.06.2000	11:00	06	34.9	10	31.9	18.06.2000	13:16	06	37.0	10	19.8	23	1806
GeoB00-088	18.06.2000	13:16	06	37.0	10	19.8	18.06.2000	14:00	06	40.7	10	20.0	7	577
GeoB00-089	18.06.2000	14:00	06	40.7	10	20.0	18.06.2000	16:53	06	43.1	10	33.3	25	2289
GeoB00-090	18.06.2000	16:53	06	43.1	10	33.3	18.06.2000	18:03	06	38.3	10	29.4	11	934
GeoB00-091	18.06.2000	18:03	06	38.3	10	29.4	18.06.2000	20:46	06	24.0	10	27.5	27	2173
GeoB00-092	18.06.2000	20:46	06	24.0	10	27.5	18.06.2000	21:32	06	23.7	10	30.9	6	590
GeoB00-093	18.06.2000	21:32	06	23.7	10	30.9	18.06.2000	22:00	06	21.2	10	30.0	5	392
GeoB00-094	18.06.2000	22:00	06	21.2	10	30.0	18.06.2000	23:37	06	28.0	10	23.2	18	1265
GeoB00-095	18.06.2000	23:37	06	28.0	10	23.2	19.06.2000	00:26	06	23.1	10	22.9	9	665
GeoB00-096	19.06.2000	00:26	06	23.1	10	22.9	19.06.2000	01:02	06	23.4	10	26.1	6	498
GeoB00-097	19.06.2000	01:02	06	23.4	10	26.1	19.06.2000	04:51	06	00.8	10	21.4	43	3044
GeoB00-098	21.06.2000	00:00	06	09.8	11	14.4	21.06.2000	11:15	05	07.2	11	10.0	116	6769
Congo Canyon														
GeoB00-099	21.06.2000	11:15	05	07.2	11	10.0	21.06.2000	15:19	04	50.1	10	51.9	46	2273
Northern Congo Margin														
GeoB00-100	21.06.2000	15:27	04	50.7	10	51.6	21.06.2000	21:05	05	19.9	10	35.0	62	3416
GeoB00-101	21.06.2000	21:05	05	19.9	10	35.0	22.06.2000	01:32	05	00.0	10	16.9	50	2674
Pockmark Area														
GeoB00-102	22.06.2000	01:32	05	00.0	10	16.9	22.06.2000	06:10	04	44.2	09	54.1	51	2689
GeoB00-103	22.06.2000	06:10	04	44.2	09	54.1	22.06.2000	06:43	04	44.0	09	56.8	5	300
GeoB00-104	22.06.2000	06:43	04	44.0	09	56.8	22.06.2000	08:05	04	51.2	09	53.5	15	837
Namibia Upwelling														
GeoB00-105	27.06.2000	12:19	19	20.4	10	10.1	27.06.2000	16:30	19	44.6	10	11.0	45	3346
GeoB00-106	27.06.2000	16:30	19	44.6	10	11.0	27.06.2000	23:00	19	43.1	10	50.0	68	4985
GeoB00-107	27.06.2000	23:00	19	43.1	10	50.0	28.06.2000	03:36	19	15.3	10	49.9	51	3862
GeoB00-108	28.06.2000	03:47	19	15.4	10	50.6	28.06.2000	12:07	19	45.5	11	30.0	89	6637
GeoB00-109	28.06.2000	12:07	19	45.5	11	30.0	28.06.2000	16:10	19	51.1	11	55.2	45	3116
GeoB00-110	28.06.2000	16:10	19	51.1	11	55.2	28.06.2000	23:42	20	09.9	11	13.1	81	6047
GeoB00-111	28.06.2000	23:42	20	09.9	11	13.1	29.06.2000	06:36	20	50.7	11	05.0	77	5456
GeoB00-112	29.06.2000	08:00	20	51.0	11	04.9	29.06.2000	21:25	21	18.9	12	29.7	155	10747
GeoB00-113	29.06.2000	21:25	21	18.9	12	29.7	30.06.2000	06:31	22	09.7	12	00.1	107	7171
GeoB00-114	30.06.2000	06:51	22	11.1	12	01.8	30.06.2000	15:22	22	39.8	12	49.8	98	6803
GeoB00-115	30.06.2000	15:32	22	40.8	12	49.4	30.06.2000	23:42	23	20.6	12	19.4	90	6121
GeoB00-116	30.06.2000	23:42	23	20.6	12	19.4	01.07.2000	08:24	23	49.8	13	09.6	101	7046
GeoB00-117	01.07.2000	08:24	23	49.8	13	09.6	01.07.2000	15:53	24	24.5	12	40.0	81	5795
GeoB00-118	01.07.2000	16:00	24	25.2	12	40.0	01.07.2000	16:48	24	29.9	12	40.1	9	632
GeoB00-119	01.07.2000	16:58	24	30.5	12	40.9	02.07.2000	01:40	25	00.0	13	30.0	99	6950
GeoB00-120	02.07.2000	01:40	25	00.0	13	30.0	02.07.2000	10:12	25	34.1	12	58.6	82	6656
GeoB00-121	02.07.2000	10:12	25	34.1	12	58.6	02.07.2000	12:00	25	46.9	12	59.1	24	882
Total													**3863**	**271088**

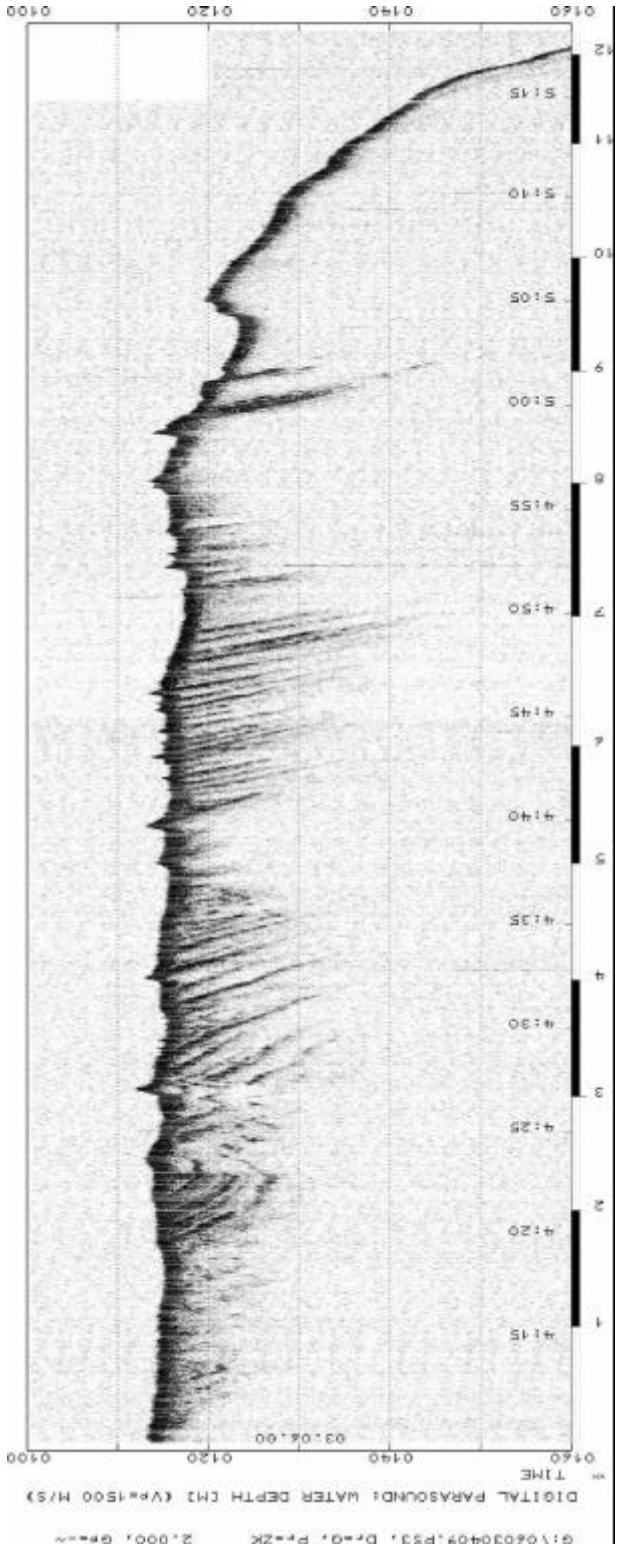

Fig. 3.8: Digital PARASOUND line from the Gabon shelf showing exposed strata at the level of the glacial sea level lowstand. Recent sedimentation is absent.

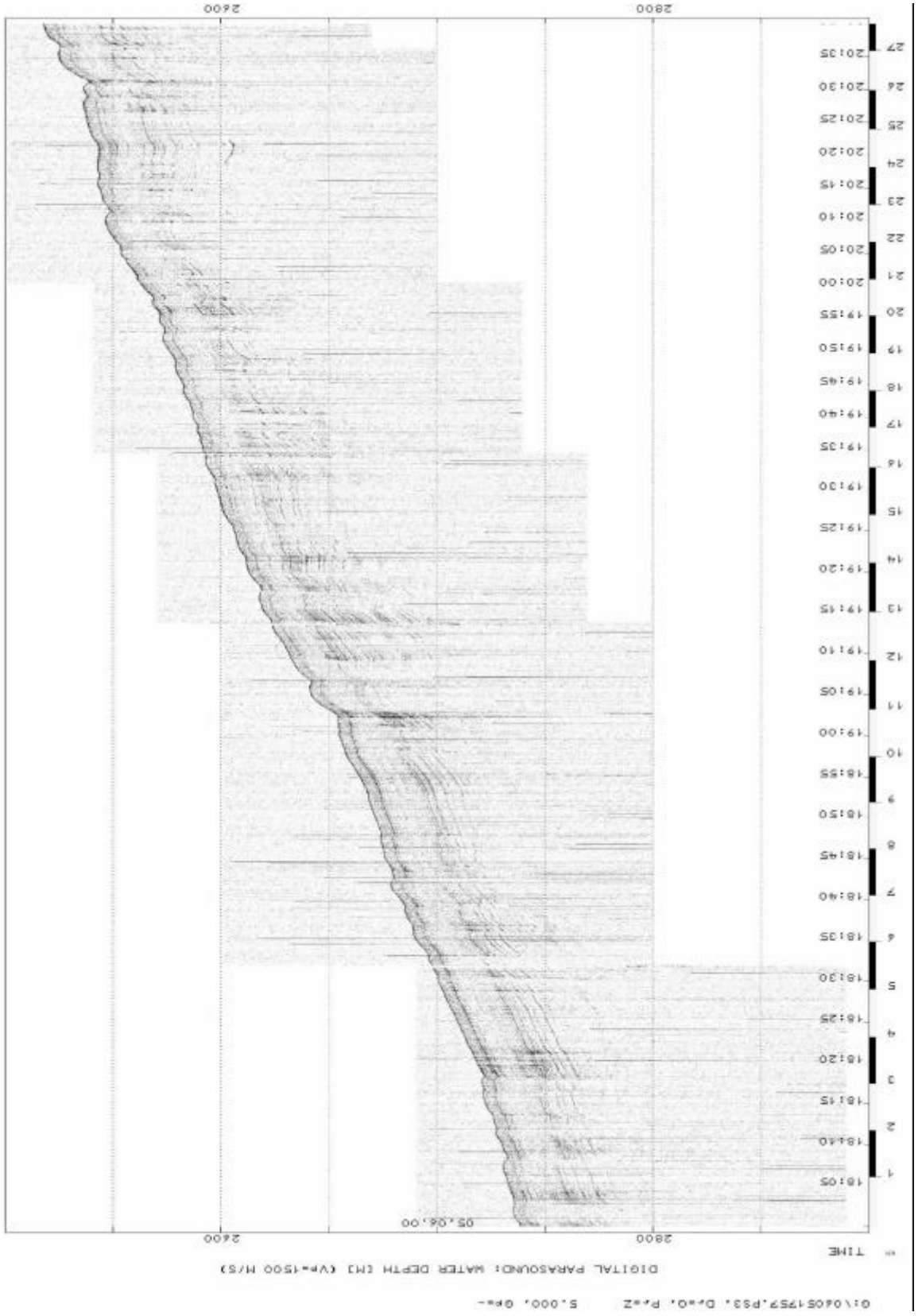

Fig. 3.9: Digital PARASOUND example along seismic line GeoB 00-045. The example reveals intense small scale sediment tectonics and faulting. Reflection amplitudes are low to moderate, with occasional anomalies near faults.

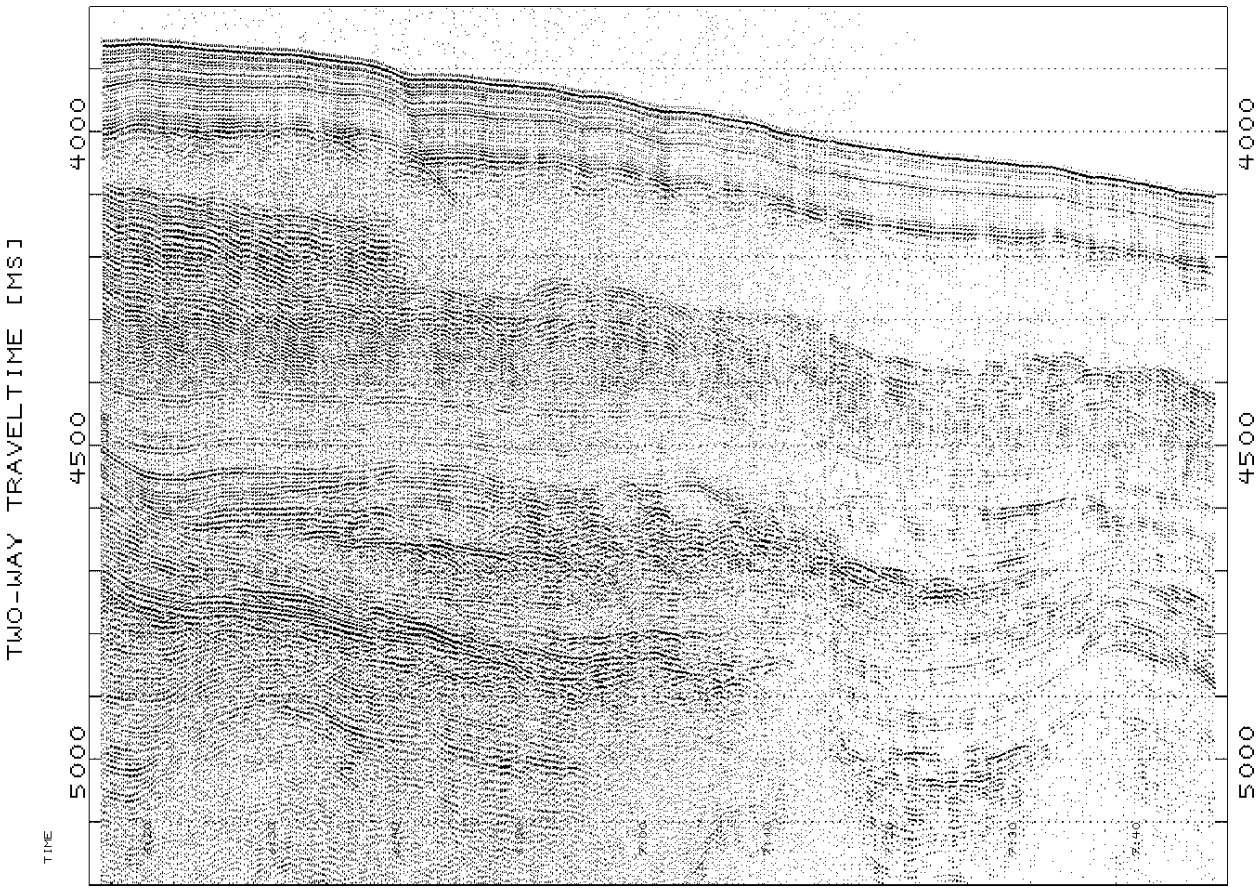

Fig. 3.10: Multichannel seismic example as part of line GeoB 00-047, shot with GI Guns. The vertical sequence of pronounced layering and transparent units indicates episodic mass wasting processes as debris flows in a hemipelagic realm. Undulating deeper layers may be caused by salt diapirism.

Deep Congo Fan

Sedimentation in the Congo Fan is dominated by the input of massive turbidites, originating from the mouth of the Congo Canyon in 3500 m water depth. At this depth a transition is observed from undisturbed, layered sediment to depositional lobes and channel levee systems. A long seismic line was shot, complimentary to another long line acquired during R/V SONNE Cruise SO 86, to study this transition. In particular, we were interested in the role of salt diapirism in the extension of the Angola escarpment, which may also have controlled fan deposition as the transition to hemipelagic sedimentation through local uplift and subsidence.

Dedicated sediment cores were taken in the vicinity of an active channel-levee system to collect material, which directly links to the coarse river input, carrying signal of continental climate and erosion (Fig. 3.12)

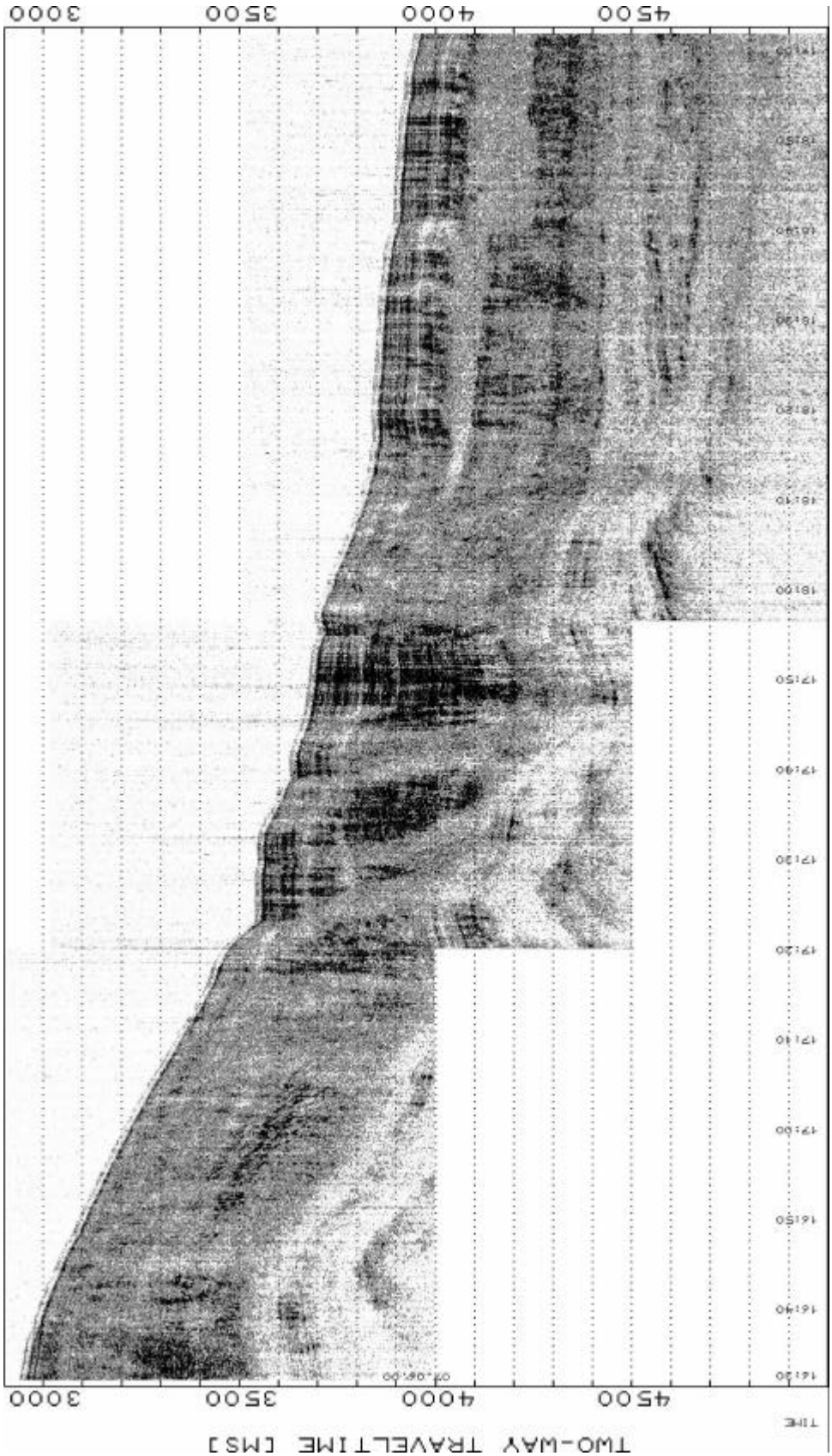

Fig. 3.11: Multichannel seismic example as part of line GeoB 00-047, shot with watergun. The example reveals pronounced lateral amplitude variations, structural disturbances, intercalated debris flows, which are related to slope instability, gas and fluid migration and postsedimentary and early diagenetic overprint.

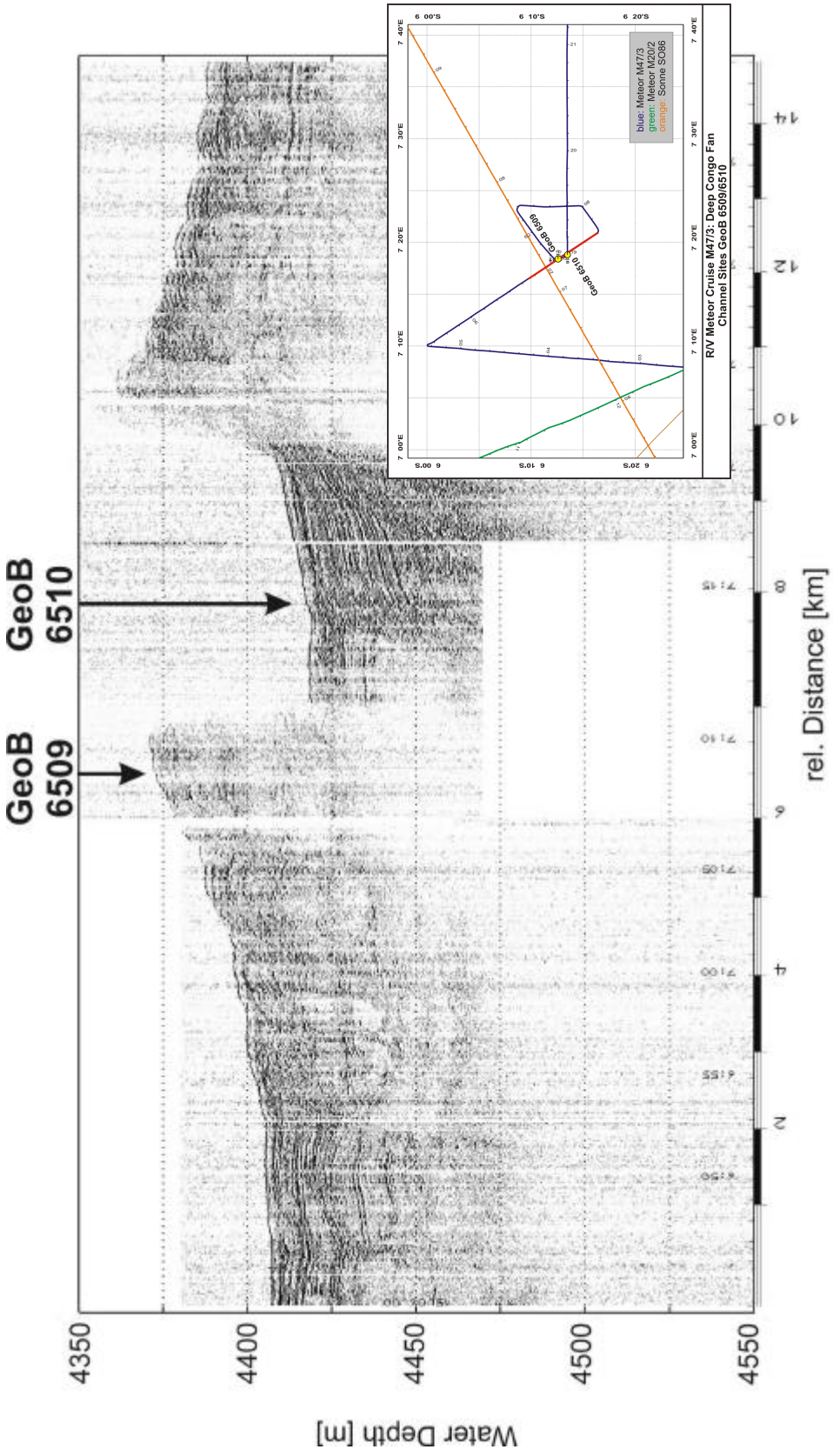

Fig. 3.12: Digital PARASOUND example from the deep Congo Fan in the vicinity of an active channel segment. Locations of coring sites GeoB 6509 and 6510 are indicated on the profile and on the insert map with cruise track.

Pockmark Area

A particular interest of this METEOR Cruise was related to fluid migration. Selected seismic and echosounder profiles were acquired in a relatively small area in water depths around 3000 m, where during the R/V SONNE Cruise SO 86 strong indication of fluid and/or gas migration was found. Criteria were: pronounced vertical and lateral amplitude variations, columnar zones of acoustic blanking, pockmarks at the sea floor, correlation between salt diapirs and high amplitude reflections above, clear relationsship between small scale and large scale faults and anomalous reflector amplitudes.

The surveys in the fluid migration area (Fig. 3.13; see also Fig. 3.7) aimed at the confirmation of previous sparse observations, and the collection of additional echsounder and seismic lines to understand the structural setting on a larger scale. It was e.g. so far unclear, what type of structure (circular or linear) may be associated with the assumed fluid venting, and whether multiple occurrences of vent sites can be expected.

In bathymetric data we could identify several pockmarks in the area, some more than 20 m deep and some kilometers wide (Fig. 3.14). All these features, which were subsequently named and sampled, provided indications for more or less active venting, as through the collection of carbonate concretions, living worms, mussle fields or massive gas hydrates. Furthermore, several linear, N-S trending structures are found at the surface within and east of the pockmark field, another linear structure also in the west. The relationship of these morphologic features to the overall tectonic regime is not yet clear, but we expect sediment tectonics to be involved in the creation of fluid pathways.

Figure 3.15 across 'Banana Hole' shows a watergun seismic record (brute stack), which images in great detail the subsurface amplitude anomaly beneath the pockmarks. The columnar blanking zone reaches deeply into the sea floor, which may hint to a possible source for upflowing gas or fluids in some hundred meters sub-bottom depth. All pockmark structures are related to columnar blanking zones beneath, imaged in all seismic frequencies applied. Characteristic of sediments in the vicinity of the pockmark field is a unit of high reflection amplitudes in appx. 50 m sub-bottom depth, as is clearly seen in the digital PARASOUND example in Figure 3.16. But there we can also observe that at two locations near the morphological anomalies the high amplitude zones come closer to the surface. Furthermore, high amplitudes often appear near fault zones or disturbances, whereas otherwise average amplitudes in the sediment column within the upper 100 m are very low, reflecting a typical signature of opal-rich and water-rich sediments. High amplitude zones appear limited in lateral extent, and it may well exist a direct relationship to fluid/gas migration.

Below 3350 m water depth, amplitudes within this unit increase significantly, and the morphology of these reflectors is rough (Fig. 3.17). Steep incisions are also found, which can be traced to the sea floor. It can be speculated that a fan depositional lobe is buried by hemipelagic sediments, but it is also possible that mass wasting is responsible for the complex morphology, associated with a gas, fluid or gas hydrate charge in the deeper unit.

As the most spectacular result of geologic sampling, gas hydrates had been found at several sites, either in massive form or disseminated in the sediment. At Site GeoB 6520 massive gas hydrate of several meters thickness was found beneath a hemipelagic sediment cover of appx. 5 meters. A second coring attempt provided appx. 50 cm gas hydrate from the sea floor without sediment cover.

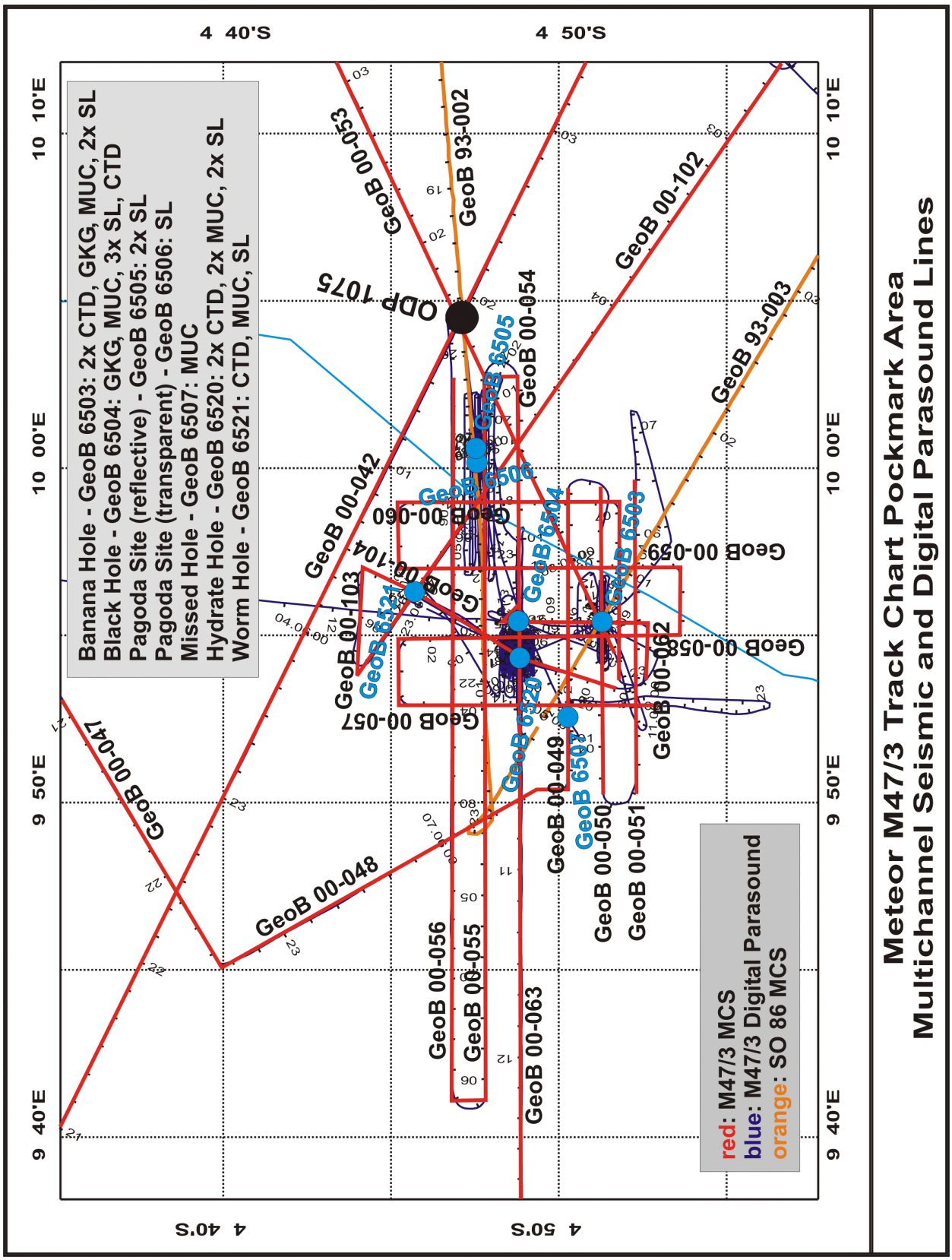

Fig. 3.13: Cruise track of R/V METEOR Cruise M47/3 in the pockmark area with echosounder (blue) and seismic lines (red), seismic lines of SONNE Cruise SO 86 (orange), coring sites GeoB 6503 through 6507, 6520 and 6521 (see also insert text for applied sampling devices) and ODP Site 1075.

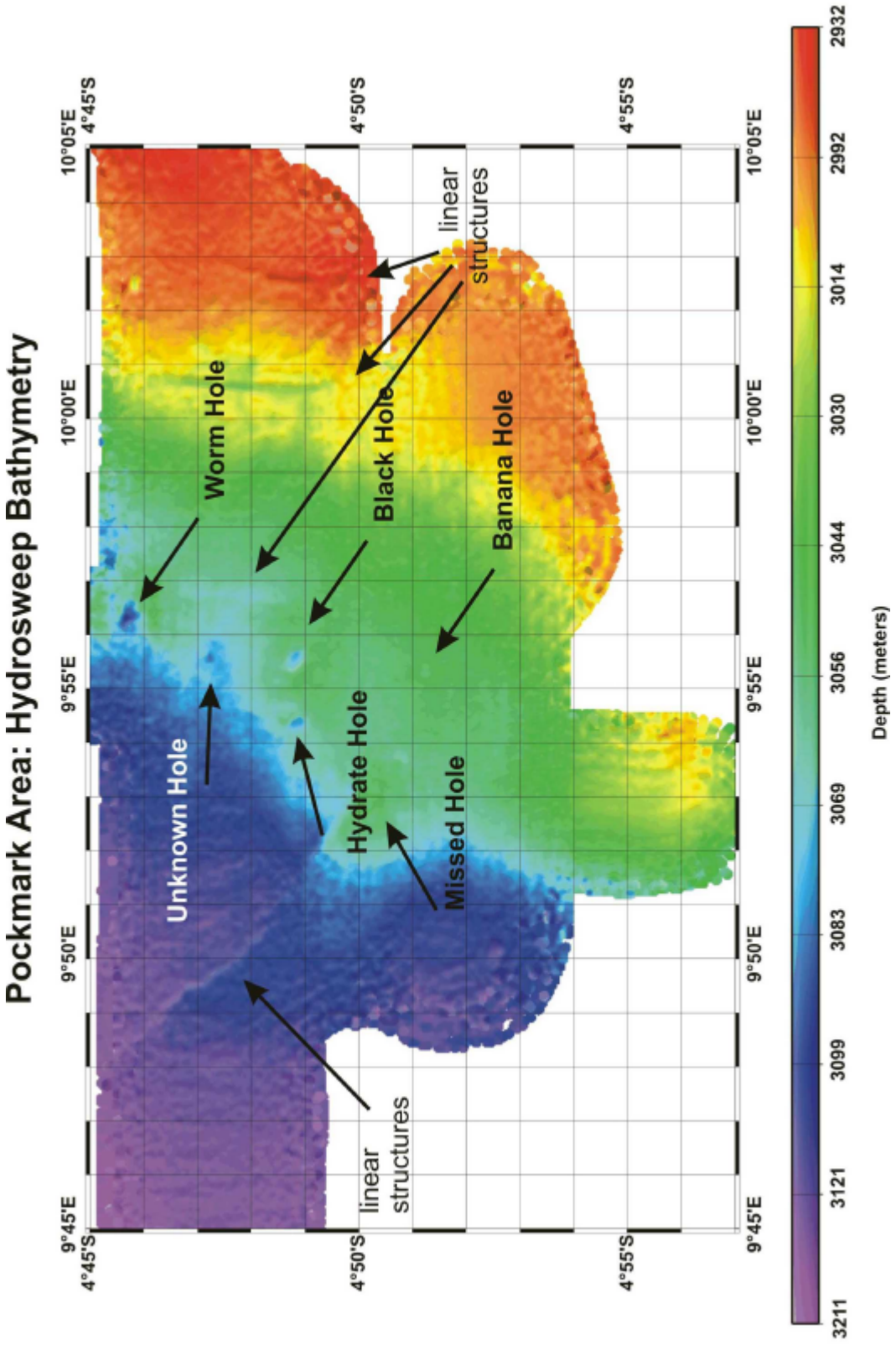

Fig. 3.14: Bathymetry of the pockmark are with names of morphologic or subsurface anomalies (pockmarks='Holes') and with linear morphologic features.

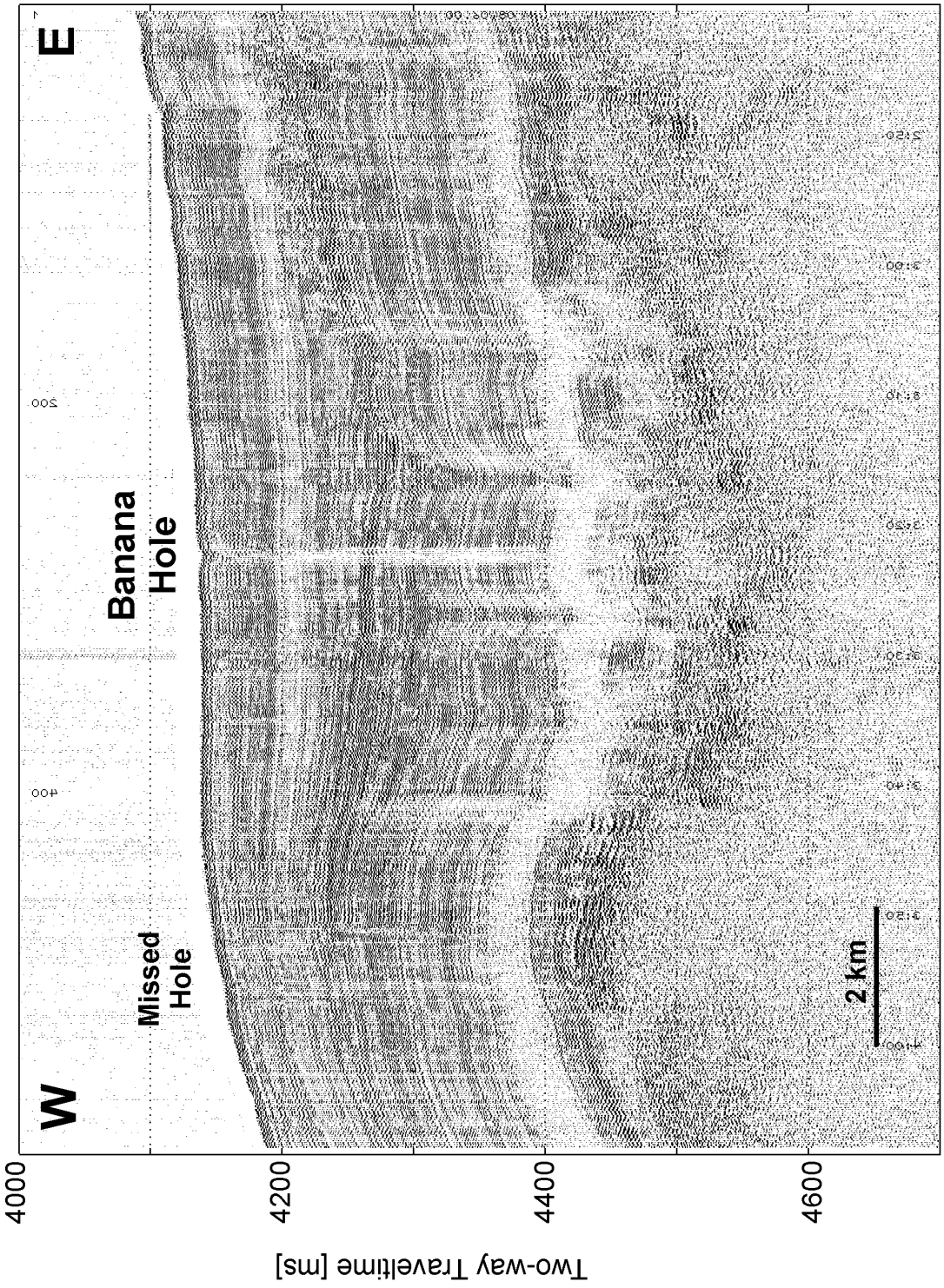

Fig. 3.15: Multichannel seismic lines GeoB 00-050, shot with watergun, across 'Banana Hole'. Pronounced columnar blanking zones can be identified beneath the pockmark, connecting the sea floor to a low-amplitude band at 250-300 ms TWT.

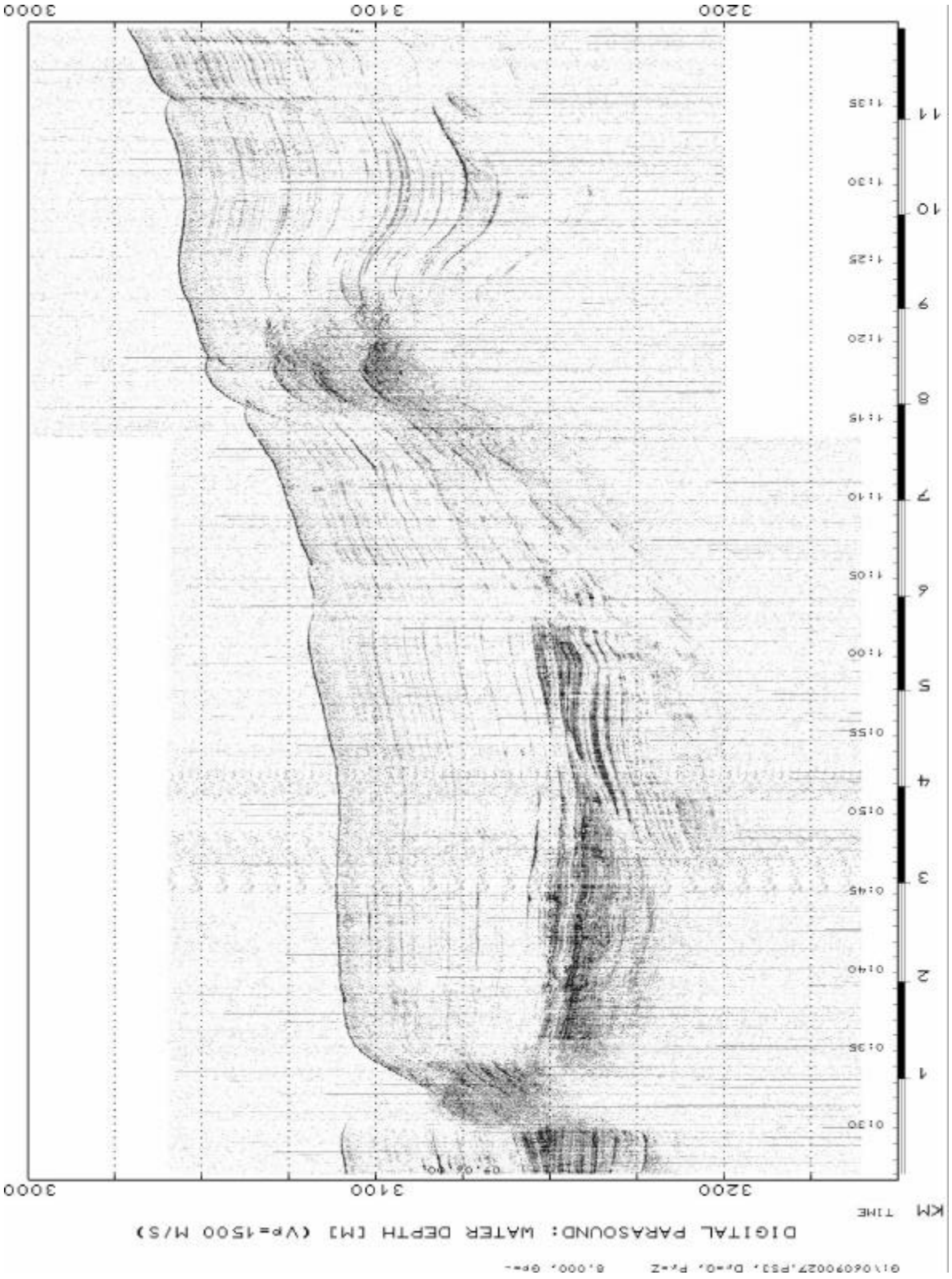

Fig. 3.16: Digital PARASOUND example from the pockmark area, indicating pronounced amplitude variations at depth and near the surface at pockmarks and near fault zones.

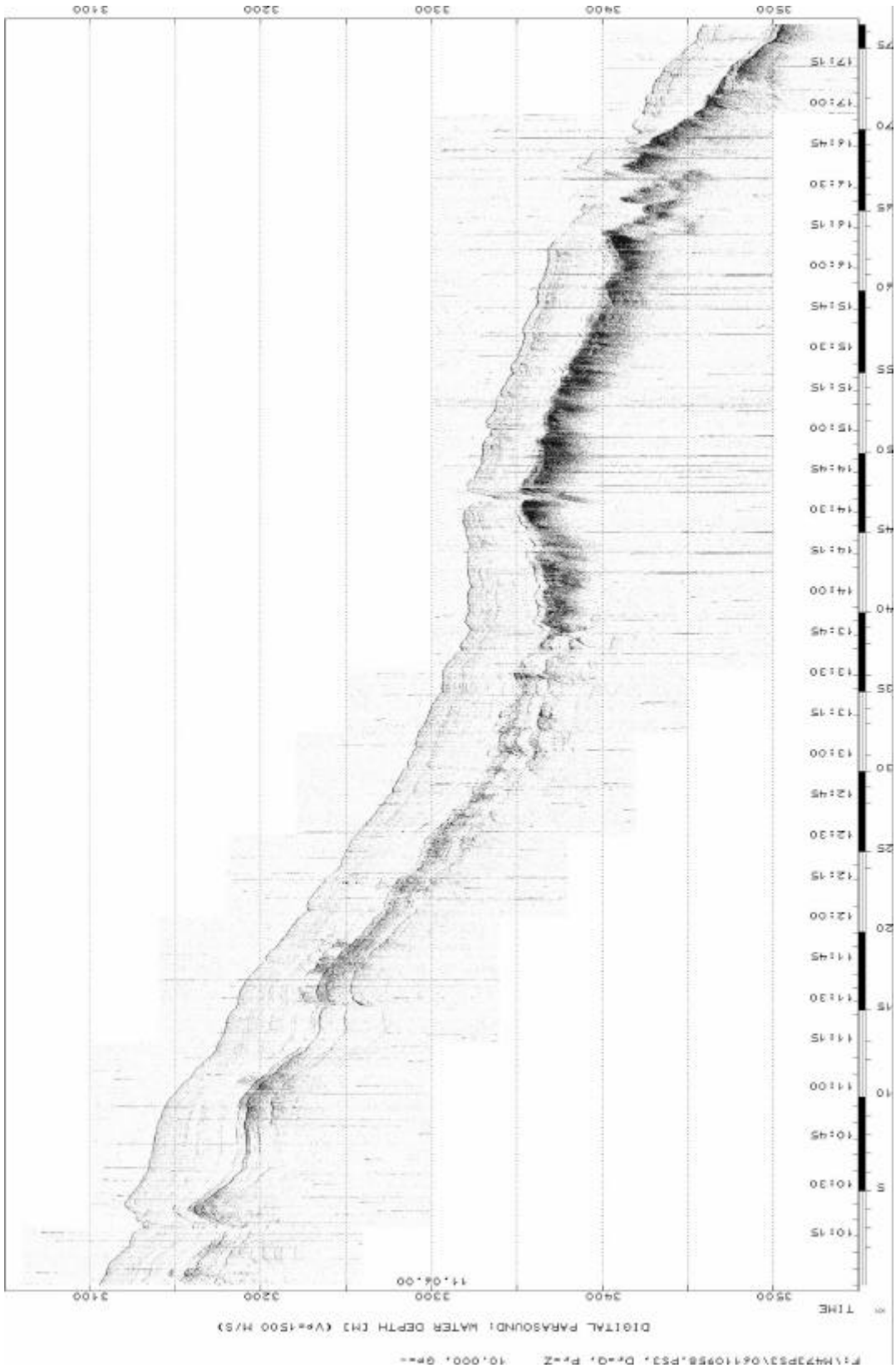

Fig. 3.17: Digital PARASOUND examples downslope of the pockmark area showing narrow incisions, probably representing buried channels. In addition, a pronounced increase in reflection amplitude is observed beyond km 40.

Figure 3.18 shows the digital PARASOUND record, which reveals at the coring location GeoB 6520, that compared to the surroundings, reflection amplitudes are very high near the sea floor. These amplitudes are comparable to amplitudes within the reflection band in 50 m sub-bottom depth elsewhere, and it may be speculated that a higher content of gas hydrate is responsible for these amplitude anomalies. Lateral inhomogeneities make it very difficult to directly relate these physical parameters to the occurrence of hydrate or gas, although increased gas content is more likely responsible for attenuation, low reflectivity and columnar blanking. If hydrates can be imaged from the distribution of high amplitudes, the network of digital PARASOUND lines (Fig. 3.19), combined with seismic data from the survey area around the pockmark field, may be used to locate the upper limit of hydrate occurrence in the sediment column and to quantify the amount of hydrate in the formation. Details about this relationship await further onshore research on seismic data and geologic and geochemical samples.

Diapir Area

As a second research activity related to fluid migration, we selected a region south of the Congo Canyon for seismic surveying and sampling. Here, fan deposition is absent and salt diapirism is responsible for significant uplift. In such an environment, major faulting is likely to open pathways for fluid and gas migration, as is well known from extensive surface sampling campaign of the oil industry, selecting specifically fault zones in the search of oil.

The main objective of the 3.5 day survey (Fig. 3.21) was to collect reference data for a comparison to the pockmark area, where conditions both with respect to salt tectonics and to sediment accumulation are very different. Amplitude anomalies in the surface sediments and their relationship to fault zones were a specific target, but also the role of small scale tectonics, small scale morphology, presence or absence of pockmarks. Whereas in the region north of the Congo Canyon units with assumed gas accumulations are found in some hundred meters sub-bottm depth as potential sources for upflow zones, these seemed to be absent in the diapir area. Consequences of these differences shall be studied by a systematic bathymetric, echosounder and seismic survey, complimented by sampling at 4 coring sites to search for active vent locations.

The bathymetry near the Angola escarpment is very complex with several coast parallel ridges and uplifted smaller plateaus (Fig. 3.22). Seismic GI Gun line GeoB 00-070 (Fig. 3.23) reveals the pronounced internal variability in structure and amplitude on scales of a few kilometers only. Without further processing and spatial analysis it will be difficult to understand the tectonic setting, but it is evident from both the GI Gun and the watergun data (Fig. 3.24) that the original layering and reflectivity in the upper sediment column, mainly derived from hemipelagic sedimentation and turbidites, over overprinted and modified by subsequent processes, as there may be: slumping, gas charge, gas initiated attenuation, fluid upflow, faulting.

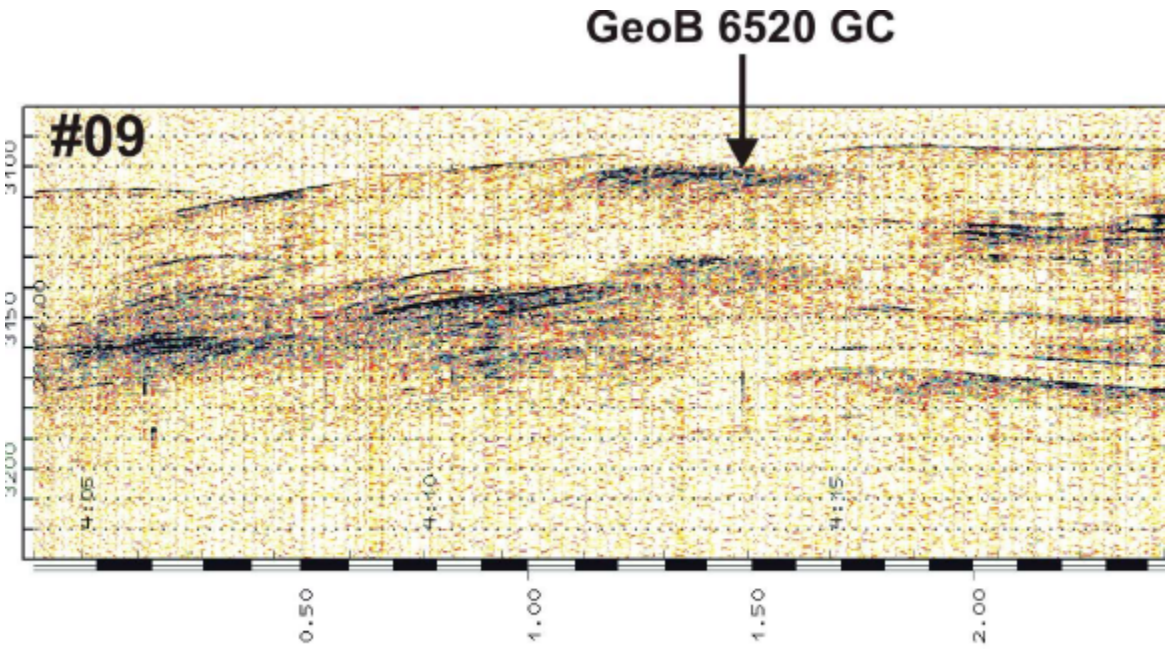

Fig. 3.18: Digital PARASOUND line across gas hydrate site GeoB 6520 ('Hydrate Hole').

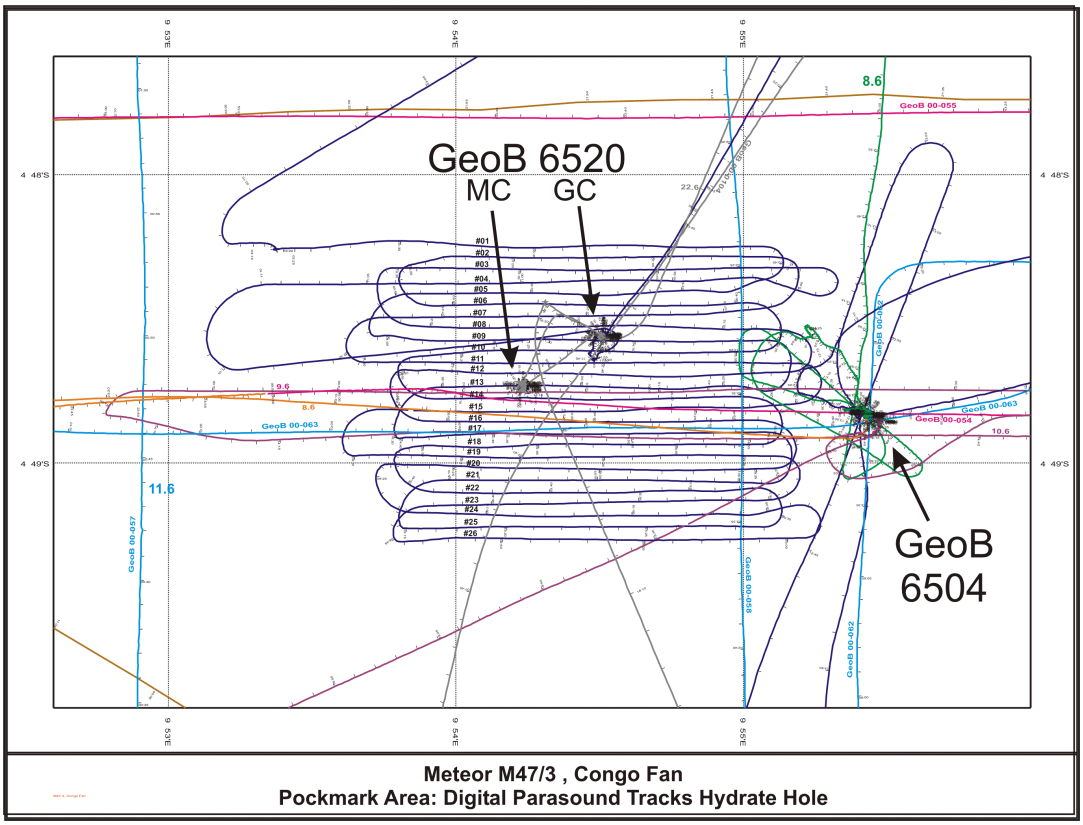

Fig. 3.19: Grid of echosounder survey lines in the vicinity of the gas hydrate site GeoB 6520 ('Hydrate Hole').

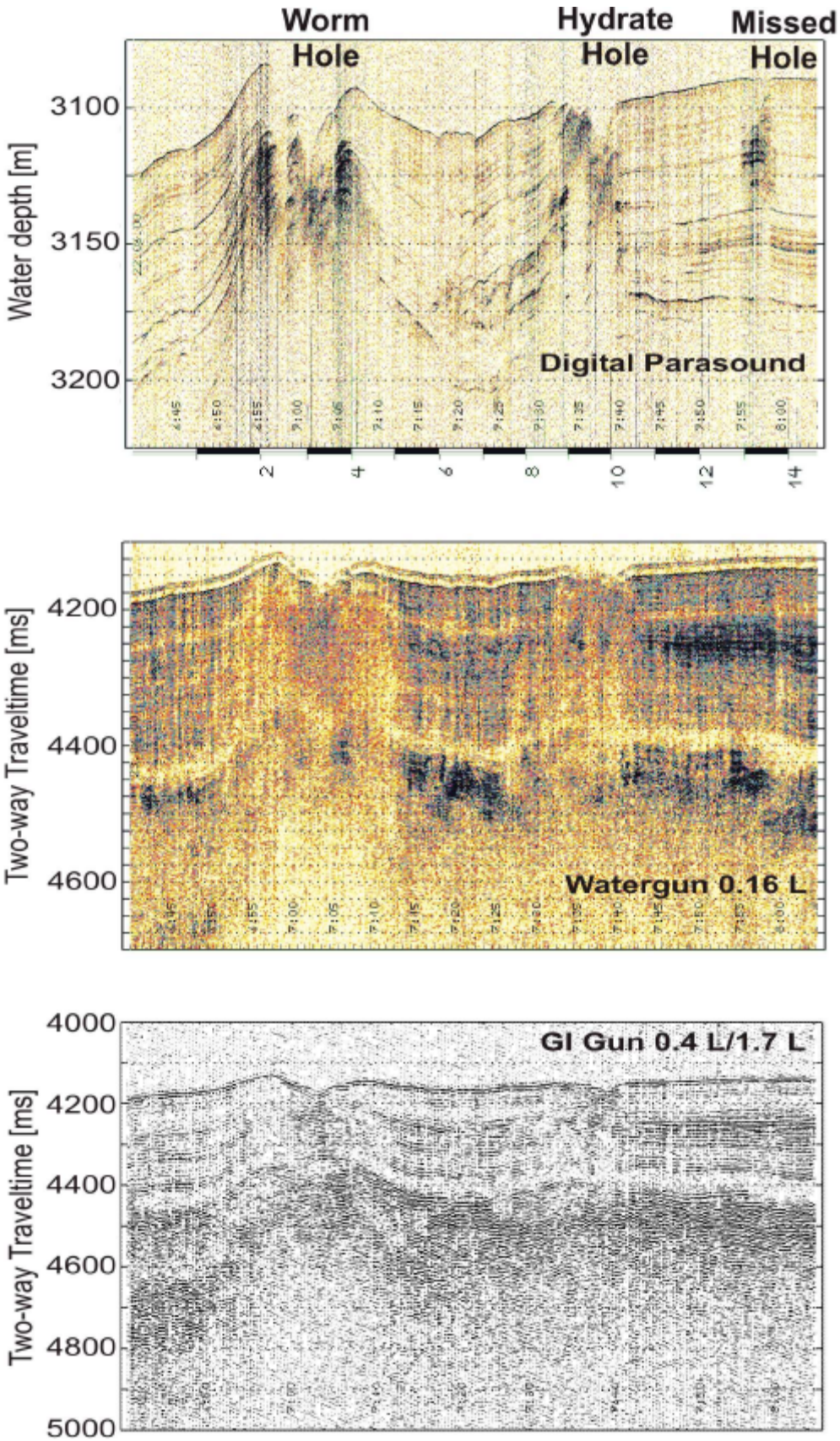

Fig. 3.20: Comparison of different seismic data sets across pockmarks and the gas hydrate site GeoB 6520. Interesting is the appearance of the columnar blanking zone beneath 'Worm Hole' and 'Hydrate Hole', where amplitudes/reflectivity varies significantly as a function of signal frequency.

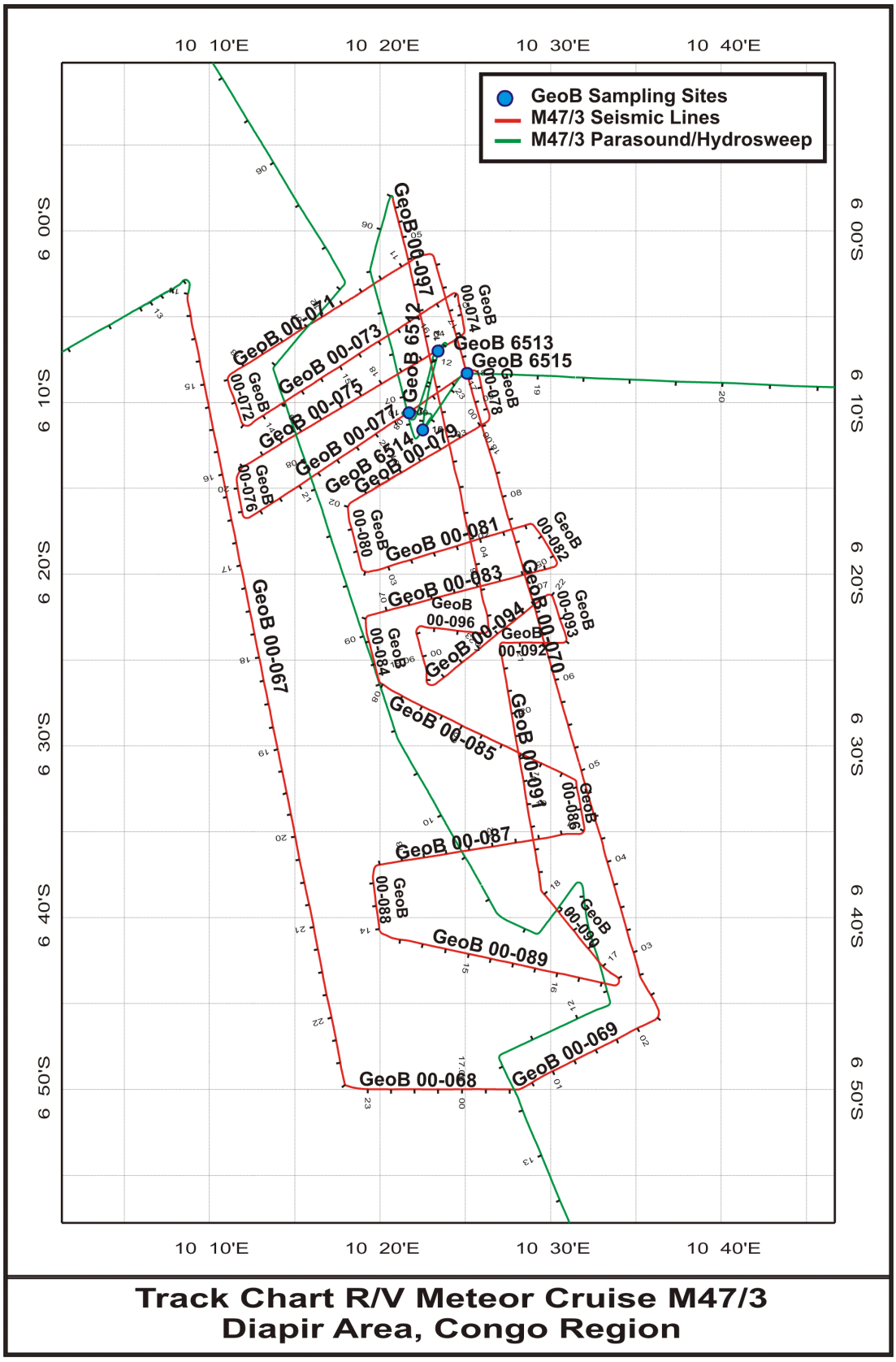

Fig. 3.21: Track Chart of R/V METEOR Cruise M47/3 seismic survey and sampling in the diapir area.

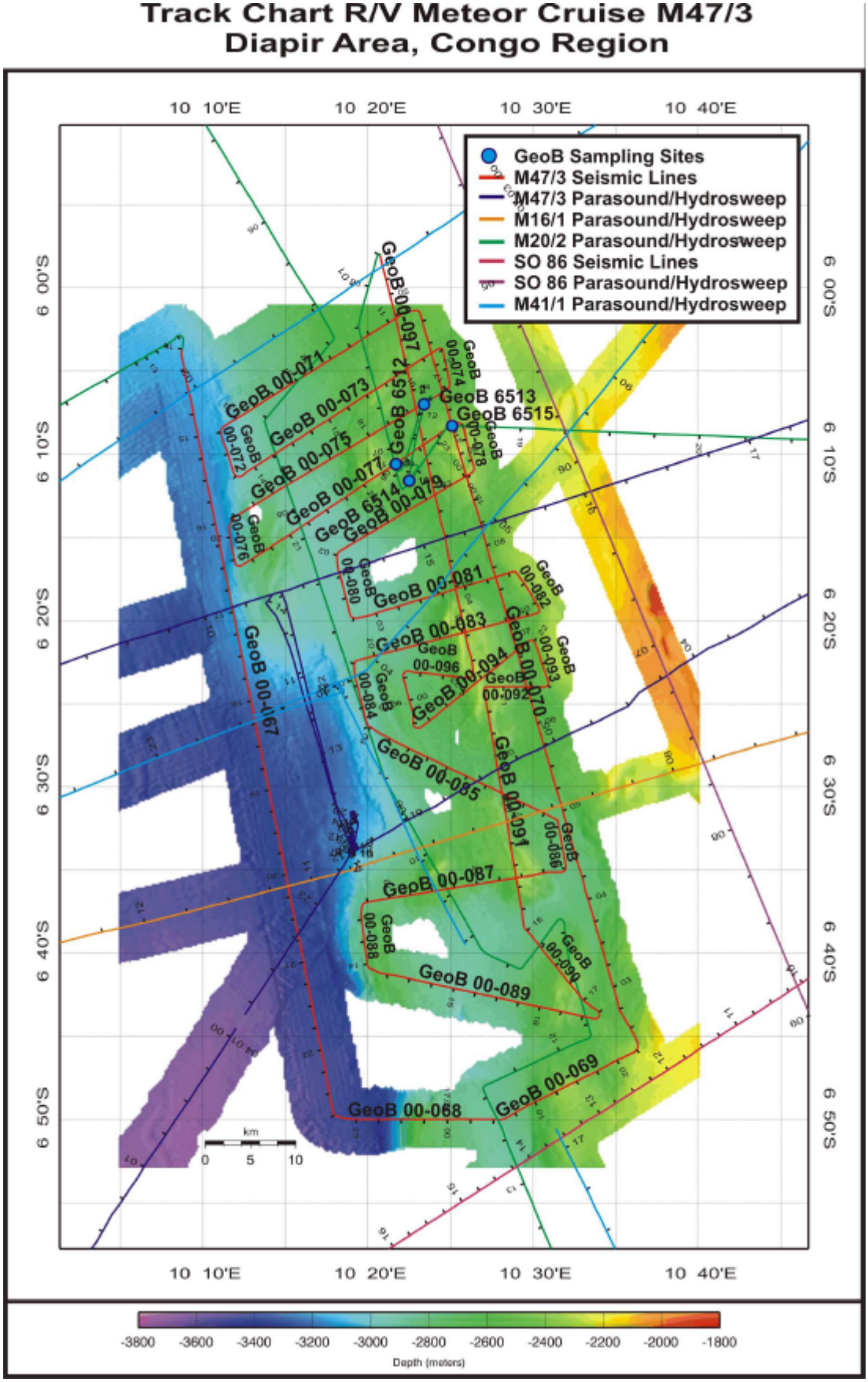

Fig. 3.22: Bathymetry of the diapir area, including data from previous Cruises M16/1, M20/2, M41/1 and SO 86.

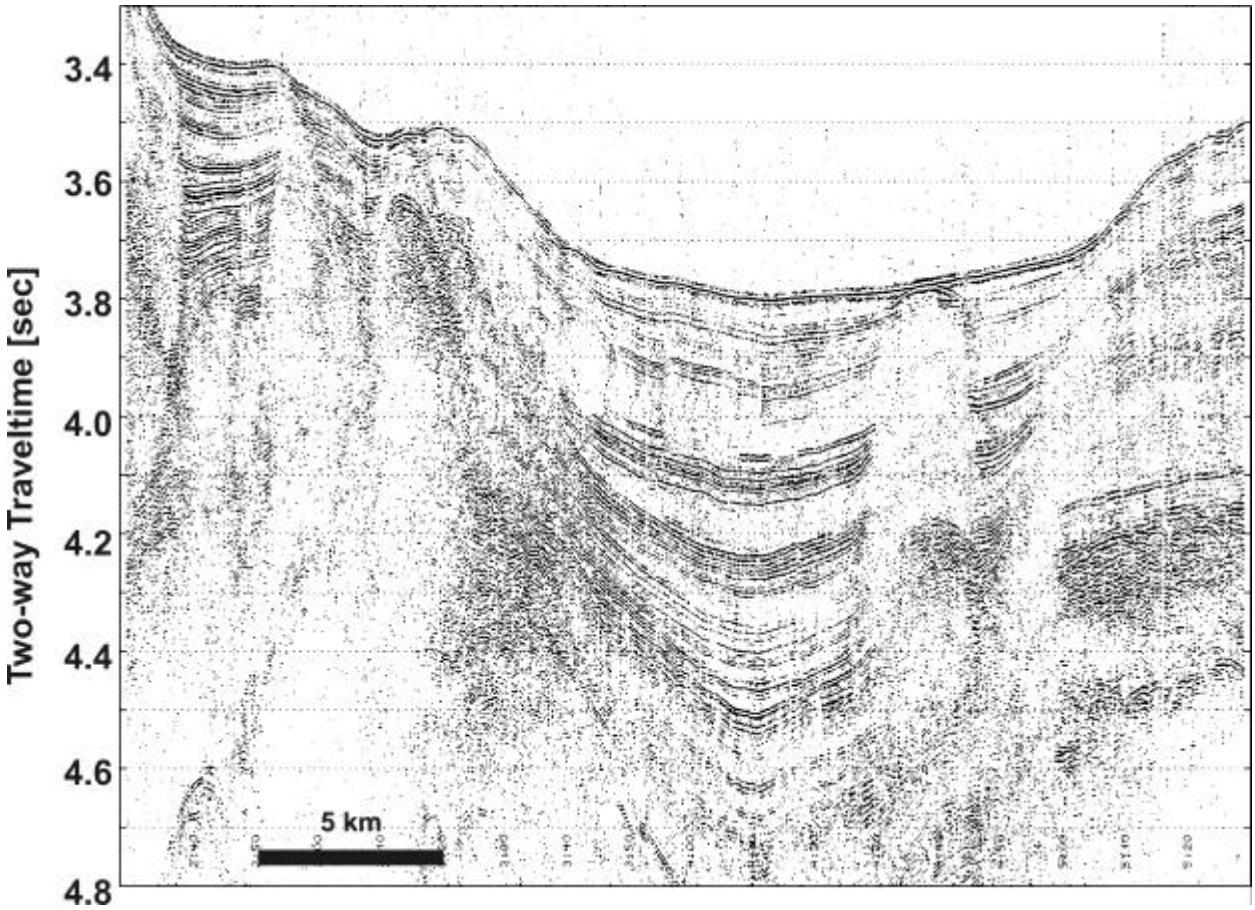

Fig. 3.23: Seismic line GeoB 00-070, shot with a GI Gun. Diapiric structures and significant amplitude anomalies are present, indicating fluid migration and gas accumulation.

Namibia Upwelling

As the last part of the research program, an exclusively multichannel and echosounder survey was carried out further south on the way to the final destination Walvis Bay. Between Walvis ridge at 18°40'S and 25°40'S off Lüderitz, seismic lines were shot in water depths between 500 m and 2500 m, including ODP Leg 175 drill sites 1081 through 1084. All of these drill sites provided samples of 'dolomitic layers', which represent lithified or coarse grained intervals. From the drilling results in comparison with the original pre-site survey data for the ODP leg, collected during R/V SONNE Cruise SO 86 and R/V METEOR Cruise M34/1, we observed, that such anomalous layers seemed to be restricted to a certain water depth range. Furthermore, the knowledge about a stronger bottom water current with a core in 1200 to 1700 m water depth, which had also caused small scale mud waves, may be also responsible for a distinct distribution of such dolomitic layers.

The survey lines shown in Fig. 3.25 (see also Table 3.5) were chosen to collect high-resolution data, which are suitable to resolve layer of sub-meter thickness, complimenting the existing data to map out the dolomitic layers. Correlation with downcore logs shall be carried out to link drilling data to reflectors or reflector bands. This work will be carried out onshore after full processing of the data.

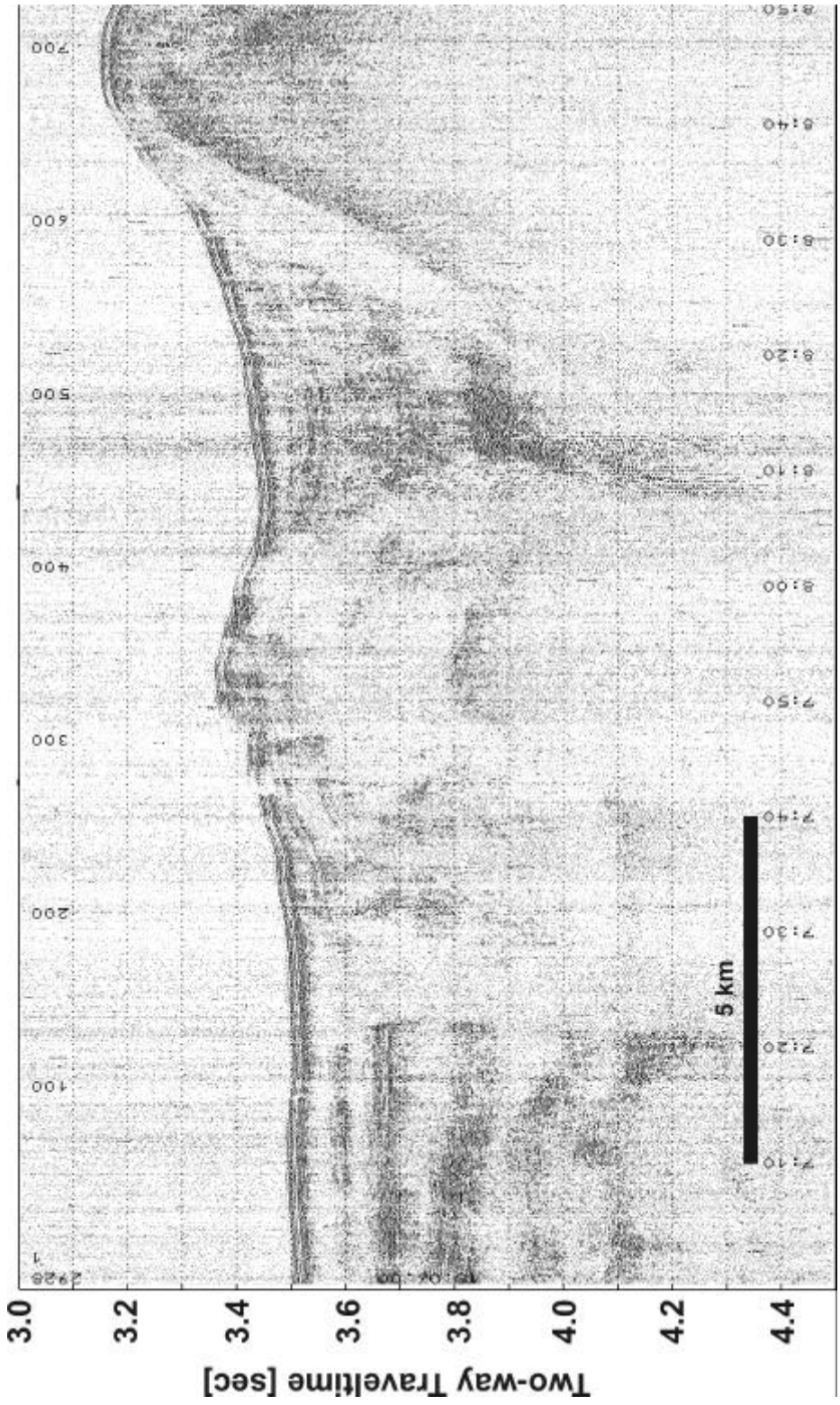

Fig. 3.24: Seismic line GeoB 00-077, shot with a watergun. Pronounced lateral amplitude variations indicate fluid migration, gas accumulations and perhaps gas hydrates.

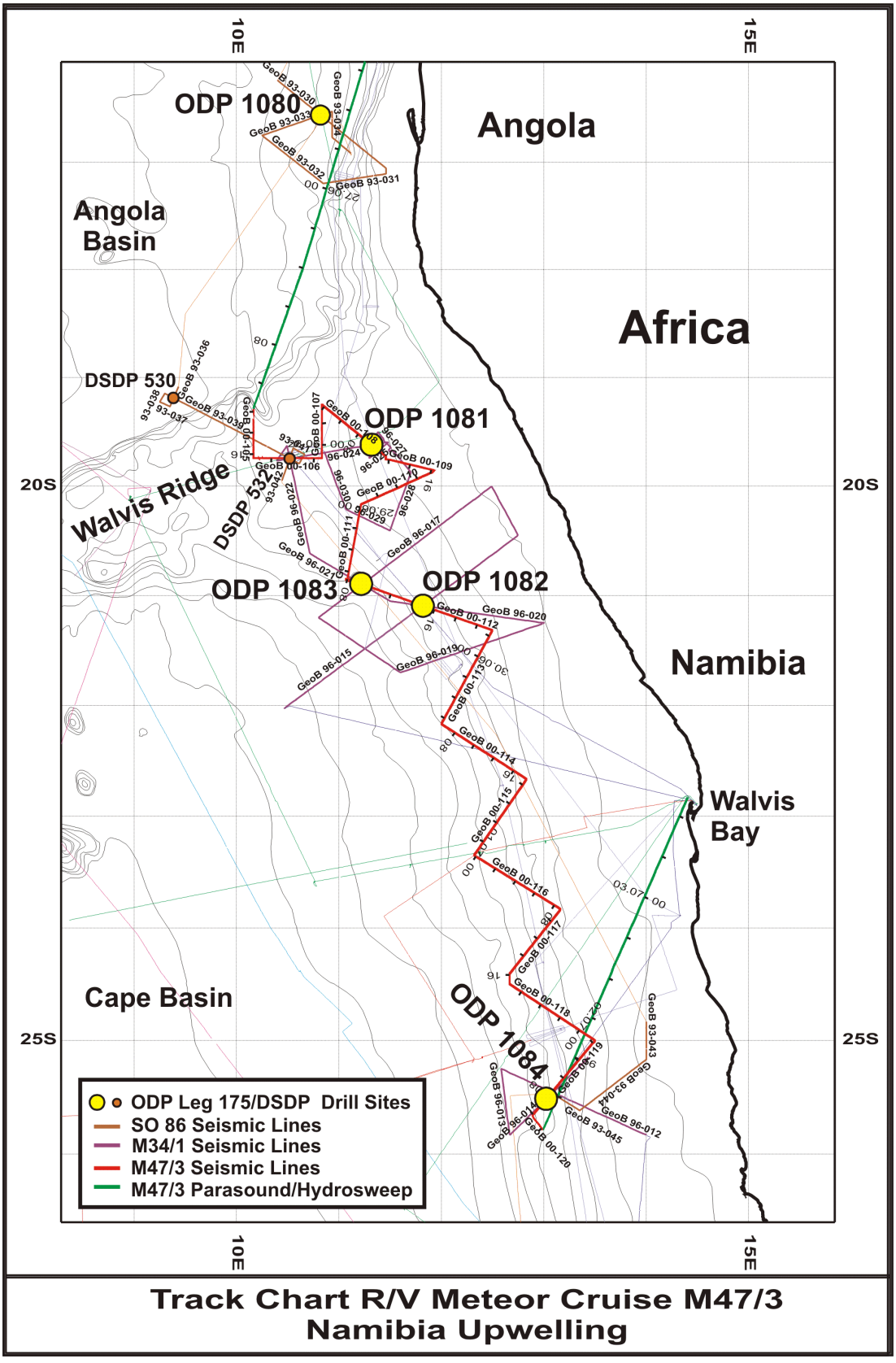

Fig. 3.25: Track chart of multichannel seismic survey (red line) during R/V METEOR Cruise M47/3 in the Namibia Upwelling System. Additional survey lines from previous cruise are added. ODP drill sites are plotted as yellow dots, DSDP sites as red dots.

3.4.2 Marine Geology

(D. Grotheer, B. Meyer-Schack, U. Rosiak, R. Schneider, S. Schulte, G. Versteegh)

3.4.2.1 Sediment cores

On this cruise we used multicorer, box-corer and a gravity corer in order to recover surface and late Quaternary sediments from the continental slope north of the Zaire (Congo) Fan and from the fan itself, north and south of the central deep-sea canyon. During M47/3 we carried out 21 sampling stations at water depths between 680 and 4460 m. The coring locations and related water depths are given in the station list (Tab. 3.6). This table also shows the devices used for our program at all stations and the core lengths recovered.

Gravity Core Sampling

With the gravity corer sediment cores between 4.86 and 15.94 m core length were taken at 19 stations. During M47/3 altogether 200 m of fan sediments were recovered with this device. Before using the coring tools, the liners were marked with a straight line lengthwise, in order to be able to sample the core segments afterwards in the same orientation, in particular for paleomagnetic purposes. When the core was retrieved on deck, the core liners were cut into 1-m segments, closed with caps at both ends and inscribed, following standard rules of GeoB core repository protocols.

All cores except those from the diaper field in the southern part of the fan (stations GeoB 6512 to 6514) were cut along-core in two half pieces: one Archive and one Work half. The sediments were described, smear-slide samples were taken from distinctive layers and spectrophotometric measurements were carried out on the Archive half (see chapter 3.4.3.2), which was stored in a cool room at +4° C. Two parallel series and a third series of syringe samples (10 ccm) were taken from the Work-Half at a depth interval of 5 cm and 10 cm, respectively. These samples were taken for the measurements and determination, stable isotopes, foraminiferal and dinoflagellate assemblages, as well as for mineralogy and organic geochemistry. On purpose, additional syringe and bulk samples were taken at irregular intervals for determination of physical properties. In order to get a first impression about the composition of planktonic foraminifera and changes in sand content for each core, 5 ml syringe samples from selected cores where wet sieved onboard.

A detailed list of samples available from the sediment cores taken on this Cruise M47/3 can be requested from the library of the Marine Geology Section, Fachbereich Geowissenschaften, University of Bremen.

Table 3.6 Geologic Station List M 47/3
(Abbreviations: MUC: Multicorer, ROS: Rosette, CTD: Conductivity, Temperature, Pressure Profiler, GKG: Box corer, SL: gravity corer, n.o.: not opened, WD: Water depth)

GeoB No.	Date 2000	Equipment	Time Sea floor (UTC)	Location Latitude	Location Longitude	Water Depth (m)	Core Length (cm)	Remarks
NORTHERN RIM OF THE CONGO FAN								
6501-1	02.06.	ROS14/CTD CH4-sensor	18:21	03°33.5 S	009°46.9 E	684		To 681 m WD, 14x10L, isotopes, CH4, nutrients
6501-2		GKG	19:29	03°33.5 S	009°46.9 E	695	45	Surface samples, 4 tubes
6501-3		MUC	20:18	03°33.5 S	009°46.8 E	703	35	8 big and 4 small tubes
6501-4		SL12	21:26	03°33.4 S	009°46.8 E	692	486	CC: olive hemipelagic mud, H2S, mollusks
NORTHERN CONGO FAN, Central Part								
FaultZone or Channel?								
6502-1	04.06.	GKG	17:49	05°16.4 S	009°52.9 E	2936	50	Surface samples, 3 tubes
6502-2		MUC	20:01	05°16.4 S	009°53.0 E	2932	44	8 big and 4 small tubes
6502-3		SL18	22:18	05°16.4 S	009°52.9 E	2933	1396	CC: olive hemipelagic mud, geochemistry sampling
Banana Hole								
6503-1	07.06.	ROS14/CTD CH4-sensor	15:42	04°51.1 S	009°55.3 E	3101		To 3078 WD, 14x10L, CH4, isotopes, nutrients, Nd/Sr
6503-2		GKG	18:30	04°51.2 S	009°55.3 E	3103	> 50	surface disturbed, watery, surface samples, 4 tubes
6503-3		SL18	20:30	04°51.3 S	009°55.3 E	3093	736	Banana, CC: concretions,
6503-4	22.06. revisit	ROS14/CTD CH4-sensor	10:44	04°51.2 S	009°55.3 E	3090		To 3074 WD, 14x10L, CH4, isotopes, nutrients
6503-5		MUC	12:56	04°51.2 S	009°55.3 E	3089	42-44	2 big and 1 small tubes for geochemistry, geology surface samples
6503-6		SL12	14:52	04°51.2 S	009°55.3 E	3089		Surface lost ?m through the weight, CC: olive mud
Black Hole								
6504-1	08.06.	GKG	15:14	04°48.8 S	009°55.4 E	3118	> 50	surface disturbed, watery, surface samples, 3 tubes
6504-2		MUC	17:15	04°48.9 S	009°55.4 E	3117	42-44	7 big and 4 small tubes, olive to black mud, clams
6504-3		SL6	19:29	04°48.8 S	009°55.4 E	3117	--	No core, through weight
6504-4		SL12	22:01	04°48.8 S	009°55.4 E	3117	--	No core, through weight
6504-5	09.06. revisit	ROS14/CTD CH4-sensor	13:41	04°48.8 S	009°55.4 E	3120		To 3093 WD, 14x10L, CH4, nutrients
6504-6		SL18	16:12	04°48.8 S	009°55.4 E	3117	1594	CC: olivegrey mud, H2S, geochemistry, concretions
6504-7	10.06. revisit	SL18	16:56	04°48.9 S	009°55.5 E	3120	576	CC: mud, geochemistry
Reflector Zone								
6505-1	09.06.	SL12	20:10	04°47.6 S	010°00.6 E	3060	--	No core, through weight
6505-2	10.06. revisit	SL18	08:45	04°47.6 S	010°00.6 E	3051	1554	CC: hemipelagic mud
Transparent Zone								
6506-1	10.06.	SL18	11:13	04°47.6 S	010°00.7 E	3057	954	CC: hemipelagic mud
Missed Hole								
6507-1	10.06.	MUC	21:01	04°50.3 S	009°53.0 E	3089	42-44	8 big and 4 small tubes
DEEP CONGO FAN								
6508-1	14.06.	ROS/CTD CH4-sensor	07:46	06°38.4 S	005°08.7 E	4992		To 3000 WD, 14x10L, CH4, isotopes, nutrients, Nd/Sr
Channel levee								
6509-1	15.06.	MUC	11:00	06°12.6 S	007°18.4 E	4379	24-26	8 big and 4 small tubes
6509-2		SL12	13:59	06°12.6 S	007°18.4 E	4372	1152	CC: hemipel. mud, black

Channel fill								
6510-1	15.06.	SL12	16:57	06°13.5 S	007°18.8 E	4411	1070	CC: hemipel.mud, silt
6510-2		ROS/CTD CH4-sensor	18.33	06°13.5 S	007°18.8 E	4446		To 500 WD, 14x10L, Sd/Nd isotopes, nutrients

GeoB No.	Date 2000	Equipment	Time Sea floor (UTC)	Location Latitude	Longitude	Water Depth (m)	Core Length (cm)	Remarks
SOUTHERN CONGO FAN								
6511-1	16.06.	ROS/CTD CH4-sensor	10:33	06°13.6 S	009°50.0 E	3422		To 500 WD, 14x10L, Sd/Nd isotopes, nutrients
Diapir field								
6512-1	19.06.	MUC	08:47	06°10,6 S	010°21.7 E	2552	41-43	8 big and 4 small tubes
6512-2		SL9 (n.o.)	10:32	06°10,6 S	010°21.6 E	2561	730	CC: olive clay, glauconite
6513-1	19.06.	SL9 (n.o.)	13:19	06°07.0 S	010°23.4 E	2596	601 (701)	CC: olive hemipelagic mud, 1m surface lost.
6514-1	19.06.	SL9 (n.o.)	15.32	06°11.6 S	010°22.5 E	2615	745	CC: olive mud, 5cm surface in plastic bottle
6515-1	19.06.	SL9 (n.o.)	17:40	06°08.3 S	010°25.1 E	2451	763	CC: olive-black mud
UPPER CONGO FAN								
6516-1	20.06.	ROS/CTD CH4-sensor	04:47	05°29.7 S	011°18.9 E	856		To 830 WD, 14x10L, CH4, isotopes, nutrients
6516-2		MUC	05:48	05°29.7 S	011°18.9 E	856	40-42	8 big and 4 small tubes
6516-3		SL12	06:42	05°29.7 S	011°18.9 E	856	600	CC: olive mud, pteropods
6517-1	20.06.	MUC	11:59	05°37.0 S	011°19.9	648	34-36	8big and 4 small tubes
6517-2		SL12	12:47	05°37.0 S	011°19.9	642		CC: olive mud
6517-3		ROS/CTD CH4-sensor	13:30	05°36.5 S	011°19.6	638		To 500 WD, 14x10L, CH4, isotopes, nutrients, Nd/Sr
6518-1	20.06.	SL12	15:23	05°35.3 S	011°13.3 E	962	741	CC: olive mud
6518-2		MUC	16:09	05°35.3 S	011°13.3 E	962	41-43	8 big and4 small tubes
6519-1	20.06.	MUC	20:58	06°10.1 S	011°11.2 E	946	--	All tubes empty
6519-2		MUC	21:45	06°10.1 S	011°11.2 E	946	40-42	8 big and 4 small tubes
6519-3		SL12	22:31	06°10.1 S	011°11.3 E	940	641	CC: olive mud, pteropods
NORTHERN CONGO FAN, Central Part								
Hydrate Hole, Center								
6520-1	22.06.	ROS/CTD CH4-sensor	18:05	04°48.7 S	009°54.2 E	3122		To 3101 WD, 14x10L, CH4, isotopes, nutrients
6510-2		MUC	20:21	04°48.7 S	009°54.2 E	3124	44-46	Only surface and geochem. samples, olive mud.
Hydrate Hole, Northern flank								
6520-3		SL18	22:34	04°48.6 S	009°54.5 E	3112	9-10 m	CC: Gashydrates , olive mud, stiff, strong gas release from liners, H2S, concretions at the surface
6520-4	23.06. revisit	ROS/CTD CH4-sensor	12:45	04°48.6 S	009°54.5 E	3112		To 3083 WD, CH4, isotopes deepest sample
6520-5		SL18	14:59	04°48.6 S	009°54.5 E	3114	Banane	2 clasts of mud with gas hydrates in the deepest section, concretions in CC
6520-6		MUC	17:08	04°48.6 S	009°54.5 E	3116	18-20	5 big and 4 small tubes, surface with concretions and mollusks, sampling at 5 cm intervals
Worm Hole								
6521-1	23.06.	MUC	01:34	04°45.6 S	009°56.3 E	3131	35-36	8 big and 4 small, surface with worms, molluscs, and concretions, sampling at 5 cm intervals.
6521-2	23.06. revisit	SL18	19:32	04°45.7 S	009°56.3 E	3131	1154	CC: olive mud
6521-3		MUC/CTD CH4-sensor	21:48	04°45.7 S	009°56.3 E	3114		To 3106 WD, 13x10L, CH4

Lithologic Core Summary

This preliminary lithologic summary of the sediments retrieved with the gravity corer during M47/3 is based on visual description (mainly MUNSELL soil color chart, and sedimentary structures), colour scanner readings and microscopic inspection of smear slides taken from distinctive sediment horizons. For digital colour profiles a Minolta CM - 2002 hand-held spectrophotometer was used to measure percent reflectance values of sediment colour at 31 wavelength channels over the visible light range (400-700 nm). The digital reflectance data of the spectrophotometer readings were routinely obtained from the surfaces of split archive halfs immediately after core opening to provide a continous record of the sediment color variation. The surfaces of all core segments were scraped with a knife to expose a fresh, unsmeared surface for measurements at 2 cm intervals. A thin, transparent plastic film (HOSTAPHAN) was used to cover the wet surface of the sediment to protect the photometer from being soiled. Before measuring each core the spectrophotometer was calibrated for white color reflectance by attaching a white calibration cap. The spectrophotometer readings were transfered to a PC and a graphic representation for selected wave band reflection (550, and 700/400 nm ratio) of each core is given in the lithogenic core summary. The color reflectance measurements provide a more detailed picture of alternating intervals of more grey to light green versus dark olive green sediment colour. It is likely, that these slight color changes are due to changes in the sediment composition - particularly the ratio of carbonate, and opal (light and high reflection values) to organic residue and terrigenous clay mineral (dark or low reflection values) content. The red/blue (700/400 nm ratio) in Congo fan sediments generally is a measure of changes in the content of oxic and sulfidic iron phases. More subtle changes in this ratio may be considered as slight changes in terrigenous iron supply to the fan sediment. Nonetheless, these high resolution color reflectance profiles are the immediate tool to correlate sediment cores form the all fan areas. As a first measure of sediment grain size variation is we looked at the sand content in the stratigraphy samples (all grains and foraminiferal tests > 63 microns), however, the sampling density of this sample series and the sporadic occurrence of coarser layers of authigenic minerals resulted in un-interpretable plots of grain size variations in the coarse fraction that we refrained from plotting them here. All the fan sediments cored consists of diatom-bearing hemipelagic muds with traces of foraminifera. They all are olive green in color with only very minor changes in lightness and green shading that are very difficult to detect visually. Therefore the digital reflectance curves shown in the following section have been the basis for correlation amongst cores and also for preliminary stratigraphic information. Sediment core visual descriptions and biostrat results of foram miscroscopy can be found in the GeoB core archive.
The sediments recovered and opened onboard can be described as follows:

The sediments at site GeoB 6501 (Fig. 3.26) from the upper slope north of the fan consist of olive-green diatom- and foram-bearing, hemipelagic mud. Sedimentation rates are probably low, the bottom of the 486 cm long core containing about 200,000 years old sediments. Light reflection is very low on the dark olive coloured sediments, also indicating low carbonate content and probably high organic carbon content). Light reflectance for the 550 nm wave band (Amplitude) and the 700/400 nm ratio do not reveal a pattern indicative for any climatic pattern know from older cores from that region.

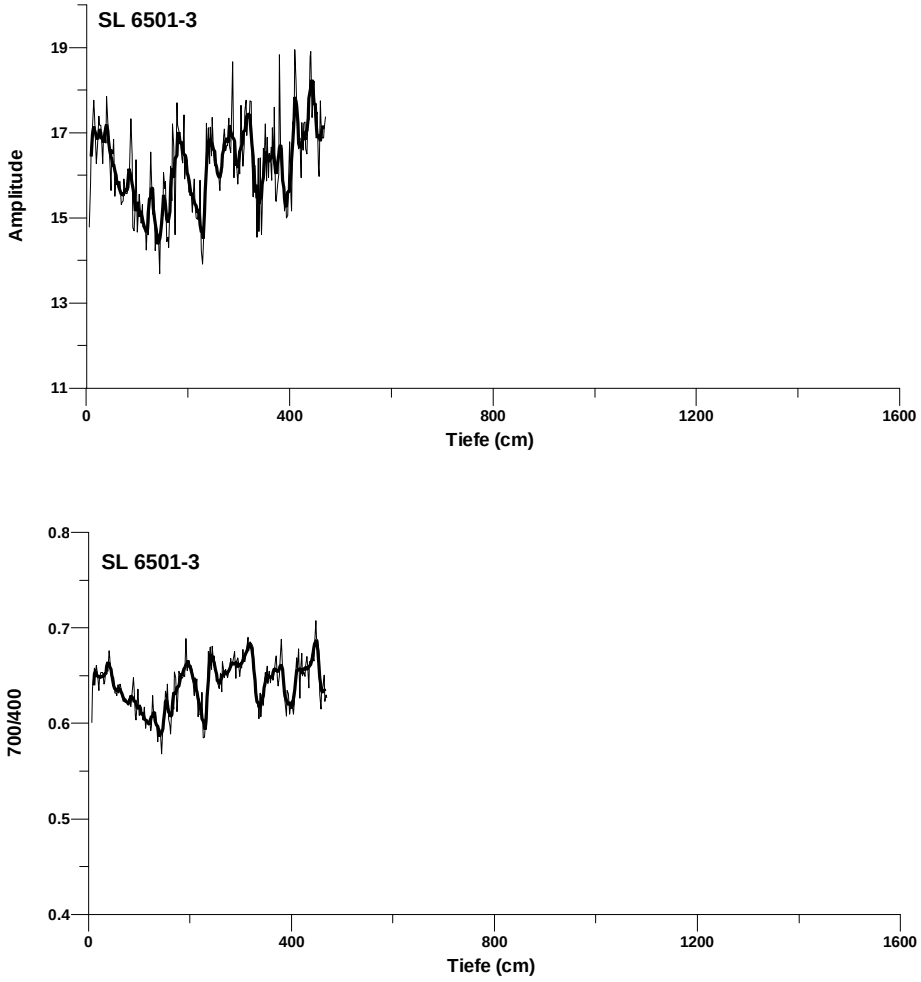

Fig. 3.26: Profiles of color reflectance over depth in core GeoB 6501-3. Amplitude is reflectance changes in the 550 nm wave band, the red/blue or 700/400 nm wave bands ratio represents subtle changes in oxic versus sulfidic iron contents.

Sediment cores 6503-6 and 6503-3 were taken from the same station (Table 3.6) and both consists of dark olive-green, diatom-bearing mud with low abundance of foraminifera. Despite the close vicinity of coring in a pockmark, the 18m long gear only retrieved about 7 m of sediment while the 12 m long gear was completely filled and even had some sediment in the weight set. Also, the reflectance patterns are difficult to compare between both cores (Fig 3.27) and indicate, together with the huge difference in core recovery, that the sediments are very heterogeneous in some sense. Probably the occurrence of a layer of massive authigenic carbonates prevented deeper core penetration at site 6503-3. From preliminary shipboard results it is assumed that small scales changes in pore water chemistry, sediment redox conditions and precipitation of authigenic minerals throughout the sediment column in an area of fluid migration assigned by pockmark structures is very heterogeneous, thus causing the observed differences in the color profiles and in core retrieval.

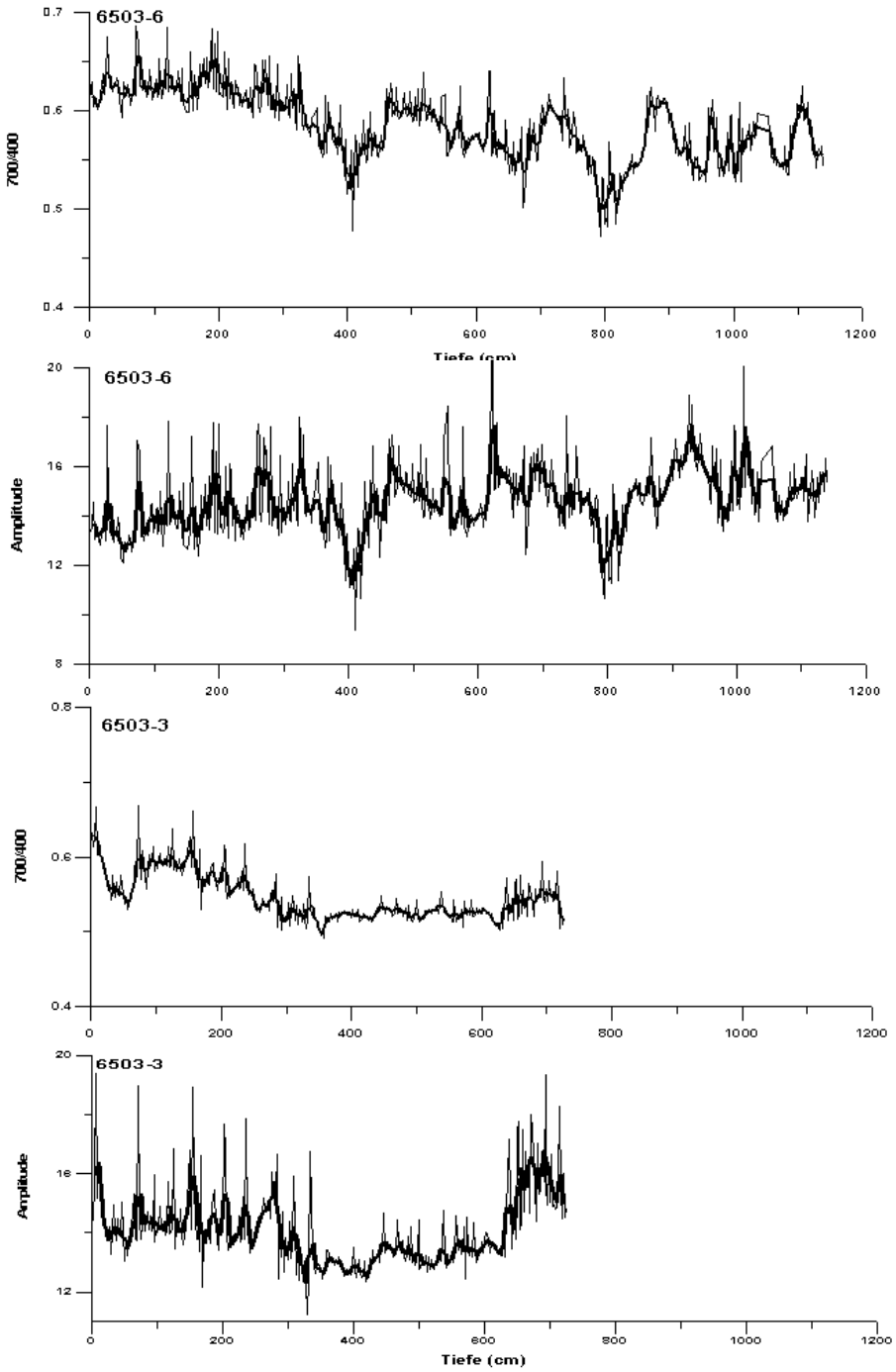

Fig. 3.27: Profiles of color reflectance over depth in cores GeoB 6503-6 and 6503-3. Amplitude is reflectance changes in the 550 nm wave band, the red/blue or 700/400 nm wave bands ratio represents subtle changes in oxic versus sulfidic iron contents.

Core GeoB 6504-6 was recovered from another pockmark structure near to site GeoB 6504, but at site 6504 a much longer core of about 16 m could be retrieved. Although from probably a similar environment, color reflectance records do not allow correlation between sites GeoB 6503 and 6504 (Fig. 3.28). Preliminary shipboard counting showed only very minor foraminifera abundances, thus biostratigraphic inferences were not possible to make.

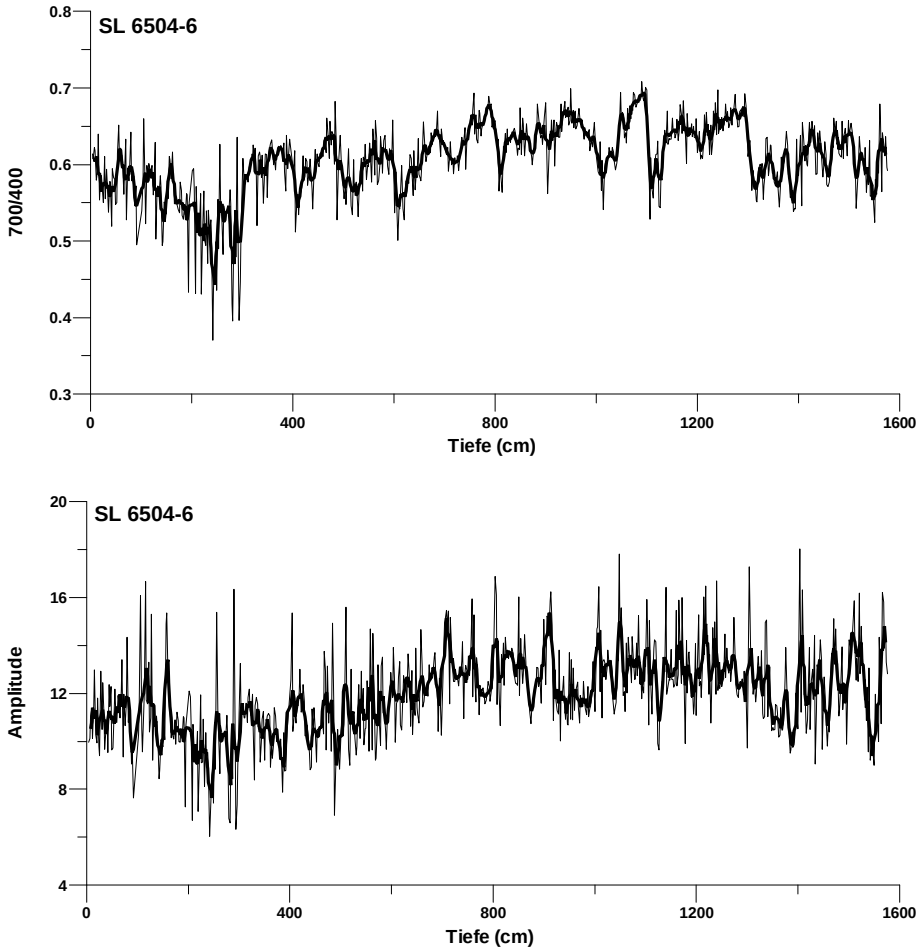

Fig. 3.28: Profiles of color reflectance over depth in core GeoB 6504-6. Amplitude is reflectance changes in the 550 nm wave band, the red/blue or 700/400 nm wave bands ratio represents subtle changes in oxic versus sulfidic iron contents.

Cores GeoB 6505-2 and 6506-1 were taken from a region of "normal" sedimentation in between two pockmark structures. The exercise here was to retrieve two cores for normal fan sedimentation which show differences in the intensities of sediment acoustic (PARASOUND) and high resolution seismic reflectors in the upper 20 meters of the sediment column. The longer core GeoB 6505-2 was retrieved from an area of more pronounced reflectors while the shorter core GeoB 6506-1 comes from an area of more diffusive and hardly to distinguish reflectors, the so-called transparent zone. Both cores consists again of soft dark, olive-green, diatom-bearing hemipelagic mud with minor abundances of foraminifera. Color reflectance patterns (Figs. 3.29 and 3.30) allow weak correlation of the upper 7 m in core GeoB 6505-2 with the upper 5 m in core GeoB 6506-1. The latter core probably contains pronounced lithologic variance and/or experienced small scale changes in redox conditions as is indicated by rapid oscillations in the reflectance data below 7 m core depth at site GeoB 6506. This feature prevented correlation to site 6505 for the deeper core sections.

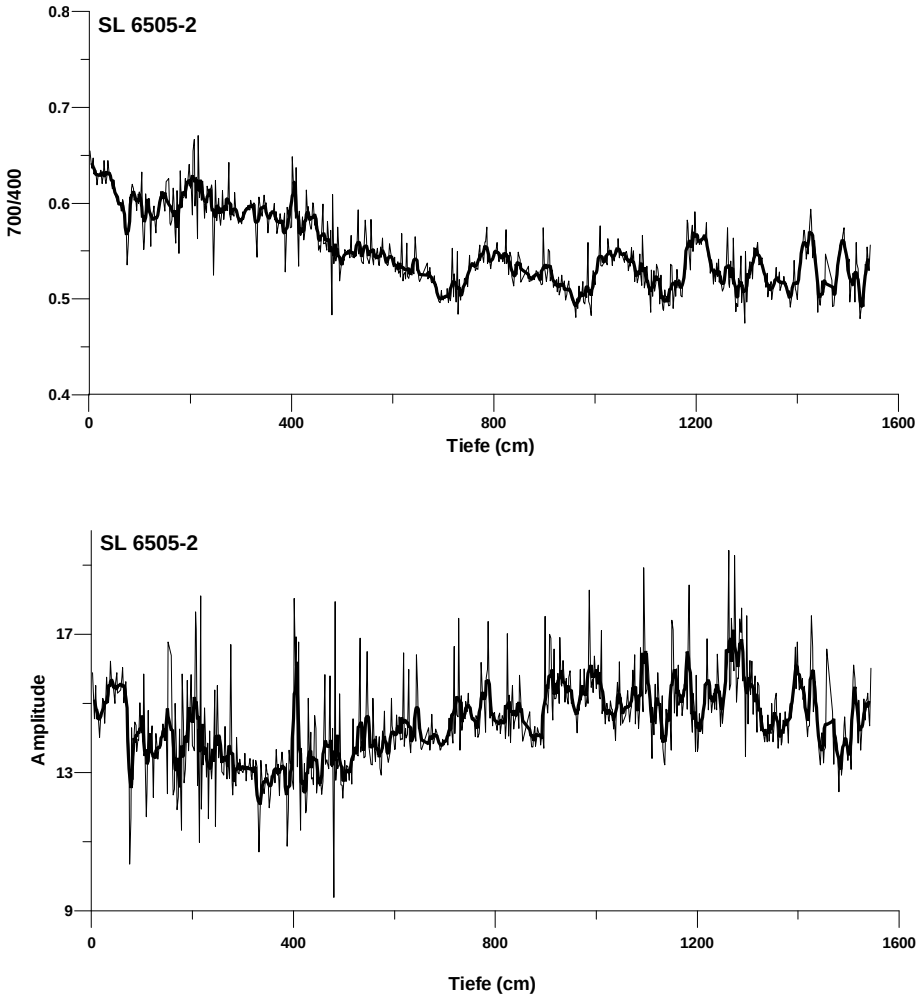

Fig. 3.29: Profiles of color reflectance over depth in core GeoB 6505-2. Amplitude is reflectance changes in the 550 nm wave band, the red/blue or 700/400 nm wave bands ratio represents subtle changes in oxic versus sulfidic iron contents.

The reason why acoustic reflectors where so different between these two core sites could not be detected from these shipboard data. In general it was found that these 2 cores contained no authigenic carbonate precipitates as it was the case for the cores from pockmark structures. Detailed studies of physical properties will be carried out in the shore-based labs in Bremen later in order find explanations for this “acoustic”. difference An age of about 100,000 years for the bottom of core 6506-1 was inferred from the occurrence pattern of the planktonic foraminifera *Glorotalia menardii*, while core GeoB 6505-2 probably extents back to 200,000 years BP. This accounts for a sedimentation rate of 6 to 10 cm / 1000 years, values that are very similar to sedimentation rates found in previous cores from about 3000 m water depths in the northern fan area.

From the deepest part of the Zaire (Congo) fan that was surveyed during M47/3 we took two cores from the central canyon. One core, GeoB 6509-2, was retrieved from channel levee sediments, at 4380 m water depth, while the other, GeoB 6510-1, was taken from the canyon infill at 4410 m water depth. Both cores should enable the characterisation of mainly the terrigenous sediment input by the Zaire River and transported through this major distributary canyon, channelling almost all of the river-bed sediment load to the deep sea.

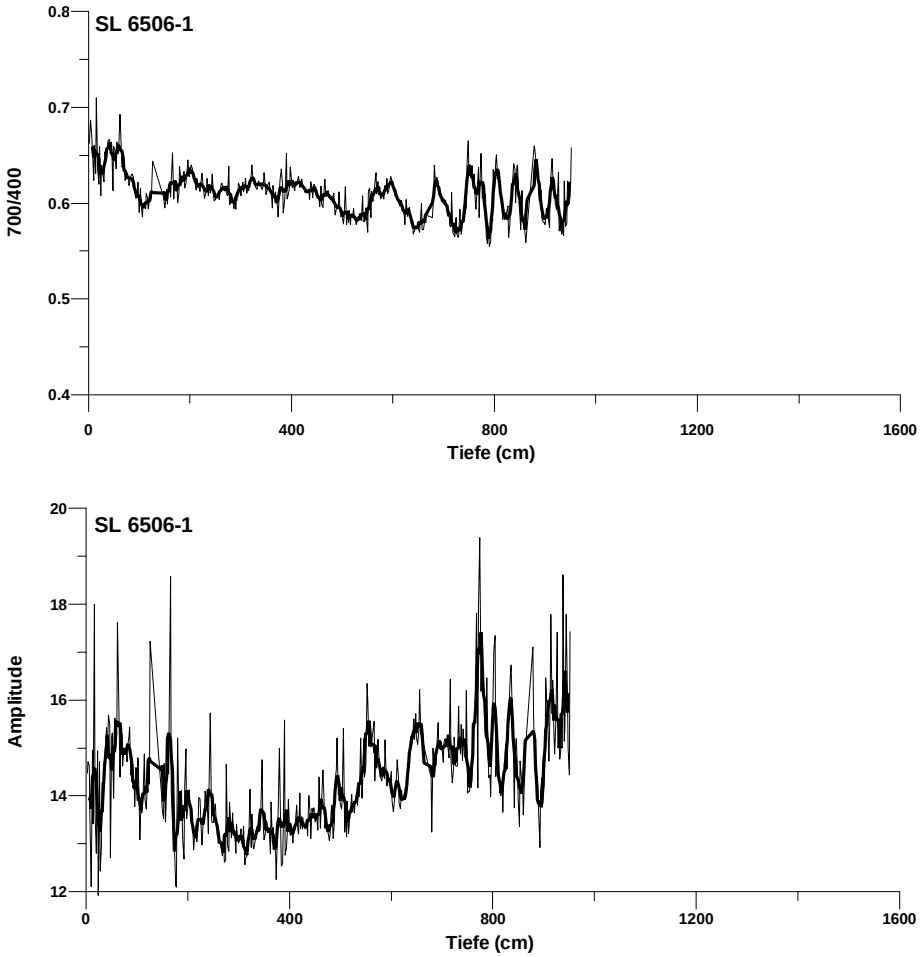

Fig. 3.30: Profiles of color reflectance over depth in core GeoB 6506-1. Amplitude is reflectance changes in the 550 nm wave band, the red/blue or 700/400 nm wave bands ratio represents subtle changes in oxic versus sulfidic iron contents.

The sediments consists mainly of dark green to brown, terrigenous silty clays, containing fragments of wood and leaves while diatoms and fragments of foraminifera a rare. The color reflectance records (Fig. 3.31) show a distinct pattern that is characterised by a trend from high reflectance in the 550 nm wave band and high 700/400 nm ratio at the top of both cores to lowest values in both parameters at about 1 m core depth. Below 1 m, both parameters remain very constant downcore at low values on average. This pattern is interpretated as the change from more oxidised terrigenous sediments in the top one meter of the two cores that change to more suboxic/anoxic conditions and higher contents of organic matter below this first meter in core depth. We consider this change in color governed by the sediment composition and redox state as an indication for the transition from Last Glacial to Holocene sediments in the channel infill and levee sediments.

Another four cores were taken on the southern flank of the Zaire fan at water depths of about 2600 m, above a field of salt diapirs in the deeper sediment column. These cores were not opened onboard. The cores will serve for specific investigation of hydrocarbons within the surface sediments that may be indicative of fluid and oil migration in that specific area.

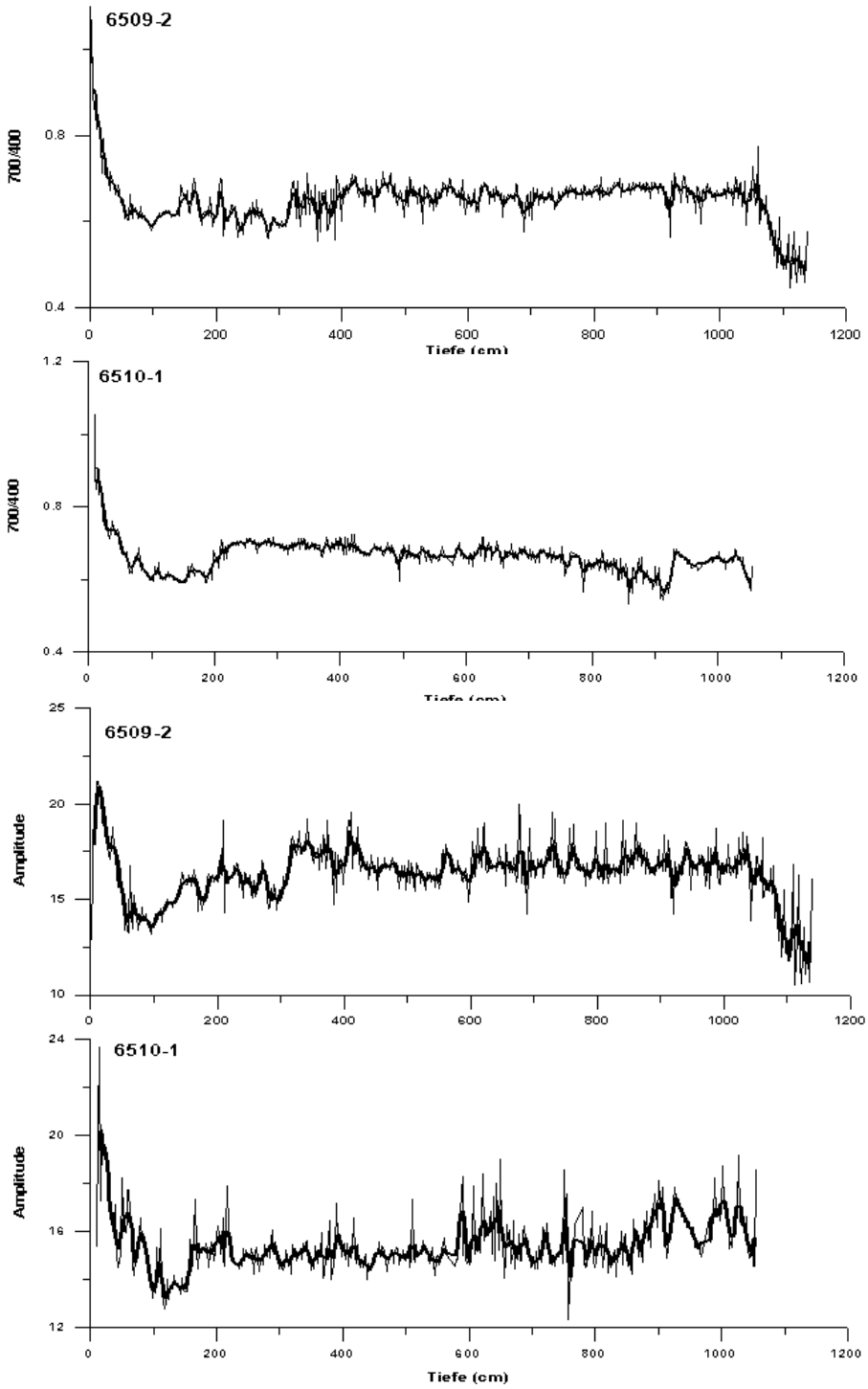

Fig. 3.31: Profiles of color reflectance over depth in cores GeoB 6509-2 (Levee) and GeoB 6510-1 (Channel fill). Amplitude is reflectance changes in the 550 nm wave band, the red/blue or 700/400 nm wave bands ratio represents subtle changes in oxic versus sulfidic iron contents.

Back from the southern flank of the fan we took another suite of four cores form the upper fan in water depths between 850 and 960 m (Figs. 3.32. and 3.33.).

The objective for these four cores was the search for high resolution proxy records of climate change in the Angola Basin and the adjacent continents over the last glacial - interglacial cycle. We therefore took cores in a fan area where we expected high sedimentation rates due to

proximal distance to the river mouth but which is prone to a continuous and undisturbed sedimentation process, because most of the turbiditic sediment flow goes through the central canyon.

As can been see in figure 3.32, the thickness of Holocene sediments, characterised by higher 700/400 nm ratios, which was about 1 m in the levee and channel infill sediments at 4400 m water depth (see above) is now about 2 to 4 m in the cores from the upper slope.

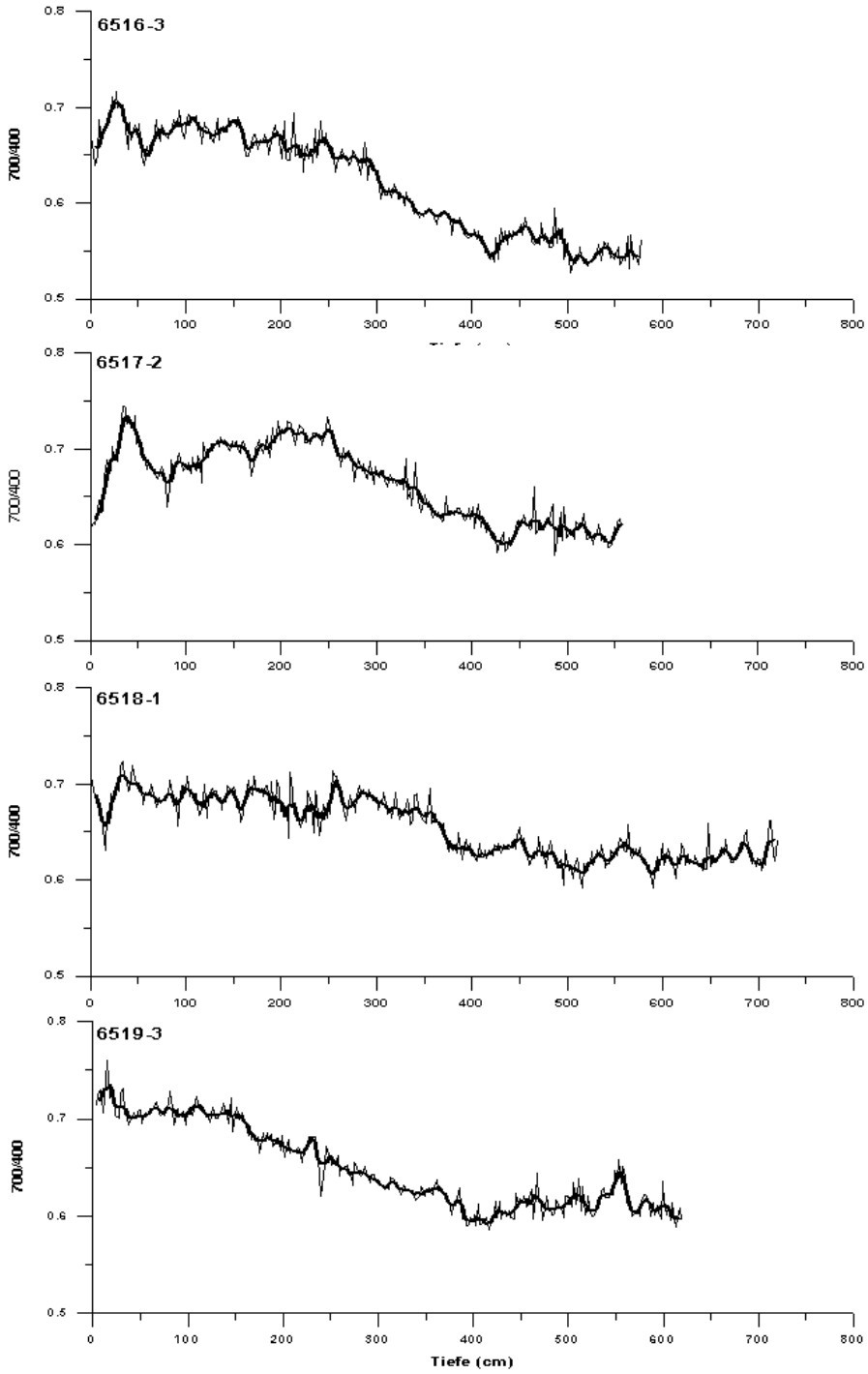

Fig. 3.32: Profiles 700/400 nm ratio over depth in cores GeoB 6516-3, 6517-2, 6518-1, and 6519-3. The red/blue or 700/400 nm wave bands ratio represents subtle changes in oxic versus sulfidic iron contents.

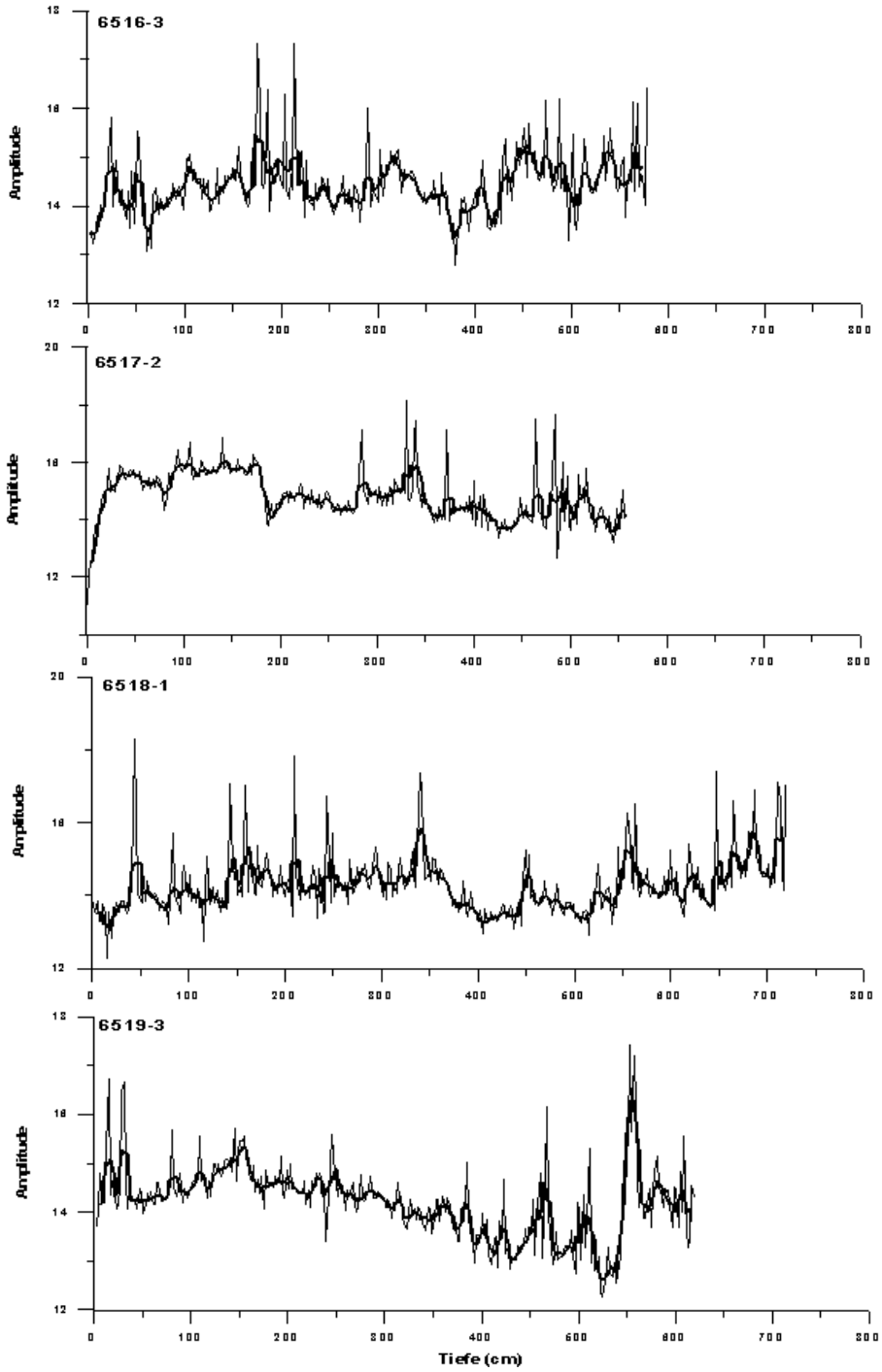

Fig. 3.33: Profiles of reflectance amplitude over depth in cores GeoB 6516-3, 6517-2, 6518-1, and 6519-3. Amplitude is reflectance changes in the 550 nm wave band.

From this we infer that the transition from the last Glacial Maximum at about 3 m core depth in all of these for cores. Preliminary counts of the abundance changes in the planktonic foraminifera *Globorotalia menardii* support this assumption. Changes in light reflectance (amplitude) are not that different between Glacial and Holocene sediments from the upper fan (Fig. 3.33), because closer to the river mouth the sedimentation on the upper fan is dominated by terrigenous input, strongly diluting the content of any whitish calcareous or grayish diatom tests in the bulk sediments. However, since marine productivity increased during glacials, organic

carbon contents are much higher in the glacial sediment sections and thus caused more suboxic and/or anoxic conditions indicated by low values in the 700/400 nm ratio in all for cores below 4 m core depth. From this we expect have cored sediments with an average sedimentation rate of 20 to 40 cm / 1000 years.

The final destination for coring during M47/3 were pockmark structures in the northwestern part of the deep sea fan at water depths of about 3100 m water depths. Here one gravity core, GeoB 6520-3, sampled a 6 m thick sediment layer of hemipelagic muds, intercalated with individual pieces and layers of gas hydrates (Fig. 3.34).

Fig. 3.34: Photograph of a core section of Congo Fan sediments containing layers of solid gas hydrates.

In this core the zone of gas hydrates was superimposed by 4 meters of hemipelagic sediments containing high amounts of authigenic carbonate precipitates. Both sediment zones are were separated by the transition from methane-rich to sulphate rich pore-waters at about 3 m core depth (see Geochemistry Section of this report). The core GeoB 6520-3 was sampled and color-scanned only down to 4 m core depth, while the lower gashydarte-bearing sediment sections were immediately stored in the freezer. A second core, GeoB 6521-2, taken from a pockmark structure nearby, was also cored in order to retrieve solid gas hydrates, however this core only reached the pore-water sulphate-methane transition zone which occurred just above the gas hydrates at site GeoB 6520. Similar to the upper 4 m in core GeoB 6520-3, the 11 m of hemipelagic sediments in core 6521-2 contain high amounts of authigenic carbonate precipitates. As was the case for cores GeoB 6503-6, 6503-3, and 6504-6, the color reflectance records of cores GeoB 6520-3 and 6521-2 from the pockmark structures at 3100 m water depth (Fig. 3.35) are heavily controlled by the occurrence of authigenic precipitates and individual redox conditions in the sediment column. Therefore, correlation of color records between sites GeoB

6520 and 6521 is not possible, nor can the patterns of reflectance changes attributed to any sedimentological features related to climate change as was the case for the cores from sites GeoB 6516 to 6518.

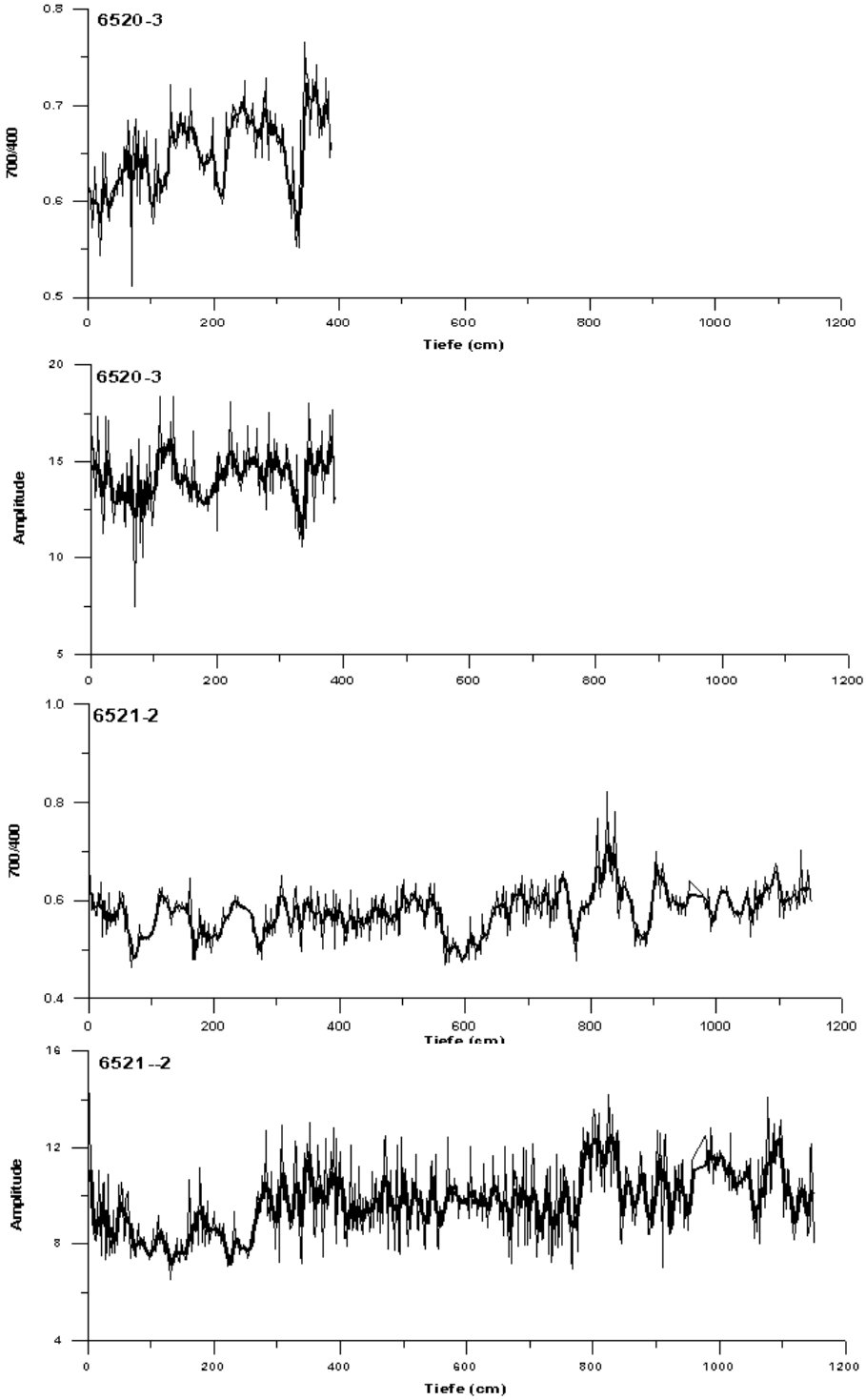

Fig. 3.35: Profiles of color reflectance over depth in cores GeoB 6520-3 (Gas hydrates and shallow methane to sulphate transition zone) and GeoB 6521-1 (deep methane to sulphate transition zone). Amplitude is reflectance changes in the 550 nm wave band, the red/blue or 700/400 nm wave bands ratio represents subtle changes in oxic versus sulfidic iron contents.

Multicorer and Box Corer Sampling

The box corer was only used at the first two stations for retrieving high amounts of surface sediments (Tab. 3.7). Afterwards this instrument was not used anymore because the sediment surface quality obtained was not sufficient for the purposes of the planned investigation program. Alternatively only the multicorer was used with multiple runs if needed. The multicorer is designed to recover undisturbed surface sediment sections and the overlying bottom water. The model used on M47/3 was equipped with 4 small plastic tubes and 8 larger tubes (6 and 10 cm in diameter). At most of the stations all tubes were filled with the uppermost 20 to 45 cm of sediment and the superimposed bottom water (Tab. 3.8). This table also describes how the tubes were sampled. In some cases, where pockmark structures were sampled, the tubes where filled with big mollusc shells and authigenic carbonate precipitates. Here the sampling of multicorer tubes in 1 cm slices was not possible (see Table 3.8)

3.4.3.2 Pumped plankton samples

Marine plankton from surface waters was sampled during the survey over the Zaire fan (Table 3.9). We used the shipboard installed fire pump system to filter about 10000 to 20000 l each day, mostly during daylight. The amount of water filtered, was depended on the plankton mass caught in the plankton net. The sea-water was pumped through a net with a mesh size of 63 microns in order to mainly get high numbers of planktonic foraminifera. When the water flow was stopped by the material closing the net openings, the plankton was washed into plastic bottles and the sampling was continued with the cleaned net. For each day the wet plankton samples were concentrated into one bottle and stored at 4° C.

Distinct samples for the detailed investigation of typical fan sediment physical properties were collected onboard from gravity cores and will be analysed by Glenn Spinelli (University of California, Santa Cruz) from METEOR Cruise 47/3 (Table 3.10).

Table 3.7: Box corer (GKG) samples

GeoB No.	Surface Sediment Samples (Size in cm^2)	Archive Tubes (diameter 12 cm)	Remarks
6501-2	Forams ca. 400, Corg 200, Biomarker 200	Geology, Corg, Biomarker, all 45 cm	
6502-1	Forams ca. 400, Corg 200, Biomarker 200	Geology, Corg, Biomarker, all 50 cm	
6503-2	Forams ca. 400, Corg 200, Bimarker 200	Geology, Corg, Biomarker, all >50 cm	Surface partly disturbed
6504-1	Forams ca. 400, Corg 200, Biomarker 200	Geology, Corg, Biomarker, all >50 cm	Surface partly disturbed

Table 3.8: Multicorer Sampling

Abbreviations: lg – large tube, sm – small tube, sl – 1 cm slices, G – geology archive, C – Corg archive, BM – biomarker archive, GS - grain size (Spinelli UCSC), PB – plastic bottles, 4sd – methane from sediment, 4bw, methane from bottom water, I – isotopes from bottom water, ss. o. – surface samples only due to molluscs and concretions, xx extra samples taken from geochemistry cores.

GeoB No.	cm	Forami-nifera	Corg	Bio-marker	TOC TW	Archives (frozen)	Geochem. / Porewater	Surface Samples Pollen, Diatoms, Magn.	MPI DNS, BM	Archaeo -bacteria
6501-1	34	2lg sl I	1lg sl	1lg sl	1lg sl	1lg 1sm G		1sm, 1sm, 1sm		
6502-2	44	2lg sl I	1lg sl	1lg sl	1lg sl	1lg 1sm G	2lg 4bw	1sm, 1sm, 1sm		
6503-5	42	ss. o. I	10 PB with mollusks from surface				2lg		1sm, xx	
6504-2	42	2lg sl I	1lg sl	1lg sl		1lg 2sm G	2lg 4bw 4sd	1sm, 3PB molluscs	1sm, xx	1l sl
6507-1	42	2lg sl I	1lg sl	1lg sl	1lg sl	2lg G BM 1sm GS		1sm, 1sm, 1sm		
6509-1	24	2lg sl I	1lg sl	1lg sl	1lg sl	2lg 1sm G BM		1lg+1sm, 1sm, 1sm		
6512-1	41	2lg sl I	1lg sl	1lg sl	1lg sl	2lg G C	1lg 1sm 4bw	1sm, 1sm, 1sm		
6516-2	40	3lg sl I	1lg sl	1lg sl	1lg sl	2lg G C 1sm G		2sm, 1sm		
6517-1	34	3lg sl I	1lg sl	1lg sl	1lg sl	1lg 1sm G		1lg 1sm, 1sm, 1sm		
6518-2	41	3lg sl I	1lg sl	1lg sl	1lg sl	1lg G 1sm BM		1lg 1sm, 1sm, 1sm		
6519-2	40	3lg sl I	1lg sl	1lg sl	1lg sl	1lg 1sm G		1sm, 1sm, 1sm		
6520-2	44	ss. o. I	7lg 3sm PB with molluscs and concretions				2lg 4sd 4bw		1sm, xx	
6520-6	18	5lg 2sm in 5cm intervals I molluscs and concretions				2sm G	1lg 4sd 4bw		1sm, xx	
6521-1	35	3lg sl I	1lg sl	1 lg sl		3sm G	1lg 4sd 4bw	1lg ss. o. mollusks	1sm, xx	1l sl

Table 3.9: Plankton Net Samples > 63 microns, Shipboard Fire Pump System

		Start Pumping					Stop Pumping				
No	Date 2000	Time UTC	Latitude S	Longitude E	Temp. °C	Sal. ‰	Time UTC	Latitude S	Longitude E	Temp. °C	Sal. ‰
1	04.06.	11:00	05°05.9	010°11.4	26.8	32.4	14:45	05°20.0	009°56.5	27.5	31.8
2	05.06	12:26	05°01.2	010°07.9	26.8	32.1	15:36	04°55.2	010°14.4	26.9	32.3
3	06.06.	09:24	04°04.5	010°44.8	25.8	34.5	11:29	04°10.2	010°35.1	26.0	34.9
4	06.06	12:05	04°11.8	010°32.4	26.8	34.1	14:45	04°19.1	010°20.2	27.0	32.7
5	07.06	07:43	04°53.4	009°57.8	26.8	31.0	12:48	04°49.0	009°55.4	27.0	31.1
6	13.06	13:12	05°41.8	005°35.8	26.8	35.2	16:40	05°49.9	005°19.9	26.0	35.2
7	18.06	14:05	06°41.1	010°20.4	25.6	35.6	17:16	06°41.7	010°32.1	25.5	35.6

3.4.3.3 Sampling for Physical Properties

The whole-rounds of sediment listed below will be used to determine sediment permeability and consolidation state. Sediment permeability determined from these samples will be compared to theoretical estimates of permeability derived from p-wave velocity measurements carried out at Universität Bremen on respective archive sections of each sediment core sampled. Any systematic variations between the measured and estimated permeabilities may be used to calibrate further permeability determinations based on p-wave velocity.

In addition, sediment physical properties (lithology, grain size, permeability, consolidation state, sediment fabric, etc.) from the two gravity cores collected at the sites GeoB 6505-2 and GeoB 6506-1 will be compared. GeoB 6505-2 was collected from a "normally" stratified section on the PARASOUND data; GeoB 6506-1 was collected from an immediately adjacent acoustically transparent section of the PARASOUND record (see sediment core descriptions before). The comparison of sediment physical properties from these two sediment cores may indicate differences between the cores that could result in their differing acoustic signatures.

Table 3.10: List of whole round physical property samples

Core ID	Section collected for permeability and consolidation state measurements at UC Santa Cruz
GeoB 6502-3	597-609 cm (depth below seafloor)
"	897-909 cm
"	1198-1210 cm
GeoB 6503-3	726-736 cm
GeoB 6504-6	1502-1512 cm
GeoB 6505-2	656-666 cm
"	856-866 cm
"	1457-1467 cm
GeoB 6506-1	666-676 cm
"	866-876 cm
GeoB 6510-1	566-576 cm
"	768-778 cm
"	970-980 cm
GeoB 6516-3	579-589 cm
GeoB 6517-2	562-572 cm
GeoB 6518-1	721-731 cm
GeoB 6519-3	620-630 cm
GeoB 6521-2	960-980 cm

3.4.4 Geochemistry

(K. Enneking, C. Hensen, S. Kasten, A. Reitz)

3.4.4.1 Introduction

The main focus of geochemical investigations carried out during this cruise was a detailed sampling of the sediments and the overlying bottom waters at and around pockmark-like depressions identified during former cruises on the Northern Congo Fan (SO 86, Bleil et al., 1994; M34/1, Bleil et al., *1996*). These pockmarks are assumed to represent sites of episodic fluid/gas discharge from vertical migration pathways. We intended to identify distinct features observed in the echosounder and seismic data and to characterize and quantify the biogeochemical processes and fluxes occurring within these sediments as well as across the sediment/water interface.

During this cruise a total of 7 multicorer cores, 5 gravity cores and 7 rosettes (NISKIN water samplers) were processed (Tab. 3.11). In addition, a methane sensor coupled with a CTD was deployed at 10 stations and sediment samples from 3 multicorer cores (GeoB 6503-5, 6504-2, 6520-6) were taken and prepared for FISH analyses at the Max Planck Institute for Marine Microbiology in Bremen.

Table 3.11: List of sediment and water samples taken during Cruise M47/3 - including deployments of the CTD/CH_4 sensor.

Multicorer	**Gravity corer**	**Rosette (vacuum degassing)**	**CTD/CH_4 sensor**
GeoB 6502-2	GeoB 6502-3	GeoB 6503-4	GeoB 6501-1
GeoB 6503-5	GeoB 6504-6	GeoB 6504-5	GeoB 6503-1
GeoB 6504-2	GeoB 6504-7	GeoB 6516-1	GeoB 6503-4
GeoB 6512-1	GeoB 6520-3	GeoB 6517-3	GeoB 6504-5
GeoB 6520-2	GeoB 6521-2	GeoB 6520-1	GeoB 6508-1
GeoB 6520-6		GeoB 6520-4	GeoB 6510-2
GeoB 6521-1		GeoB 6521-3	GeoB 6511-1
			GeoB 6516-1
			GeoB 6517-3
			GeoB 6520-1
			GeoB 6520-4
			GeoB 6521-3

3.4.4.2 Methods

To prevent a warming of the sediments on board all cores were transferred into a cooling room immediately after recovery and maintained at a temperature of about 4°C. The multicorer cores were processed within a few hours. Two samples of the supernatant bottom water were taken and

filtered for subsequent analyses. The remaining bottom water was carefully removed from the multicorer tube by means of a siphon to avoid destruction of the sediment surface. During subsequent cutting of the core into slices for pressure filtration, pH and Eh measurements were performed with a minimum resolution depth of 0.5 cm. Conductivity and temperature were measured on a second, parallel core to calculate sediment density and porosity.

The gravity cores were cut into 1 m segments on deck. At sampling locations where methane was expected to be present, syringe samples were taken on deck from every cut segment surface. Higher resolution sampling for methane analysis was carried out in the cooling laboratory immediately after storing by sawing 4 x 4 cm rectangles into the PVC liner. In this way, syringe samples of 5 ml sediment were taken every 10-20 cm and injected into 50 ml septum vials containing 20 ml of seawater. After closing and subsequent shaking methane becomes enriched in the headspace of the vial. One replicate was taken and poisoned with a $HgCl_2$ solution for determination of the stable isotopic ratios of carbon and oxygen. Within a few days after recovery, gravity cores were cut lengthwise into two halves and processed. On the working halves pH and Eh were determined and sediment samples were taken every 20 cm for pressure filtration. Conductivity and temperature were measured on the archive halves. Solid phase samples were taken at same intervals and kept in gas-tight glass bottles under argon atmosphere. The storage temperature for all sediments was -20°C to avoid dissimilatory oxidation.

All work done on opened cores was carried out in a glove box under argon atmosphere. For pressure filtration Teflon- and PE-squeezers were used. The squeezers were operated with argon at a pressure gradually increasing up to 5 bar. The pore water was retrieved through 0.2 µm cellulose acetate membrane filters. Depending on the porosity and compressibility of the sediments, the amount of pore water recovered ranged between 5 and 20 ml.

Pore water analyses

Pore water analyses of the following parameters were carried out during this cruise: Eh, pH, temperature, conductivity (porosity), sulfate, methane, chloride, ammonium, and alkalinity.

Eh, pH, conductivity and temperature were determined with electrodes before the sediment structure was disturbed by sampling for pressure filtration. Ammonium was measured photometrically with an autoanalyser using a standard method. Alkalinity was calculated from a volumetric analysis by tritration of 1 ml sample with 0.01 or 0.05 M HCl, respectively. Subsamples for sulfate and chloride determinations were diluted 1:20 and analysed by ion chromatography (HPLC). For the detection of methane 20 µl of the headspace gas were injected into a gas chromatograph. The concentrations of methane measured have to be related to the sediment porosity. Since corrected porosity data were not available we assumed a uniform porosity in all gravity cores for the calculation of preliminary methane contents. These concentrations will be recalculated with the corrected porosity values at the University of Bremen.

For further analyses at the University of Bremen, aliquots of the remaining pore water samples were either frozen (for analyses of PO_4 and NO_3) or acidified with $HNO_3^{-}{}_{(suprapure)}$ for determination of cations (Ca, Mg, Sr, K, Ba, S, Mn, Si, B) by ICP-AES and AAS. Additionally, 1 ml subsamples of the pore water were added to a ZnAc solution to fix all sulfide present as ZnS for later analysis.

Methane in the water column

Ultrasonic vacuum degassing

Concentrations of methane in the water column were determined by ultrasonic vacuum degassing of water samples according to the method described by Schmitt et al. *(1991)*. Water samples taken by NISKIN bottles (rosette) were transferred through silicone tubes into evacuated 1 L glass bottles. Ultrasonic energy applied to the samples led to gas release into the headspace. A volume of 0.5 ml gas was taken through a septum for immediate GC analysis. The 0.5 ml aliquots of the concentrated headspace were analysed for methane using a Varian Star 3400 gas chromatograph fitted with a flame ionisation detector. The fraction of the extracted water gases not used for analysis aboard was stored in evacuated glass vessels for later determination of stable carbon isotope ratios.

METS - CH_4 sensor

The METS methane sensor (CAPSUM Technologie, Geesthacht) and the battery module were attached to the CTD. The detection limit of the sensor is 20 nmol/l. Methane concentrations measured during downcast and upcast were saved in the CTD's storage unit and extracted with a specific software after each deployment.

Samples taken for FISH – fluorescence in situ hybridization

Samples from 3 multicorers (GeoB 6503-5, 6504-2, 6520-6) were taken and prepared for subsequent FISH analyses at the Max Planck Institute for Marine Microbiology. The aim of this technique is to identify the microorganisms present in sediments associated with the pockmark structures, especially focussing on consortia of archaea and sulfate reducing bacteria. These consortia have recently been identified by Boetius et al. *(2000)* in sediments of the Cascadia margin and are assumed to mediate the anaerobic oxidation of methane by sulfate.

3.4.4.3 Shipboard Results

Pore water data

Pore water concentration profiles of sulfate and methane at four pockmark stations are shown in Fig. 3.35. At all of these stations the process of anaerobic oxidation of methane could be identified by the consumption of both sulfate and methane within a narrow depth interval. The depth location of this typical sulfate/methane transition in the sediment is dependent on the methane flux from below and significantly varies between the examined sites. At station GeoB 6520 where gas hydrates were present below 5 m the sulfate/methane transition zone is located at about 2.2 m. At the other three stations shown in Fig. 3.35 the depth position of this geochemical boundary at 11 m (GeoB 6521), 13.5 m (GeoB 6504) and about 13.5 m (GeoB 6502) implies lower diffusive fluxes of methane from deeper parts of the sediment.

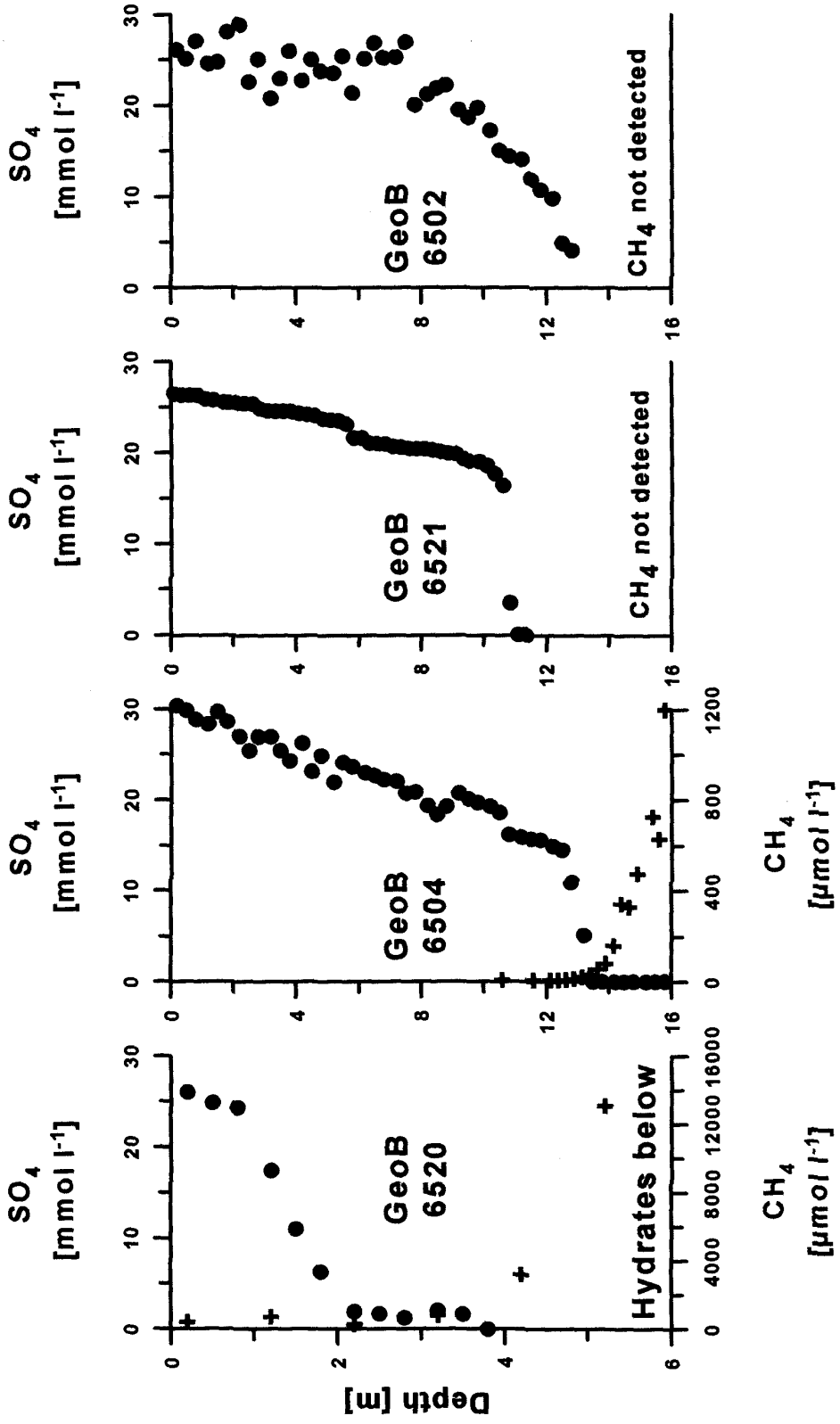

Fig. 3.35: Pore water concentration profiles of SO_4 and CH_4 in gravity cores from stations GeoB 6502, 6504, 6520 and 6521. At site GeoB 6520 massive pieces of gas hydrate were found below 5 m sediment depth.

Methane in the water column

All water column methane concentrations measured during this cruise by means of the ultrasonic degassing technique were below the METS sensors‘ detection limit of 20 nmol/l. Highest CH_4 concentrations determined using the ultrasonic degassing method were around 15 nmol/l. At most of the stations examined methane concentrations were found to increase towards the sediment surface. A typical methane profile as obtained at station GeoB 6504 is depicted in Fig. 3.36. The elevated concentrations determined close to the sediment surface indicate a supply of methane from the sediment. It is not clear yet whether the transport of methane into the overlying bottom water occurs via diffusion across the sediment/water interface or results from the dissociation of gas hydrates outcropping at the sediment surface.

A comparison of the results of the two methods revealed that the METS sensor was not suitable for measuring the comparatively low dissolved methane concentrations in the study area. The absolute values obtained by the sensor do not correspond to the concentrations analysed by means of the ultrasonic degassing technique. Moreover, the shapes of the concentration profiles during downcast and upcast are not identical. This discrepancy might results from the vertical attachment of the sensor at the rosette water sampler and/or from differences in turbulence during downcast and upcast. Largest differences between upcast and downcast occur in the surface waters (Fig. 3.37). Methane values determined during the downcast are significantly elevated compared to the upcast. This is obviously due to the time required for the surface air influence to be removed from the sensor.

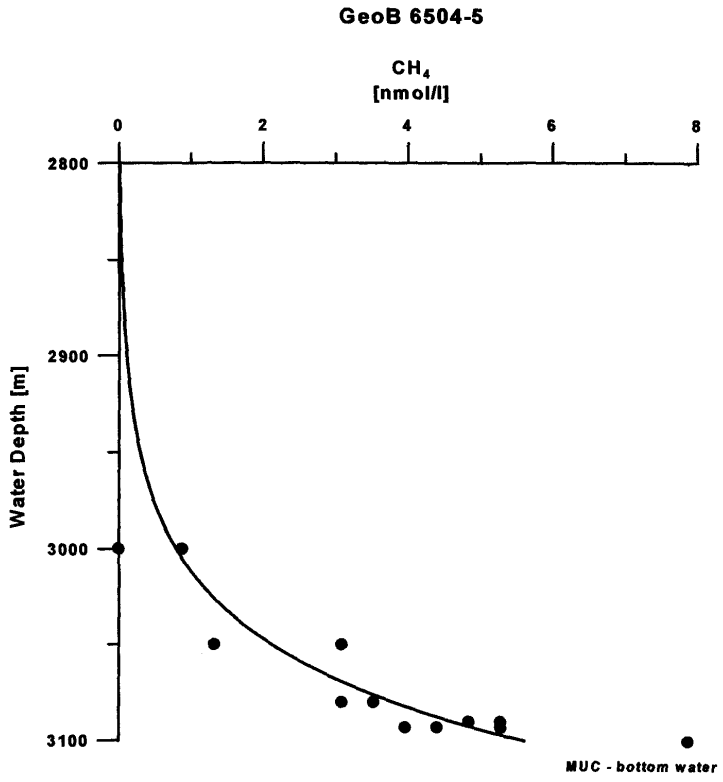

Fig. 3.36: Dissolved methane concentrations in the water column at station GeoB 6504 as obtained from vacuum/ultrasonic degassing.

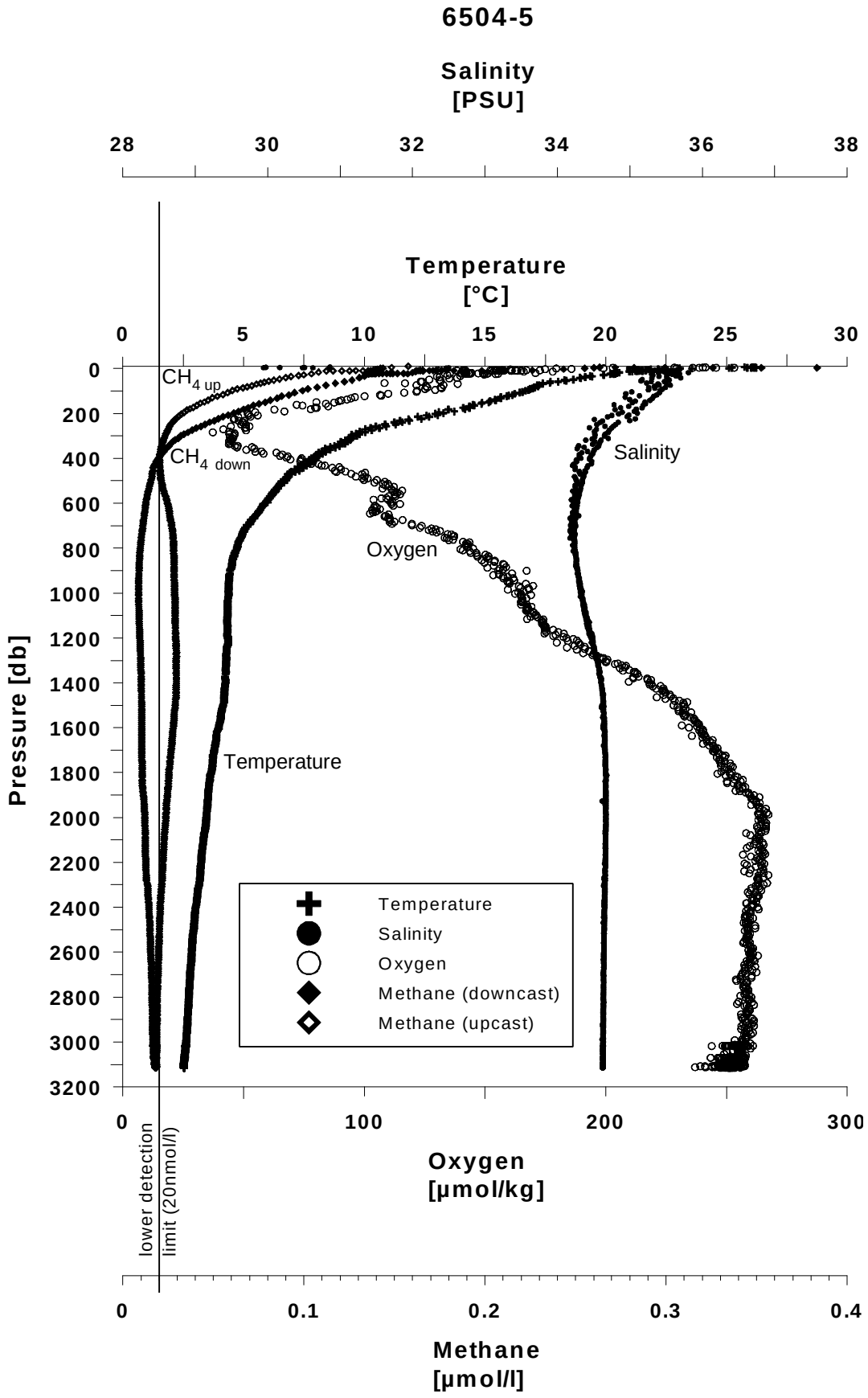

Fig. 3.37: CTD profiles of temperature, salinity, and oxygen at station GeoB 6504. The output of the METS CH_4 sensor is shown here as well. Please note the strong deviation of the CH_4 sensor output between upcast and downcast.

3.5 Ship's Meteorological Station

(C. Joppich)

The weather in the first 3 weeks of the cruise (in the area of Congo Fan) was dominated by the northward position of the Intertropical Convergence Zone (between 06 and 14°N) and the Subtropical High over the Southern Atlantic Ocean. Therefore winds from southerly to southeasterly directions were observed all the time. The wind forces mostly lay between Bft 2 and Bft 4. Only in regions far away from the coastal area Bft 5 was observed for a short time. The swell from southerly directions reached heights from 1 to 2.5 meters. Water temperatures varied between 24 and 28°C, while air temperatures lay between 23 and 27°C. Clouds mostly were cumuliform, but sometimes layered clouds in lower and medium levels were also observed.

During the last week (in the working area west of Namibia) weather conditions exclusive were formed by the intensity and westward position of the subtropical high. At first the trade winds were relatively weak, but to the end of period winds increased up to Bft 6 to 7 and the observed wave height reached 3 meters for a time. Temperatures of water and air lay between 15 and 19°C in the coldwater-upwelling area. Due to a very low atmospheric inversion the sky was free of clouds for several days.

3.6 Acknowledgements

The scientific party gratefully acknowledges the professional support and friendly atmosphere aboard RV METEOR during Cruise M47/3 provided by Captain Kull, the nautical officers, the engineers and his crew. We also appreciate the valuable help of the Leitstelle METEOR, Hamburg, in planning and realization of the cruise. The work was funded by the Deutsche Forschungsgemeinschaft.

3.7 References

Bleil, U., and shipboard scientific party, 1994, Report and preliminary results of SONNE Cruise SO 86, Buenos Aires - Capetown, 22.4.93 - 31.5.93. Berichte, Fachbereich Geowissenschaften, Universität Bremen, 51, 116 S.

Bleil, U., and shipboard scientific party (1996) Report and preliminary results of METEOR cruise M34/1, Capetown – Walvis Bay, 3.1.1996 – 26.1.1996. Berichte, Fachbereich Geowissenschaften, Universität Bremen, 77, 129 S.

Boetius, A., K. Ravenschlag, C. Schubert, D. Rickert, F. Widdel, A. Gieseke, R. Amann, B.B. Jørgensen, U. Witte U and O. Pfannkuche (2000) A marine microbial consortium apparently mediating anaerobic oxidation of methane. Nature, 407, 623-626.

Caress, D. W., and Chayes, D. N., 1996, Improved processing of HYDROSWEEP DS Multibeam data on the R/V Maurice Ewing, *Marine Geophys. Res.*, 18, 631-650.

Grant, J. A., and Schreiber, R., Modern swath sounding and sub-bottom profiling technology for research applications: The Atlas HYDROSWEEP and PARASOUND Systems, *Marine Geophys. Res*., 12, 9-19, 1990.

Schmitt, M., Faber, E., Botz, R. and Stoffers, P., 1991, Extraction of methane from seawater using ultrasonic vacuum degassing. Anal. Chem., 63, 529-532.

Spieß, V., 1993, Digitale Sedimentechographie – Neue Wegezu einer hochauflösenden Akustostratigraphie, Berichte aus dem Fachbereich Geowissenschaften der Universität Bremen, pp. 199, Fachbereich Geowissenschaften, Universität Bremen, 35.

Wessel, P. and Smith, W. H. F., 1998, New, improved version of Generic Mapping Tools released, *EOS Trans.*, American Geophysical Union, 79, 579.